NBSIR 85-3147

Evaluation of the Thermal Integrity of the Building Envelopes of Eight Federal Office Buildings

by

Richard A. Grot
Y. May Chang
Stephen Weber
Andrew K. Persily
Jin B. Fang
Lawrence S. Galowin

SEPTEMBER 1985

Center for Building Technology
National Bureau of Standards
Department of Commerce
Gaithersburg, MD 20899

Office of Design and Construction
Public Buildings Service
General Services Administration
Washington, DC 20405

NBSIR 85-3147

EVALUATION OF THE THERMAL INTEGRITY OF THE BUILDING ENVELOPES OF EIGHT FEDERAL OFFICE BUILDINGS

Richard A. Grot
Andrew K. Persily
Y. May Chang
Jin B. Fang
Stephen Weber
Lawrence S. Galowin

U.S. DEPARTMENT OF COMMERCE
National Bureau of Standards
Center for Building Technology
Gaithersburg, MD 20899

September 1985

Prepared for
Public Buildings Service
General Services Administration
Washington, DC 20405

U.S. DEPARTMENT OF COMMERCE, Malcolm Baldrige, *Secretary*
NATIONAL BUREAU OF STANDARDS, Ernest Ambler, *Director*

ABSTRACT

Diagnostic test methods were applied to eight federal office buildings in order to assess the applicability of these measurement methods for determining the thermal integrity of the building envelope. The eight federal office buildings were located in Anchorage, AK; Ann Arbor, MI; Columbia, SC; Fayetteville, AR; Huron, SD; Norfolk, VA; Pittsfield, MA and Springfield, MA. These buildings ranged in size from 20,000 ft^2 (1,900 m^2) for the building in Pittsfield to 520,000 ft^2 (48,000 m^2) for the Anchorage Federal Building. They were all constructed within the last ten years. The diagnostic tests which were applied to these buildings were ground infrared thermographic inspection, aerial infrared thermographic inspection, spot radiometry, air infiltration and ventilation rate measurement using tracer gas decay, building tightness testing using fan pressurization, component tightness testing, and measurement of the thermal conductance of major wall sections using portable calorimeters and heat flow meters. This report presents and discusses the results of these tests.

Key Words: Air infiltration, building diagnostics, building thermal integrity, fan pressurization, field measurements, spot radiometers, thermal bridges, thermographic inspection, tracer gas techniques, U-value measurements.

EXECUTIVE SUMMARY

Background

The federal government presently owns and leases thousands of buildings throughout the United States. The General Services Administration (GSA) and other federal agencies are also constructing new buildings each year. In recent years, an increasing awareness of energy use has led to greater concern regarding energy consumption in existing buildings and the expected energy use in new buildings. In fact, GSA has developed energy guidelines for new buildings in units of Btu/ft^2 (MJ/m^2) per year. However, many new and existing buildings consume excessive amounts of energy due, in part, to thermal defects in their exterior envelopes. These defects are due to poor construction practice, misunderstanding of construction specifications, and deterioration of building materials, as well as specific design details which lead to thermal breaks in the building envelope.

Several diagnostic techniques have been developed to evaluate the thermal integrity of building envelopes. In order to investigate the implementation of such diagnostic procedures the GSA had the National Bureau of Standards (NBS) develop a multi-phased research effort. The first phase was devoted to the development of in-situ and nondestructive procedures that the GSA could use to evaluate the thermal integrity of building envelopes. This effort was developed under guidelines of a peer reiew group consisting of representatives from the GSA, the Departments of Defense, Housing and Urban Development and Energy, and Public Works of Canada, and resulted in a report which addresses measurement techniques, inspection procedures and data anlaysis procedures [1].

In Phase II of the project, reported on in this document, the diagnostic procedures developed in Phase I were applied to eight federal buildings located throughout the United States. This group of buildings includes four large buildings (over 100,000 square feet) and four small buildings (less than 100,000 square feet), all of relatively recent construction. The eight buildings, located in a range of climates, include:

Large	Small
Anchorage, AK	Ann Arbor, MI
Columbia, SC	Fayetteville, AR
Norfolk, VA	Huron, SD
Springfield, MA	Pittsfield, MA

All of the buildings, except the Fayetteville building, were constructed after the GSA energy guidelines were in effect.

Seven different diagnostic techniques were applied to all or some of the buildings in order to locate and/or quantify deficiencies in the thermal integrity of the building envelopes. The techniques were applied by NBS personnel or by subcontractors and include the following:

Ground-based infrared thermography for locating thermal defects in the envelope.
Aerial infrared thermography for locating defects in roof systems.

Spot radiometry for locating and quantifying thermal defects.
Tracer gas measurements of infiltration and ventilation rates.
Pressurization testing for measuring envelope airtightness.
Heat flow meters and portable calorimeters for measuring wall thermal conductance and quantifying the effects of thermal bridges.

These diagnostic techniques performed well in locating and quantifying the defects in the thermal integrity of the eight building envelopes. The results of the application of each technique are summarized below.

Ground-Based Infrared Thermography

Though seven of these eight federal office buildings were built to the new federal energy guidelines, thermographic inspection revealed serious defects in each building. Thermal defects in the insulation system were observed to be in the range of 6 to 18 percent of the wall areas of these buildings. Leakage around windows and seams were observed in all buildings. Other thermal anomalies found in these buildings included missing insulation in the wall, thermal bridges, defective ceiling and floor insulation, and convection within insulation. Buildings with overhangs and indentations appeared to have severe problems in those areas.

Thermographic inspections performed on commercial buildings are capable of determining the thermal integrity of the building envelopes and detecting defects in the mechanical system. For new buildings, thermography can be used for quality control during construction. Had such inspections been done on these buildings, most of the observed defects could have been corrected at no cost to the building owner. After buildings are occupied, thermographic inspections can still identify degradation of materials and locations of poor performance of building envelopes. However, correction of these defects at this stage are costly and only justified in extreme cases.

Aerial-Based Infrared Thermography

The quality of the aerial thermographic surveys produced by the three private contractors indicated that aerial thermographic surveys can yield information from which roof damage can be assessed. For detection of roof anomalies on single buildings, the economic benefits of aerial thermography have not been determined. For the multi-building complex or large areas, aerial surveys have shown that many buildings can be evaluated by flyovers. Since it is necessary to follow-up with walk-on inspections, the cost factors for also conducting the aerial survey may not be justifiable. On the other hand, the demonstration that all thermal roof problems on a building can be detected without an aerial survey should be undertaken. If proven, cost savings by elimination of the aerial study may then be realized.

Roof anomalies revealed through aerial infrared surveys are often not related to deficiencies resulting from the roofing system. Instead, they are attributable to building system components or equipment. The analysis of such sources requires building and roof inspections by experienced and/or trained staff.

Roof-top level inspections with infrared equipment were required to define potential deficiencies. Other testing, such as core-sampling or water content measurements in thermal insulation by destructive means was recommended by contractors for evaluation of the extent of deterioration.

Thermography did not prove to be a useful tool for inspecting the inverted membrane roof of the Anchorage federal building. It helped to detect the beginning of water damage to a section of the roof of the federal building in Columbia, SC. The repair of this area before extensive damage is done would prevent the need for replacement of the roof system at a later date.

Spot Radiometry

Results from spot radiometer inspections performed on two office buildings indicated there were larger errors in the results for surface components of high R-values than those of low R-values. This may be due to the sensitivity of the instrument as well as inappropriateness of the steady state assumption used to derive the equations used for calculations. However, the thermal resistance values provided qualitative indications of the surface's thermal performance, though the absolute measurements lacked accuracy. Due to the simplicity and portability of the spot radiometer, it can be used to qualitatively evaluate regions of building envelope components.

Tracer Gas Measurements of Infiltration and Ventilation

The average natural air infiltration rates measured in these buildings varied from 0.2 air changes per hour for the Huron federal building to 0.70 air changes per hour for the Ann Arbor federal building. The infiltration component of the design heating load from these buildings ranged from 23% for the uninsulated Fayetteville federal building to 61% for the new Springfield federal building. In four of the buildings air infiltration contributed to over 50% of the heating loads. Two of the federal buildings, Anchorage and Huron, have low air infiltration rates (0.28 and 0.20 air changes per hour). However, even for these buildings air infiltration was a very important part of the heating load.

Ventilation rates under occupied conditions were also measured in the eight buildings. It was found that for hot and cold outside temperatures, the buildings are operated at minimum ventilation levels to reduce space conditioning loads. At mild temperatures, outside air is used to cool the buildings and the ventilation rates increases significantly. The minimum ventilation rates show little temperature dependence in most of the buildings, but some of the buildings exhibit a dependence on wind speed. When the minimum ventilation rates did vary with weather conditions, this implied that uncontrolled air leakage or weather induced infiltration is a significant portion of the net ventilation rate. In most of the buildings, the summer and winter minimum ventilation rates are similar, but in some buildings there is a notable difference between the two minimum ventilation rates. The minimum ventilation rates were compared to minimum outside air intake levels suggested by ASHRAE, and it was found that most of the buildings were operated very close to or below the ASHRAE recommendation. Two of the buildings were operated well below this recommended ventilation rate. Local variations in air distribution and problems of ventilation efficiency can lead to effective ventilation rates in specific areas of a

building which are significantly lower than the average rate for the building. Three of the buildings, Springfield, Ann Arbor and Columbia, had minimum ventilation rates from 20 to 50% more than required, thus wasting energy during periods of extreme weather.

Pressurization Testing of Airtightness

As part of this project, the airtightness of the envelopes were evaluated using pressurization techniques. Seven of the buildings were subjected to whole building pressurization tests and were found to possess airtightness levels similar to tight houses in units of exchanges per hour at an induced pressure difference. The airtightness of the buildings in units of flow per envelope area were generally higher than for tight houses due to the low surface to volume ratios of the federal buildings. Therefore, the airtightness in exchanges per hour from the pressurization tests provides a misleading indication of the federal buildings' airtightness. A small number of windows in six of the buildings were pressure tested individually, and while a wide range of leakiness levels was evident, they were generally leakier than a common window tightness standard. The fraction of total building leakage associated with windows was calculated to be about 10 to 20%, a percentage similar to that found in houses. The large building infiltration model of Shaw and Tamura was applied to the seven buildings which were pressure tested, and the predictions were lower than the infiltration rates measured with tracer gas.

Thermal Resistance Measurements

Reliable thermal resistance values of building envelopes can be derived from in-situ measurements of indoor-to-outdoor air temperature differences and of heat flow across test structures, provided that the measurements are carried out over a sufficiently long period. A measurement period of at least two days is recommended, but an entire week of data collection is advisable when possible. Both the heat flow meters and the portable calorimeter were found to be useful tools for measuring heat flow through large, non-homogeneous building assemblies in the field. Wall thermal resistances derived from data obtained using a portable calorimeter yield lower values than those obtained with heat flow meters. This difference is attributed to the additional heat flow through highly conductive framing members in the structure. The thermal resistance values of masonry exterior walls of seven of the buildings was found to vary widely, from approximately 8 to 39 ft^2-h-^oF/Btu (2 to 7 m^2-K/W). The measured thermal resistances deviated from the design thermal resistances by an average of 14%, the worst case being 45%.

Heat Losses Due to Thermal Bridges

The inspection of the exterior envelope of four federal office buildings using infrared thermography revealed the existence of thermal bridges. The measurement of the heat flow through these thermal bridges using heat flow meters showed that the heat flux at the thermal bridges were from 62 to 118% greater than the heat flux through the insulated sections of the walls. Examination of thermograms and architectural drawings showed that the thermal bridges represented from 9 to 18% of the buildings insulated wall areas. Therefore, the thermal bridges increased the wall heat loss by approximately 10 to 21% relative to the same wall structure without thermal

bridges. A two-dimensional finite difference heat flow model was used to simulate the transient response of the thermal bridge representing an exterior wall/intermediate floor system. At points at which heat flow measurements could be made, the model predicted the measured heat flux well. Moreover, the model predicted even higher heat fluxes at other points on the thermal bridge where measurements could not be made. Therefore, the total contribution of thermal bridges to heat loss is probably even greater, perhaps by a factor of two, than that cited above. Additional experimental work is needed to confirm this possibility.

A brief summary of the findings of the diagnostic testing of each federal office building follows:

Anchorage

The Anchorage federal building uses about 28,500 Btu/yr·ft^2 (89.8 kWh/yr-m^2) for space heating. This is a well constructed building which is tight and well insulated - though air infiltration accounts for over 55% of the building load. The major defect is the thermal bridging resulting from the manner in which the precast panels were suspended (increasing the wall heat loss by about 20%). The wall area in the section above the suspended ceiling was not insulated to the same level as the wall area below the suspended ceilings. This was done by design; however, it is not justifiable from a heat transfer point of view. Visual inspection of the roof showed many areas with separations and fissures in the rigid insulation; however, limited heat flow measurement did not detect a serious reduction in thermal resistance in the roof insulation system. During the extreme winter conditions, this building is often operated with closed dampers during occupied periods and has ventilation rates which are only 39% of those recommended by the ASHRAE ventilation standard for a building with smokers.

Ann Arbor

This building is a very poor energy performer. It is consuming about 132,000 Btu/yr·ft^2 (416 kWh/yr-m^2) for space heating. It has a high air infiltration rate of about 0.7 air changes per hour, which accounts for about 48% of the building heating load. The building has over 14,000 ft^2 (1,300 m^2) of glass area which contributes to about 26% of the heat load. The opaque walls constitute 18% of the heat load and the roof about 8%. About 18% of the wall area showed thermal defects when inspected by thermography. The thermal resistances of the wall section were close to the predicted values when the insulation was properly installed. The design of the building resulted in thermal bridging which increased the wall heat loss by about 8%.

Columbia

The Columbia federal building uses about 20,035 Btu/yr·ft^2 (63.1 kWh/yr-m^2) of energy for space heating. Air infiltration accounts for about 52% of the space heating load (0.4 air changes per hour). Air conditioning accounts for about 23% of the electrical energy use of the building. The building has operable windows which are quite leaky and which account for about 31% of the building leakage. About 17% of the wall area of the building has thermal defects, the most serious of which was air penetration

around the insulation. This was caused by the manner in which the steel framing was installed in the building; an approximately one inch gap was left between the exterior concrete panels and the framing, and the insulation was hung in the framing cavaties. The building also had thermal bridging which increased the heat flow through the wall by about 10%. The manner in which the insulation was installed in the wall area about the suspended ceiling was incorrect, allowing air movement through the insulation and leaving exposed exterior wall uninsulated. The minimum ventilation rate of this building was 51% above that required for an office building with smokers, thus adding to the space conditioning loads in extreme weather conditions.

Fayetteville

The Fayetteville federal building uses about 30,000 Btu/ft^2·yr (94.5 kWh/yr-m^2) for space heating. It is basically an uninsulated building built before the federal energy conservation guidelines were developed. In terms of energy use per unit floor area per degree day it is the second worst performer. The space heating load consists of 48% transmission through the opaque walls, 25% through the glass, 23% by air infiltration (0.33 air changes per hour) and 3% through the roof. The major deficiency of the building is the existence of large, uninsulated wall areas including large sections of spandrel glass. The building has serious leakage problems at the interface of the glass and spandrel walls and the structural columns. The first and fourth floors have serious leakage in the overhangs in the return air plenum. The building has adequate minimum ventilation; however, the ventilation rate is strongly wind dependent, indicating that much of the ventilation is being supplied by air leakage and not through the outside air supply ducts.

Huron

The Huron federal building used 21,514 Btu/ft^2·yr (67.8 kWh/yr-m^2) for space heating. This building is the tightest building of the eight tested, having an air infiltration rate of 0.2 air changes per hour. The space heating load consists of 19% transmission through the glass area, 31% through the opaque wall areas, 17% through the roof and 33% by air infiltration. The framing members of the opaque wall increased the heat flow by about 30% above the design value of the insulation. Thermal bridging at the floor/wall interface caused another 10% increase in heat flow through the opaque wall areas. The minimum ventilation rate of this building was only 26% of the minimum requirements for a building with smokers.

Norfolk

The Norfolk federal building uses about 10,588 Btu/ft^2·yr (33.4 kWh/yr-m^2) of electricity (on-site) for space heating. The building heat loss consists of 27% transmission through the glass areas, 15% through the opaque wall areas, 6% through the roof and 15% by air infiltration (0.52 air changes per hour). The building had serious defects in the insulation in the overhangs over the garage and front entrance. The thermal resistance of the insulated walls was only 54% of the predicted values. The minimum ventilation rate was 90% of that recommended for an office building with smokers.

Pittsfield

The federal building in Pittsfield, MA uses about 51,200 Btu/ft^2· (161 kWh/yr-m^2) for space heating. The largest component of the heat load is air infiltration, accounting for 36% of the load (0.3 air changes per hour). The opaque walls contribute about 22% of the heat transmission, the roof 21% and the glass area 19%. The minimum ventilation rate of the building is 90% of the requirement for a building with smokers. Thermography showed that about 18% of the exterior wall area had defects, the most serious being air penetration around the insulation. The measured thermal resistance of the walls was about 13% less than the predicted thermal resistance.

Springfield

The Springfield federal building was a newly constructed office building and therefore there were no previous fuel records for the building. Twenty-three percent of the heat loss of the building is due to transmission through the glass areas, 11% through the opaque wall areas, 5% through the roof and 61% by air infiltration (0.52 air changes per hour). The insulation of the exterior walls consist of rigid foam insulation applied to the concrete panels in such a way that air could leak around the insulation and into the air cavity between the steel framing. The effective thermal resistance of this wall construction was only 52% of the predicted value. The ventilation and air infiltration rates of the building had a strong temperature dependence which could be due to the leakiness of the building or a ventilation system control problem.

Acknowledgments

The authors wish to express their appreciation to Erma Striner and David Eakin of the Public Building Service of the General Services Administration for guidance and assistance throughout the project. The GSA staff at the test sites also provided invaluable assistance in this project and the authors acknowledge the following personnel: Anchorage - Building Managers, Jesse Avila and Jack Froiland, Building Engineers, Paul Zinn and Wes Young; Ann Arbor - Building Manager, Nils Strand, Building Engineer, Bob Yeoman; Columbia - Building Managers, Jack Terry and Herb Drakeford; Fayetteville - Building Manager, Neil Rogers, Building Engineer, Ken Collier; Huron - Building Manager, George Green, Building Engineers, James Round and Raul Rios; Norfolk - Building Managers, Thomas Coulbourne and Lee Smith, Building Engineer, Ed Akins; Pittsfield - Building Manager, Eugene Raymond, Building Engineer, Allen Creel; Springfield - Building Manager, Philip Haddad, Building Construction Engineer, Steve Mastoyin, Building Engineer, Richard McCorkindale. The assistance of Doug Pruitt and Samuel Silberstein of NBS was also instrumental in the completion of this project, along with the efforts of Phil Engers, Charlene Frith, Pat Lane, Jay Murphy, and Steven Schweinfurth. Very special thanks are expressed to Robin Bickel for her efforts in preparing this report.

Preface

This work was sponsored by the Public Building Service of the General Services Administration through an interagency agreement with the National Bureau of Standards, Interagency Agreement No. PBS-80-1.

Table of Contents

List of Figures

List of Tables

1. INTRODUCTION

The federal government presently owns and leases thousands of buildings throughout the United States. The General Services Administration (GSA) constructs new buildings each year, some of which have thermal defects in the building envelopes due to either poor workmanship or a misunderstanding of the construction specifications. A strong need exists for viable, in situ and nondestructive survey techniques to verify the thermal integrity of the envelope systems of office buildings under construction. In this way, thermal defects can be identified and located, and the contractor can carry out remedial action prior to departure from the construction site. All buildings degrade with age and require periodic maintenance. The potential causes of serious deterioration in the building often produce thermal anomalies long before serious damage has occurred. The detection of these anomalies can lead to corrective action before more costly repairs are required. Areas where thermal anomalies occur can also lead to poor thermal comfort and cause adverse reactions from the building occupants. In order to develop a diagnostic program for assessing the thermal performance of federal office buildings, GSA and NBS developed a two-phase project to identify and assess existing measurement methods which could be implemented by GSA using either government employees or private sector contractors.

Phase I

In phase I, a technical report entitled "Measurement Methods for Evaluation of Thermal Integrity of Building Envelopes", NBSIR 82-2605 was prepared [1]. This report reviewed the technical methods which could be used to assess the integrity of the exterior envelopes of Federal buildings. The inspection techniques considered were: ground-based infrared thermographic surveys, aerial infrared surveys; tracer gas air infiltration measurement; pressurization tests for measuring building envelope tightness; and spot radiometer measurements (both the temperature measuring and radiosity-measuring types) for detecting gross defects. Heat flow meters, a portable calorimeter and an envelope thermal testing unit developed by Lawrence Berkeley Laboratories were also considered for determining the thermal characteristics of the envelope.

The techniques described in the phase I report could be used to find, locate and assess the heat loss resulting from the following deficiencies:

1) uninsulated walls
2) uninsulated ceilings/roofs
3) partially insulated areas
4) air leakage
5) heat loss at joints
6) thermal by-passes
7) below-grade heat loss
8) thermal bridges
9) wet insulation
10) shrinkage in foam insulation
11) settling of loose-fill insulation
12) air movement around vapor barriers

In addition to locating deficiencies, the techniques could be used to quantify heat losses, to determine the extent of deterioration, and to suggest remedial action. They are applicable to both new and existing buildings, although the manner in which they are applied will differ.

A common presentation format was adopted to describe the required method, equipment and instrumentation; wherever applicable the information was organized as follows:

Summary
Description of Equipment
Theory
Guidelines for Conducting Measurements
Interpretation of Results
Accuracy of Techniques
Availability of Equipment and Services
Previous Usage
Personnel Training Requirements
Program Application Restrictions

Phase II

The methods described in the phase I first report had not previously been applied systematically to office buildings. Phase II was designed to assess the usefulness of various diagnostic procedures described in the phase I report by having the National Bureau of Standards perform a series of the tests on eight Federal office buildings during the period from September 1982 to August 1983. The buildings were located in Anchorage, AK, Columbia, SC, Norfolk, VA, Springfield, MA, Pittsfield, MA, Huron, SD, Ann Arbor, MI, and Fayetteville, AR. The tests which were performed on these buildings consisted of: fan pressurization to assess the tightness of the building envelope, tracer gas measurements of the natural air infiltration rates and ventilation rates of the buildings, ground-based infrared thermography, aerial thermography, inspection of the buildings with spot radiometers, determination of the thermal conductance or U-value using heat flow meters and a portable calorimeter, and leakage testing of the components of the building. Table 1.1 gives a schedule of the tests performed. A detailed technical description of these tests methods can be found in the report of the first phase of this project [1].

It was originally intended to analyze the costs of the tests and appropriate retrofit procedures and of the expected energy savings in order to develop an economic evaluation of the benefits of the diagnostic techniques. However, an insufficient amount of data was available. It does not appear that such a diagnostic and retrofit approach is economical in existing buildings due to the expense of repairs in existing buildings. Such a diagnostic program probably makes sense in new buildings before they are finished-off and the contractor has left the site.

Chapter 2 of this report describes the eight federal office buildings evaluated. The data presented in this chapter include the building dimensions, the designed thermal parameters of the building envelopes, pertinent characteristics of the building HVAC systems and the energy used in the fiscal year 1981.

Table 1.1 Schedule of Tests

	Inspection Visit	Tracer Air Infiltration	Fan Pressurization	Component Pressurization	Ground Thermography	Aerial Thermography	Spot Radiometer Inspection	Thermal U-Value
Anchorage	8-82	9-82 1-83 5-83	9-82	5-83	1-83	5-83	-	5-83
Ann Arbor	4-82	10-82 2-83 5-83	10-82	5-83	2-83	-	3-83	2-83
Columbia	8-82	11-82 1-83 5-83 8-83	11-82 5-83	5-83	1-83	3-83	-	2-83
Fayetteville	8-82	11-82 2-83 6-83	11-82	6-83	3-83	-	-	-
Huron	8-82	10-82 1-83 6-83	10-82	-	-	-	3-83	3-83
Norfolk	8-82	10-82 1-83 5-83 8-83	10-82	5-83	1-83	-	-	2-83
Pittsfield	8-82	10-82 2-83 6-83	10-82	6-83	2-83	-	-	3-83
Springfield	8-82	11-82 2-83 6-83	11-82	-	2-83	3-83	-	3-83

Chapter 3 describes the results of ground infrared thermographic inspection of the buildings. Both interior and exterior thermographic inspections were performed by NBS staff members. These inspections were performed using both short wavelength (2-5 micron) and long wavelength (8-12 micron) imaging systems. Sample thermograms for each building are given, indicating the major deficiencies found. The thermographic data were analyzed to produce a classification of the types of defects located and the area of the exterior envelope affected by the defects.

Chapter 4 discusses the results of the aerial infrared thermographic inspections performed by private contractors on three of the large office buildings. The purpose of the aerial infrared inspections were to assess the integrity of the building roofs. Two of the inspections were performed using infrared imaging systems from helicopters, the third was performed using a line scanner from a fixed wing aircraft. The two contractors who used imaging systems also inspected the roofs by a walk-on procedure.

Chapter 5 presents the results of an audit of two small office buildings performed by two private contractors using spot radiometers. These contractors used the spot radiometers to estimate the thermal resistance (R-value) of the building envelope. These results are compared with the building specifications.

In Chapter 6 the results of the air infiltration and ventilation measurements using a tracer gas are given. Sampling and injection tubing were installed in the fall of 1982 and an automatic air infiltration monitor previously designed by NBS was used to measure the air infiltration and ventilation rates during each of the major climatic seasons (three automated air infiltration systems were used on this project). The data are analyzed to determine average air infiltration and ventilation rates for the buildings, the weather dependence of the air infiltration and ventilation rates, the minimum ventilation rates experienced by the buildings and the influence of air infiltration on the building's thermal performance.

Chapter 7 describes the results of the building tightness tests using fan pressurization. Whole building pressurization tests were performed on seven of the federal office buildings using the building HVAC fans. The results of these tests are compared to the results of the air infiltration tests using a tracer gas. The results of component pressurization tests are also presented and the importance of windows on the tightness of the building envelope is assessed. A comparison is made between predicted infiltration rates, based on a model which uses the results of the building tightness tests, and measured air infiltration rates.

Chapter 8 gives the results of the measurement of the thermal resistance of the building envelopes. These tests were performed using both heat flow meters and portable calorimeters and a micro-computer for recording the data. Two such systems were deployed to measure the thermal resistance of sections of the exterior envelope of seven of the buildings.

Chapter 9 gives a quantitative estimate of the importance of thermal bridges on the performance of the building insulation system. Thermal bridges were detected in four of the office buildings during the thermographic inspection. An analysis of the thermographic data and the

results of heat flow meter tests are used to calculate the increase in heat flow due to the thermal bridging.

Chapter 10 presents a summary of the results of the diagnostic tests. A comparison is made between the results of the diagnostic tests and the energy used by the buildings.

This report contains three appendices. In Appendix A, a methodology is presented for assessing the economics of diagnostic measurements. Appendices B and C give the specifications used by NBS for procuring the services of private contractors for performing audits using spot radiometers and aerial infrared thermographic inspections. These serve as models of specifications for procuring the services of private contractors for the other measurement methods.

2. Building Descriptions

The eight federal office buildings are located in the cities shown in the map in figure 2.1. In general these are new buildings (less than three years old), designed to the GSA energy guidelines of less than 55,000 Btu/ft^2 (630 MJ/m^2) per year of on-site energy and less than 100,000 Btu/ft^2 (1,100 MJ/m^2) per year of off-site energy. The building in Fayetteville, AR is about ten years old and was built before these energy guidelines for new federal office buildings were in effect. Though these buildings tend to perform better than most existing federal office buildings, none has met the energy guidelines during its first few years of occupancy. However, the guidelines were not intended for energy use prediction, but to influence the design process. In addition, the guideline makes no distinction between the actual building and a generic building with features including ten hour a day, five day a week occupancy, no food service, no computer space and no site lighting.

For the purpose of this study the buildings in Anchorage, AK; Springfield, MA; Norfolk, VA; and Columbia, SC are considered large office buildings (over 100,000 ft^2 (92,900 m^2) of occupiable floor area). Columbia is 15 stories high, Norfolk 8 stories, Anchorage between two and six depending on the module, and Springfield five stories. The buildings in Pittsfield, MA; Huron, SD; Ann Arbor, MI; and Fayetteville, AR are considered small office buildings (less than 100,000 ft^2 (92,900 m^2) of floor area). These small office buildings range in height from two to five stories. Schematic diagrams and a photograph of each building are given in figures 2.2 through 2.9.

All but two of the buildings have variable volume air handlers in the major zones of the buildings. They are all heated by perimeter heating systems, which are generally hydronic. The building in Columbia has two perimeter heating systems. In the Norfolk building, heaters and air conditioners have been added to the air system on floors which have proved difficult to heat and cool. They all have central chiller systems for cooling the core spaces of the buildings. The buildings in Anchorage and Springfield have underground garages. The Norfolk building has an exterior garage. The physical dimensions of the buildings are given in Table 2.1.

The characteristics of the exterior walls of the buildings are summarized in Table 2.2. The buildings have masonry type construction of the wall systems, though the manner in which the insulation was applied varied. All of the buildings have insulating glass windows. Table 2.3 describes the construction of the roof systems for each building. A summary of the thermal properties of the building envelopes (above grade) is given for each building in Tables 2.4 to 2.11. The effective design thermal resistance R_{eff} of the walls varies from 17.2 F·ft^2·hr/Btu (3.0 m^2·K/watt) for the Anchorage federal building to 3.2 F·ft^2·hr/Btu (0.6 m^2·K/watt) for the Fayetteville federal building. The effective design thermal resistance of the roofs varies from 9.6 F·ft^2·hr/Btu (1.7 m^2·K/watt) for the Ann Arbor federal building to 26.3 F·ft^2·hr/Btu (4.6 m^2·K/watt) for the Fayetteville federal building. The total envelope conductive resistance varies from 3.5 F·ft^2·hr/Btu (0.6 m^2·K/watt) for the Fayetteville federal building to 9.4 F·ft^2·hr/Btu (1.7 m^2·K/Watt) for the Anchorage federal building.

Descriptions of the HVAC systems are given in Tables 2.10 to 2.19. The mechanisms for controlling outside air intake vary among the eight buildings. In most buildings, outside air intake is kept to a minimum when the building is being heated or cooled in order to reduce the space conditioning load. During mild weather, outside air is often used to cool the building. The amount of outside air intake, and the times when outside air intake is increased, are controlled by a variety of schemes. An economizer control uses the outside temperature to determine when outside air should be used for cooling. Enthalpy control uses indoor and outdoor humidity levels in addition to temperature. The amount of outside air intake for cooling is generally determined by a control system which compares the discharge or return air temperature to some temperature setting. The ventilation control strategies and the air handling systems in each building are outlined below, along with other information on mechanical systems and the zoning of the buildings.

The Anchorage building is divided into six modules, (each with its own ventilation system) which are connected by an open lobby/atrium and communicate freely. Anchorage is the only building without return fans. The mechanical systems are computer controlled and use a minimum of outside air during the heating season. During warmer weather, outside air is used to cool the building, with the outside air intake level determined by the supply air temperature.

In Ann Arbor, the building's main mechanical system serves most of the building with separate systems for the lobby and post office. The outside air intake is based on the outside air temperature (an economizer), and the amount of outside air intake is controlled by the return air temperature.

Columbia has a single mechanical system for floors two through fifteen and separate systems for the lobby and the first floor/basement zones. The mechanical system is controlled by a computer and uses an enthalpy controller to determine outside air intake levels.

There are two fan systems on each of the five floors of the Fayetteville building with an additional system for the courtroom on the fifth floor. The outside air intake is controlled manually by the building operator.

The Huron building has two mechanical systems, one for the north zone and another for the south zone. On each floor, the north and south zones are open to each other. The outside air intake is based on enthalpy control.

Norfolk has one mechanical system for most of the building, and a smaller system for the lobby area. The main HVAC system uses enthalpy control to regulate the outside air intake.

The Pittsfield building has a separate fan system for each of its two floors. The outside temperature is used to determine whether outside air can be used to cool the building.

There are three fan systems in the Springfield building, one each for the north zone, the south zone and the lobby/atrium. The outside air dampers are adjusted to maintain a supply air temperature of about 13°C (55°F) during the entire year. Thus, outside air is used to condition the

building unless the outside temperature is below the supply air temperature setting.

Table 2.20 gives the average degree days for each site. These vary from 2567 F·Days (1426 C·Days) for Columbia, SC to 10,804 F·Days (6035 C·Days) for Anchorage, AK. The fuel records for fiscal year 1981 are given in Tables 2.21 to 2.27 for seven of the buildings. The Springfield federal building had no previous fuel records since it was a new building. The summer months are those with an insignificant amount of heating. Table 2.28 gives an estimate of the electrical base load and summer excess load for each building (approximate air conditioning load). Note that the base load contributed from 67% to 92% of the electric usage of the building, while the air conditioning loads were from 5% to 23% of the electric usage.

Table 2.29 gives a summary of the energy used for space heating per floor area per degree day for each building. This varied from 2.6 Btu/F·day·ft^2 (0.35 KW/(K·m^2)) for the Huron federal building to 11.9 Btu/F·day·ft^2 (1.62 KW/(K·m^2)) for the Ann Arbor federal building. The values in Table 2.29 give a relative measure of the energy performance of each building.

Table 2.1

Building Dimensions

	Conditioned Volume ft^3	Conditioned Volume (m^3)	Rentable Floor Area ft^2	Rentable Floor Area (m^2)
Anchorage	6,140,000	(174,000)	490,000	(45,500)
Ann Arbor	1,120,000	(31,700)	52,700	(4,900)
Columbia: Tower	4,420,000	(125,000)	216,000	(20,100)
Only				
Total	5,610,000	(159,000)	266,000	(24,700)
Fayetteville	751,000	(21,300)	36,600	(3,400)
Huron	972,000	(27,500)	69,100	(6,420)
Norfolk	2,130,000	(60,300)	186,000	(17,300)
Pittsfield	301,000	(8,520)	18,600	(1,730)
Springfield	2,040,000	(57,700)	146,000	(13,500)

	Total Floor Area ft^2	Total Floor Area (m^2)	Exterior Envelope Area ft^2	Exterior Envelope Area (m^2)
Anchorage	522,000	(48,500)	248,000	(23,000)
Ann Arbor	56,700	(5,270)	71,400	(6,630)
Columbia: Tower	223,000	(20,700)	149,000	(13,800)
Only				
Total	286,000	(26,600)	213,000	(19,800)
Fayetteville	39,400	(3,600)	52,400	(4,830)
Huron	74,400	(6,910)	71,300	(6,620)
Norfolk	200,000	(18,600)	130,000	(12,100)
Pittsfield	20,000	(1,860)	24,800	(2,300)
Springfield	157,000	(14,600)	96,200	(8,940)

Table 2.2

Description of Typical Exterior Walls of Each Building

Building Location	No. of Modules	No. of Stories	Typical Wall Construction
Anchorage	6	2-6	Precast concrete panel, semi-rigid glass fiber insulation board, gypsum wallboard on metal studs.
Ann Arbor	1	4	Quarry tile, metal lath and mortar bed, semi-rigid glass fiber insulation board, acoustic wall panel.
Columbia	2	2,15	Granite siding, concrete, glass fiber blanket insulation, gypsum wallboard.
Fayetteville	1	5	Face brick, concrete block.
Huron	1	4	Face brick, lightweight concrete masonry unit, semi-rigid glass fiber insulation board, gypsum wallboard.
Norfolk	1	8	Face brick, air space, gypsum board sheathing, glass fiber blanket insulation, gypsum wallboard.
Pittsfield	1	2	Face brick, semi-rigid glass fiber insulation board, brick.
Springfield	1	5	Precast concrete panel, semi-rigid glass fiber insulation board, gypsum wallboard on metal studs.

Table 2.3

Description of the Roof Insulation Systems

Anchorage	Protected membrane - concrete pavers, 3 in. (7.6 cm) rigid foam insulation, membrane, 6 in. (15.2 cm) concrete.
Ann Arbor	Built-up roof membrane, 1-1/2 in. (3.8 cm) rigid insulation on 1-1/2 in. (3.8 cm) x 20 ga. composite concrete and steel deck.
Columbia	Built-up roof membrane 2 in. (5.1 cm) rigid insulation, 3 in. (7.6 cm) lightweight concrete, 6 in. (15.2 cm) structural concrete.
Fayetteville	Built-up roof membrane 4 in. (10.2 cm) lightweight insulating concrete, 2 in. (5.1 cm) insulation board.
Huron	Built-up roof membrane 3 in. (7.6 cm) rigid insulation, 2 in. (5.1 cm) concrete.
Norfolk	Built-up roof membrane 4 in. (10.2 cm) built-up roof membrane, 1/2 in. (1.3 cm) plywood, 2 in. (5.1 cm) rigid insulation, 5-1/2 in. (14.0 cm) concrete slab on steel roof deck.
Pittsfield	Built-up roof membrane 3/4 in. (1.9 cm) built-up roof membrane, 2-1/2 in. (6.4 cm) rigid insulation (R-20), concrete slab on 1-1/2 in. (3.8 cm) x 20 ga. steel deck.
Springfield	Built-up roof membrane, rigid insulation (R-14), metal deck.

Table 2.4

Thermal Characteristics of Building Envelope
for Anchorage, AK Federal Building

	Area		Design Transmission Loss		Effective Resistance R_{eff}	
	ft^2	(m^2)	Btu/F·hr	(W/K)	$F \cdot ft^2 \cdot hr/Btu$	($m^2 \cdot K/W$)
Opaque Wall	98,932	(9,191)	5,736	(3,023)	17.2	(3.0)
Glass	35,154	(3,266)	14,648	(7,719)	2.4	(0.4)
Roof	112,228	(10,426)	5,754	(3,032)	19.5	(3.4)
Total	246,314	(22,883)	26,138	(13,775)	9.4	(1.7)

Table 2.5

Thermal Characteristics of Building Envelope for
Ann Arbor, MI Federal Building

	Area		Design Transmission Loss		Effective Resistance R_{eff}	
	ft^2	(m^2)	Btu/F·hr	(W/K)	$F \cdot ft^2 \cdot hr/Btu$	($m^2 \cdot K/W$)
Opaque Wall	26,776	(2,487)	5,424	(2,858)	4.9	(0.9)
Glass	14,487	(1,346)	7,968	(4,199)	1.8	(0.3)
Roof	24,062	(2,235)	2,499	(1,317)	9.6	(1.7)
Total	65,325	(6,069)	15,891	(8,375)	4.1	(0.7)

Table 2.6

Thermal Characteristics of Building Envelope for Columbia, SC Federal Building

	Area		Design Transmission Loss		Effective Resistance R_{eff}	
	ft^2	(m^2)	Btu/F·hr	(W/K)	$F \cdot ft^2 \cdot hr/Btu$	$(m^2 \cdot K/W)$
Tower						
Opaque Wall	103,412	(9,607)	8,667	(4,568)	11.9	(2.1)
Glass	16,091	(1,494)	15,527	(8,183)	1.0	(0.2)
Roof	23,336	(2,168)	1,553	(818)	15.2	(2.7)
Total	142,839	(13,270)	25,747	(13,569)	5.5	(1.0)
Courthouse						
Opaque Wall	22,478	(2,088)	3,313	(1,746)	6.8	(1.2)
Glass	6,132	(570)	5,917	(3,118)	1.0	(0.2)
Roof	35,455	(3,294)	2,832	(1,492)	12.5	(2.2)
Total	64,065	(5,952)	12,062	(6,356)	5.3	(0.9)
Volume						
Tower	4.42×10^6 ft^3		$(1.25 \times 10^5$ $m^3)$			
Courthouse	1.19×10^6 ft^3		$(3.36 \times 10^4$ $m^3)$			

Table 2.7

Thermal Characteristics of Building Envelope for Fayetteville, AR Federal Building

	Area		Design Transmission Loss		Effective Resistance R_{eff}	
	ft^2	(m^2)	Btu/F·hr	(W/K)	$F \cdot ft^2 \cdot hr/Btu$	$(m^2 \cdot K/W)$
Opaque Wall	29,737	(2,763)	9,306	(4,904)	3.2	(0.6)
Glass	8,837	(821)	4,684	(2,468)	1.9	(0.3)
Roof	13,402	(1,245)	509	(268)	26.3	(4.6)
Total	51,976	(4,829)	14,499	(7,641)	3.5	(0.6)

Table 2.8

Thermal Characteristics of Building Envelope for Huron, SD Federal Building

	Area		Design Transmission Loss		Effective Resistance R_{eff}	
	ft^2	(m^2)	Btu/F·hr	(W/K)	F·ft^2·hr/Btu	(m^2·K/W)
Opaque wall	36,003	(3,344)	3,071	(1,618)	11.7	(2.1)
Glass	4,853	(451)	1,990	(1,048)	2.4	(0.4)
Roof	20,989	(1,950)	1,733	(388)	12.1	(2.1)
Total	61,845	(5,745)	6,794	(3,580)	9.1	(1.6)

Table 2.9

Thermal Characteriscs of Building Envelope for Norfolk, VA Federal Building

	Area		Design Transmission Loss		Effective Resistance R_{eff}	
	ft^2	(m^2)	Btu/F·hr	(W/K)	F·ft^2·hr/Btu	(m^2·K/W)
Opaque Wall	83,173	(7,726)	6,099	(3,214)	13.6	(2.4)
Glass	17,948	(1,667)	9,692	(5,108)	1.9	(0.3)
Roof	32,272	(2,998)	2,259	(1,190)	14.3	(2.5)
Total	133,393	(12,392)	18,050	(9,512)	7.4	(1.3)

Table 2.10

Thermal Characteristics of Building Envelope for Pittsfield, MA Federal Building

	Area		Design Transmission Loss		Effective Resistance R_{eff}	
	ft^2	(m^2)	Btu/F·hr	(W/K)	F·ft^2·hr/Btu	(m^2·K/W)
Opaque Wall	10,596	(984)	1,052	(554)	10.0	(1.8)
Glass	1,760	(164)	915	(482)	1.9	(0.3)
Roof	12,444	(1,156)	1,032	(544)	12.0	(2.1)
Total	24,800	(2,304)	2,999	(1,580)	8.3	(1.5)

Table 2.11

Thermal Characteristics of Building Envelope for Springfield, MA Federal Building

	Area		Design Transmission Loss		Effective Resistance R_{eff}	
	ft^2	(m^2)	Btu/F·hr	(W/K)	F·ft^2·hr/Btu	(m^2·K/W)
Opaque Wall	50,203	(4,664)	4,292	(2,261)	11.7	(2.1)
Glass	18,762	(1,743)	9,117	(4,805)	2.1	(0.4)
Roof	25,784	(2,395)	1,865	(982)	13.8	(2.4)
Total	94,749	(8,802	15,274	(8,049)	6.2	(1.1)

Table 2.12

Air Handler Characteristics of HVAC System for
Anchorage, AK Federal Building

	Fan Capacity cfm (m^3/s)	Volume Served ft^3 (m^3)	Type
Module A	31,500 (14.8)	567,000 (16,046)	VAV
Module B	32,800 (15.4)	661,000 (18,706)	VAV
Module C	63,000 (29.6)	1,108,000 (31,356)	VAV
Module D	51,600 (24.25)	987,000 (27,932)	VAV
Module E	50,100 (23.5)	1,100,000 (32,715)	VAV
Module F	61,200 (28.8)	1,100,000 (31,130)	VAV

VAV - variable volume system

Table 2.13

Air Handler Characteristics of HVAC System for
Ann Arbor, MI Federal Building

	Fan Capacity cfm (m^3/s)	Volume Served ft^3 (m^3)	Type
Floors 1 to 4 except Mail Room	56,000 (15.3)	919,000 (26,007)	VAV
Mail Room	8,300 (3.9)	153,900 (4,355)	CV
Lobby	4,050 (2.3)	47,900 (1,356)	CV

VAV - variable volume
CV - constant volume

Table 2.14

Air Handler Characteristics of HVAC System for
Columbia, SC Federal Building

	Fan Capacity cfm (m^3/s)	Volume Served ft^3 (m^3)	Type
Tower Core		2,575,000 (72,873)	
#1	106,000 (49.8)		VAV
#2	106,000 (49.8)		VAV
Tower Perimeter			
West	10,200 (4.8)	209,000 (5,915)	VAV
North, South, East	33,700 (15.8)	645,000 (18,254)	VAV
1st Floor & Basement	20,000 (9.4)	347,000 (9,820)	VAV
1st Floor Lobby	8,000 (3.8)	71,104 (2,012)	CV
Courthouse	75,000 (35.3)	1,039,000 (29,404)	VAV
Courthouse Lobby	10,000 (4.7)	76,000 (2,151)	CV

VAV - variable volume system
CV - constant volume system

Table 2.15

Air Handler Characteristics of HVAC System for
Fayetteville, AR Federal Building

	Fan Capacity cfm (m^3/s)	Volume Served ft^3 (m^3)	Type
1st Floor North	8,450 (4.0)	64,934 (1,838)	CV
1st Floor South	7,271 (3.4)	52,520 (1,486)	CV
2nd Floor North	5,290 (2.5)	63,984 (1,811)	CV
2st Floor South	6,278 (3.0)	63,607 (1,800)	CV
3rd Floor North	5,290 (2.5)	63,984 (1,811)	CV
3rd Floor South	6,278 (3.0)	63,607 (1,800)	CV
4th Floor North	4,818 (2.3)	61,956 (1,753)	CV
4th Floor South	5,750 (2.7)	64,237 (1,818)	CV
5th Floor North	6,648 (3.1)	81,018 (2,293)	CV
5th Floor South	9,515 (4.0)	93,582 (2,658)	CV
5th Floor Courtroom	4,200 (2.0	46,791 (1,324)	CV

CV - constant volume system

Table 2.16

Air Handler Characteristics of HVAC for
Huron, SD Federal Building

	Fan Capacity cfm (m^3/s)	Volume Served ft^3 (m^3)	Type
Zone 1 (North)	23,970 (11.3)	463,000 (13,103)	VAV
Zone 2 (East)	26,200 (12.3)	507,000 (14,348)	VAV

VAV - variable volume system

Table 2.17

Air Handler Characteristics of HVAC System for Norfolk, VA Federal Building

	Fan Capacity cfm (m^3/s)	Volume Served ft^3 (m^3)	Type
Floor 2 through 8	76,450 (35.9)	1,864,000 (52,751)	VAV
1st Floor	-	266,250 (7,535)	CV

Note: Heat two electric boilers ~ 300 KW each
Added 50 heaters to floors 1 through 4
Two chillers 200 tons and 125 tons

Table 2.18

Air Handler Characteristics of HVAC System for Pittsfield, MA Federal Building

	Fan Capacity cfm (m^3/s)	Volume Served ft^3 (m^3)	Type
1st Floor	6,900 (3.2)	154,295 (4,367)	VAV
2nd Floor	8,950 (4.2)	146,655 (4,150)	VAV

Table 2.19

Air Handler Characteristics of HVAC System for Springfield, MA Federal Building

	Fan Capacity cfm (m^3/s)	Volume Served ft^3 (m^3)	Type
North Zone	56,650 (2.6)	778,000 (22,018)	VAV
South Zone	35,650 (16.8)	495,000 (14,009)	VAV
Atrium	6,600 (3.1)	133,000 (3,764)	CV

VAV - variable volume system
CV - constant volume system

Table 2.20

Degree Days for Building Sites - Base 65°F (18.3°C)

	Degree Day - °F	(°C)
Anchorage, AK	10,864	(6,035)
Ann Arbor, MI	6,293	(3,496)
Columbia, SC	2,567	(1,426)
Fayetteville, AR	3,292	(1,829)
Huron, SD	8,223	(4,568)
Norfolk, VA	3,421	(1,901)
Springfield, MA	7,273	(4,041)
Pittsfield, MA	7,578	(4,210)

Table 2.21

Power and Fuel Records for Federal Building in Anchorage, AK for FY1981

	Electricity KWH	Demand KW	Gas cubic feet
January	795,200	0	2,170,200
February	596,000	0	2,292,300
March	621,600	0	1,709,900
April	690,400	0	1,347,400
May	610,400	0	280,500
June	683,200+	0	0
July	715,200+	0	0
August	718,400+	0	0
September	718,400+	0	395,000
October	615,200	0	711,400
November	624,000	0	1,842,800
December	719,200	0	4,410,200
	8,107,200	0	15,159,200

+ Summer months

Table 2.22

Power and Fuel Records for Federal Building in Ann Arbor for FY1981

	Electricity KWH	Demand KW	Gas cubic feet
January	97,380	189	631,000
February	91,280	194	591,500
March	89,520	192	385,000
April	95,180	187	282,200
May	85,160	237	28,700
June +	119,500	284	25,300
July +	145,240	282	22,900
August +	128,480	292	8,400
September +	126,880	278	106,300
October	89,160	230	417,900
November	82,360	188	591,700
December	82,680	299	858,200 *
	1,232,820	2,852	3,949,100

* Corrected
+ Summer months

Table 2.23

Power and Fuel Records for Federal Building in Columbia, SC for FY1981

	Electricity KWH	Demand KW	Oil Gallon
January	396,000	1,204	-
February	342,000	1,204	-
March	355,500	1,296	-
April	387,000 +	1,804	-
May	454,400 +	1,841	-
June	523,500 +	1,906	-
July	786,000 +	1,836	-
August	639,000 +	2,221	-
September	547,500 +	2,269	-
October	463,500 +	1,777	-
November	378,000	1,679	-
December	363,000	1,193	-
	5,635,500	20,230	19,101 *

* Total FY1981 yearly delivery (oil delivered in 8,000 gallon lots).
+ Summer months

Table 2.24

Power and Fuel Records for Federal Building in
Fayetteville, AR for FY1981

	Electricity KWH	Demand KW	Gas cubic feet
January	42,840	324	307,000
February	34,200	194	232,000
March	36,180	248	153,000
April	44,100	216	10,000
May +	43,740	227	13,000
June +	54,540	227	6,000
July +	64,980	232	6,000
August +	62,820	227	5,000
September +	49,140	226	5,000
October	38,880	203	34,000
November	36,880	185	154,000
December	39,060	118	296,000
	549,360	2,627	1,221,000

+ Summer months

Table 2.25

Power and Fuel Records for Federal Building in
Huron, SD for FY1981

	Electricity* KWH	Demand KW	Gas* cubic feet	(Oil) (Gallons)
January	60,120	206	431,800	
February	68,100	254	400,000	
March	53,350	220	213,600	
April	55,680	225	157,400	
May	53,760	224	11,200	(193)
June +	62,880	308	0	
July +	61,440	355	0	
August +	70,080	342	0	
September +	59,040	303	0	
October	55,200	333	3,600	
November	59,820	204	78,200	
December	53,640	212	190,800	
	713,340	3,186	1,486,600	

+ Summer Months
* Electricity 1981 789,100 cubic feet
Gas 1982 Fuel 1981 2,069 gallons oil

Table 2.26

Power and Fuel Records for Federal Building in Norfolk, VA for FY1981

	Electricity KWH	Demand KW	Excess Over Base KWH
January	324,480	858	176,646
February	266,880	708	119,040
March	213,120	794	65,280
April	200,000	790	52,160
May +	148,000	650	160
June +	170,000	700	22,160
July +	236,160	596	88,320
August +	213,120	612	65,280
September +	203,520	550	55,680
October	147,840	646	0
November	192,000	920	44,160
December	268,000	988*	120,160
	2,583,920	8,812	831,000

* December 1980

Excess Winter 577,000 KWH
Excess Summer 254,000 KWH
+ Summer Months

Table 2.27

Power and Fuel Records for Federal Building in Pittsfield, MA for FY1981

	Electricity KWH	Demand KW	Oil Gallon
January	12,480	50	1,400
February	12,400	56	1,000
March	13,000	52	900
April	11,760	62	750
May	12,560	65	250
June +	11,440	70	0
July +	11,440	66	0
August +	12,240	68	0
September	11,280	42	100
October	12,800	46	250
November	12,880	46	900
December	13,040	49	1,175
	147,320	672	6,725

+ Summer months

Table 2.28

Base and Excess Electrical Loads for the Federal Buildings

	Base KWH/Month	(% of Total Usage)	Summer Excess KWH	(% of Total Usage)	Winter Excess KWH	(% of Total Usage)
Anchorage	610,400	(90%)	393,600	(5%)	-	
Ann Arbor	82,360	(80%)	190,660	(15%)	-	
Columbia	355,500	(76%)	1,342,500	(23%)	-	
Fayetteville	36,180	(79%)	94,320	(17%)	-	
Huron	53,760	(90%)	59,445	(8%)	-	
Norfolk	147,840	(69%)	254,000	(10%)	577,000	(22%)
Pittsfield	11,280	(92%)	1,280	(1%)	-	

Table 2.29

Energy Used for Space Heating Per Floor Area Per Degree Day

	$Btu/(F \cdot day \cdot ft^2)$	$KW/(K \cdot m^2)$
Anchorage	2.9	0.40
Ann Arbor	11.9	1.62
Columbia	7.8	1.06
Fayetteville	10.1	1.38
Huron	2.6	0.35
Norfolk	4.2	0.57
Pittsfield	6.7	0.91

Figure 2.1 Location of the Eight Federal Office Buildings

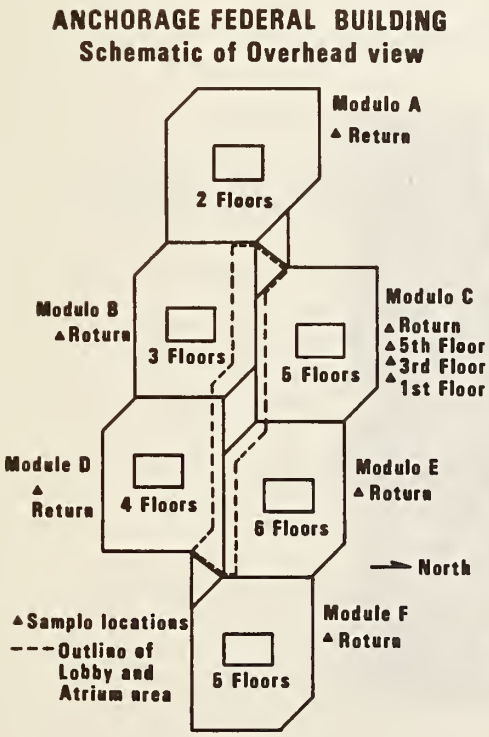

Figure 2.2 Schematic Diagram and Photograph of Federal Building in Anchorage, AK

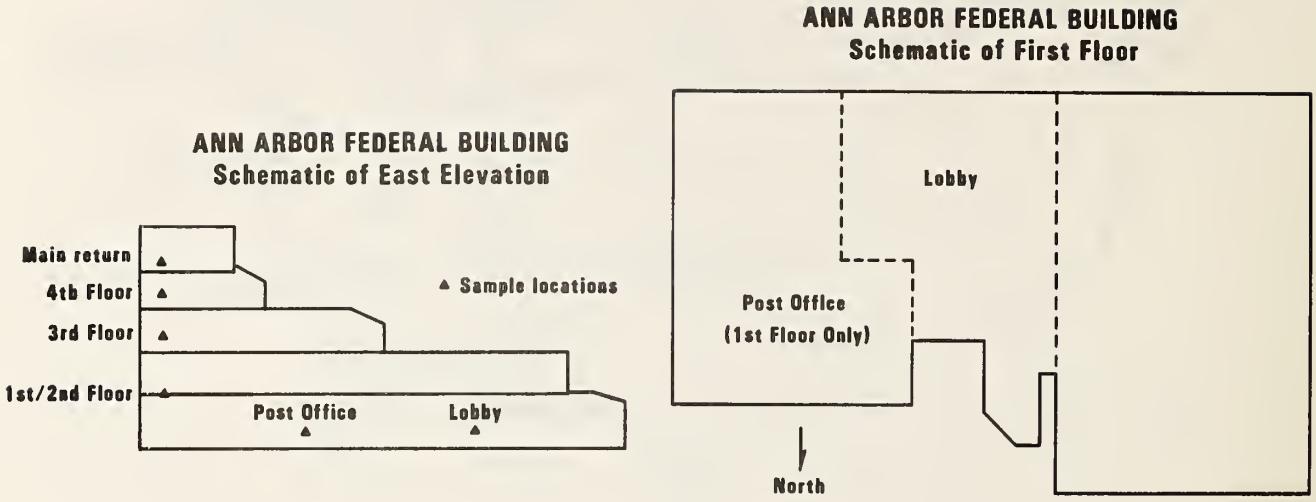

Figure 2.3 Schematic Diagram and Photograph of Federal Building in Ann Arbor, MI

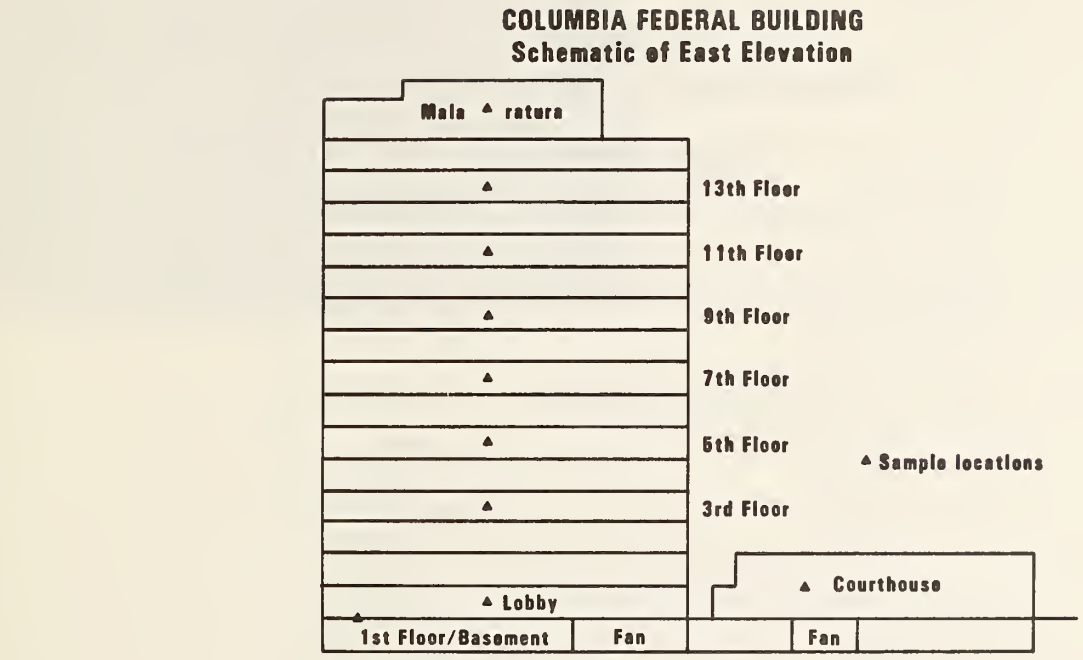

Figure 2.4 Schematic Diagram and Photograph of Federal Building in Columbia, SC

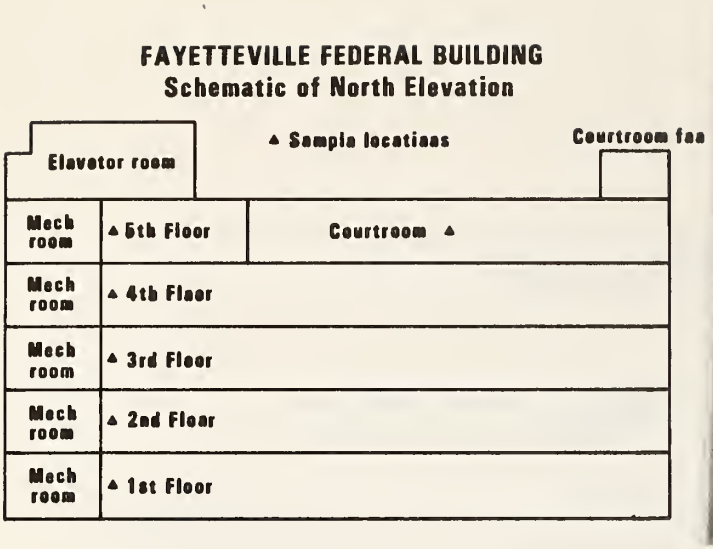

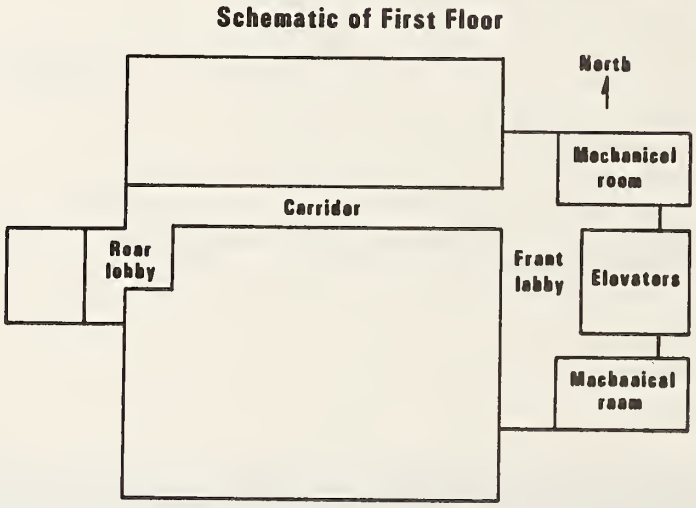

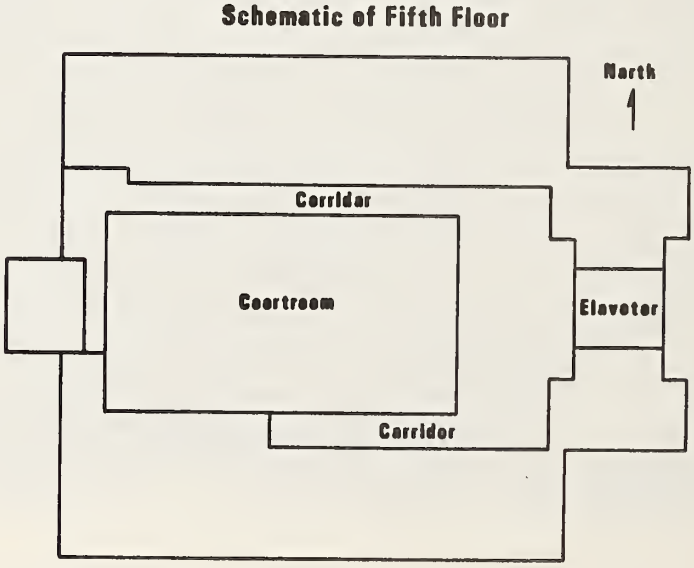

Figure 2.5 Schematic Diagram and Photograph of Federal Building in Fayetteville, AR

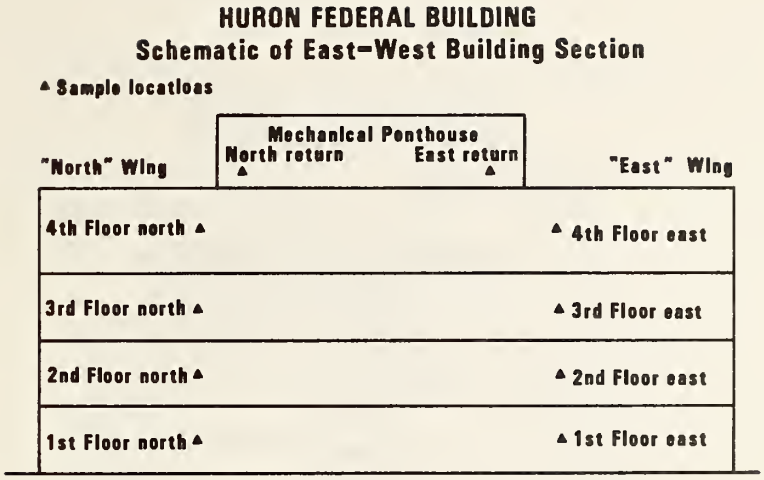

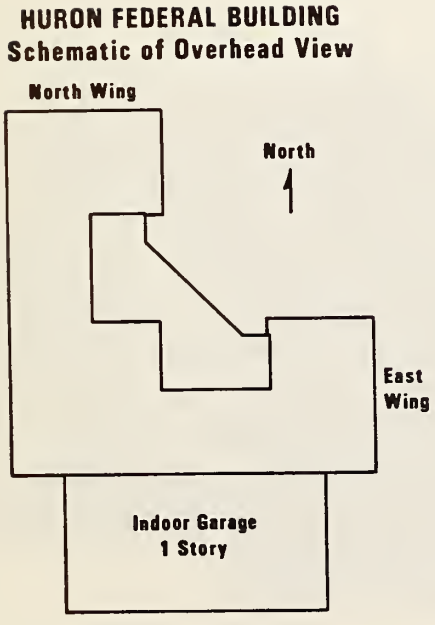

Figure 2.6 Schematic Diagram and Photograph of Federal Building in Huron, SD

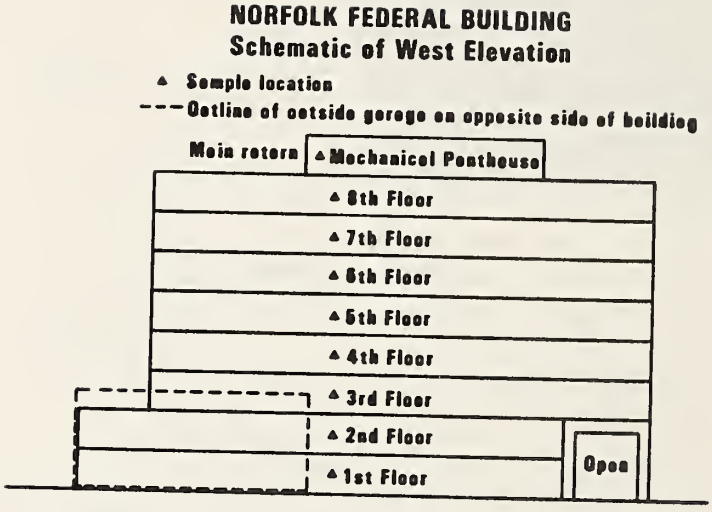

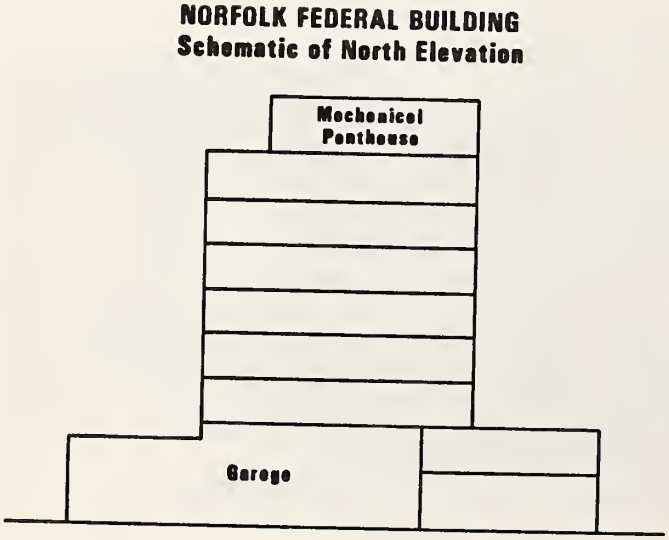

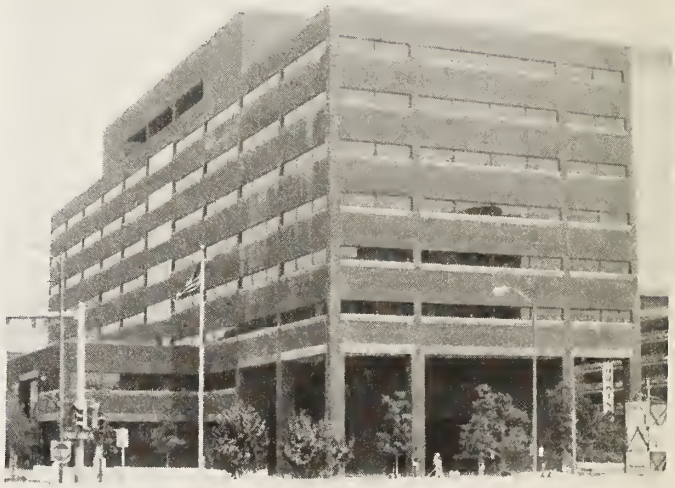

Figure 2.7 Schematic Diagram and Photograph of Federal Building in Norfolk, VA

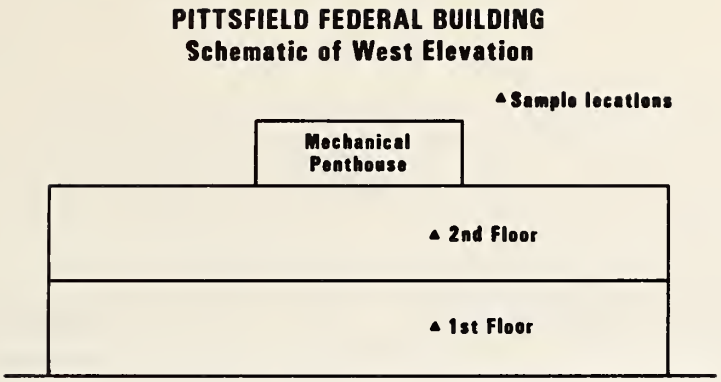

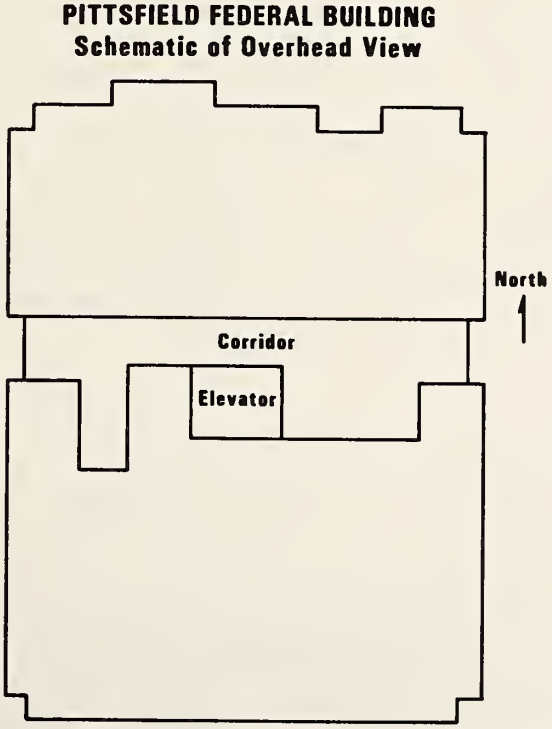

Figure 2.8 Schematic Diagram and Photograph of Federal Building in Pittsfield, MA

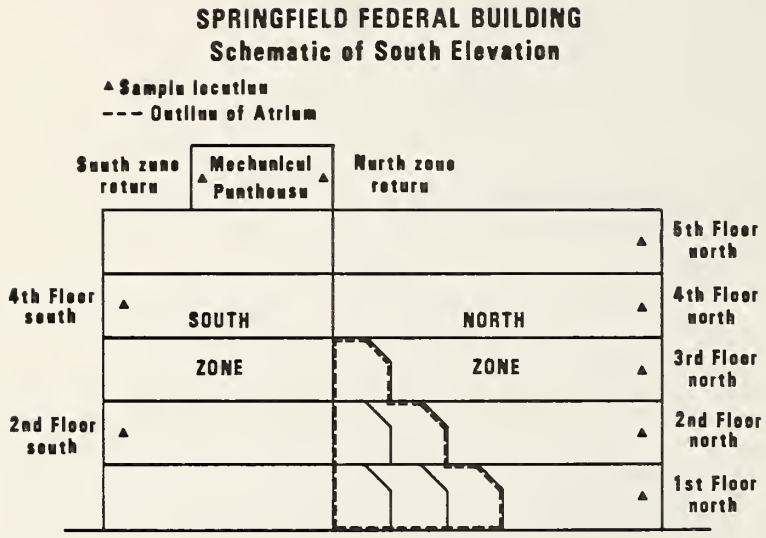

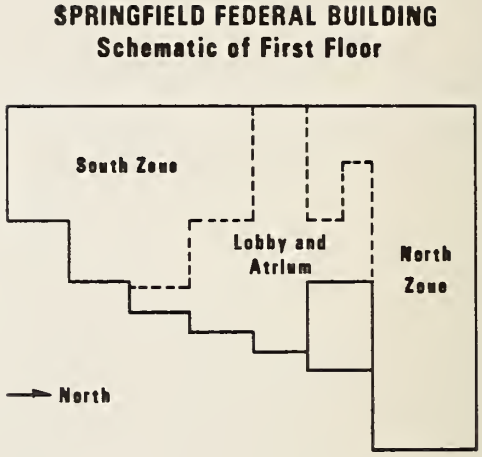

Figure 2.9 Schematic Diagram and Photograph of Federal Building in Springfield, MA

3. Ground Infrared Thermographic Inspections

3.1 Background

Thermographic inspection with infrared (IR) imaging systems is a diagnostic tool to locate thermal defects in a building envelope. IR thermography employs non-contact scanning devices to convert the IR radiation from the object surface to visible light by providing an image of the surface intensity variation. The application of IR thermographic surveys to detect thermal anomalies and to determine insulation effectiveness in large buildings permits the selection of retrofit actions to be carried out to achieve energy conservation. During field measurements, IR thermographic inspections are usually carried out both internally and externally under suitable weather conditions. Thermographic data can be collected by photographing the thermal image display of the thermographic sensing system or by recording the video output of the system directly for subsequent reproduction. Information such as the temperature range of the sensing system and the environmental conditions during inspection are also required in addition to the thermographic data. A copy of such a thermal image, which corresponds to the apparent radiance temperature distribution along the surface, is called a thermogram. A typical thermogram of a surface will provide an intensity-modulated image where the bright and dark portions represent the hot and cold regions, respectively, and the grey shades show intermediate ranges. Accordingly, the thermal integrity of the buildings can be analyzed and interpreted from the thermograms and other documentation.

3.2 Summary of Results

Thermographic surveys were conducted during the heating season of 1982-83 at all eight federal buildings. Since these are all large buildings, they were inspected thoroughly by exterior surveys with interior surveys only at some regions where thermal anomalies were detected or suspected by outside inspections. A summary of thermal deficiencies interpreted from the thermographic inspection for all eight buildings is given in table 3.1. Note that the numerical calculations of the total wall area and percentage of wall area subject to thermal defects in table 3.1 exclude the glass and window areas of the outside surfaces. As indicated in table 3.1, the most severe thermal defects that occur in these buildings, besides defects in insulation, are air leakage through joints (wall-to-wall, ceiling-to-wall, and floor-to-wall) and window seals. Other common heat loss locations observed include shrinkage of insulation, and air penetration paths in walls and ceilings. The percentage of wall area subject to thermal defects in these buildings was found to be between 6 and 18 percent, also given in table 3.1. Descriptions of the envelope thermal integrity and examples of defects observed in the thermograms are included in the following discussion.

Table 3.1 Thermal Deficiencies Observed in Each Test Building

City	ANCHR	ANNAR	COLUM	FAYET	HURON	NORFK	PITFD	SPRFD
Total Wall Area ft^2	81,800	9,700	113,900	15,900	38,300	66,400	10,900	47,300
(m^2)	7,600	904	10,580	1,480	3,560	6,170	1,010	4,390
Defective Wall Area ft^2	15,120	1,710	19,530	950	3,530	11,490	2,010	3,260
(m^2)	1,405	159	1,814	88	328	1,067	187	303
% of Wall Area Subject to Thermal Defects	18	18	17	6	9	17	18	7
Defects Observed:								
Walls								
Lack of Insulation		*	*	*			*	*
Shrinkage or Figures in Insulation	*	*	*		*	*	*	
Cross Braces		*				*	*	
Air Penetration	*	*	*		*	*	*	*
Ceilings								
Interior		*	*			*	*	*
Indentation or Overhang			*	*		*	*	*
Doors					*			
Windows	*	*	*	*	*	*	*	*
Seam Leakage								
Wall-Wall				*	*	*	*	
Floor-Wall			*	*	*		*	*
Wall-Panels	*	*	*					*
Basement			*					
Pipe or Duct			*				*	
Thermal Bridges	*	*			*	*		*

3.2.1 Description of Thermal Defects in the Anchorage Federal Building

The federal building in Anchorage, AK is rather uniform in its thermal anomalies, for the defects in the modules are consistent and regular and the modules are nearly identical to one another, discounting the differences in the number of floors. The major defects are the thermal bridging at the panel supports and the leakage that occurs at the seams of the interlocking panels, especially at the corners and along the edges of the adjoining mirror walls, as illustrated in the thermograms from figures 3.1 and 3.2. The mirror walls in figure 3.2 appear as bands of light and dark, with the light bands having one-way mirrors for the floors inside and the dark bands having walls behind them. The high rating, 18%, of wall area exposed to thermal defects is primarily due to this corner leakage and thermal bridging at the structural supports of the panels. Examples are the SW corner of the A module in figure 3.2-2 and the vertical seams in figures 3.2-3 and 3.2-4. (The bright spot in the center of figure 3.2-3 is the heat from a streetlight.) There also is extensive heat loss from the first floor windows that are on every module as illustrated by the west face of the A module in figure 3.2-4.

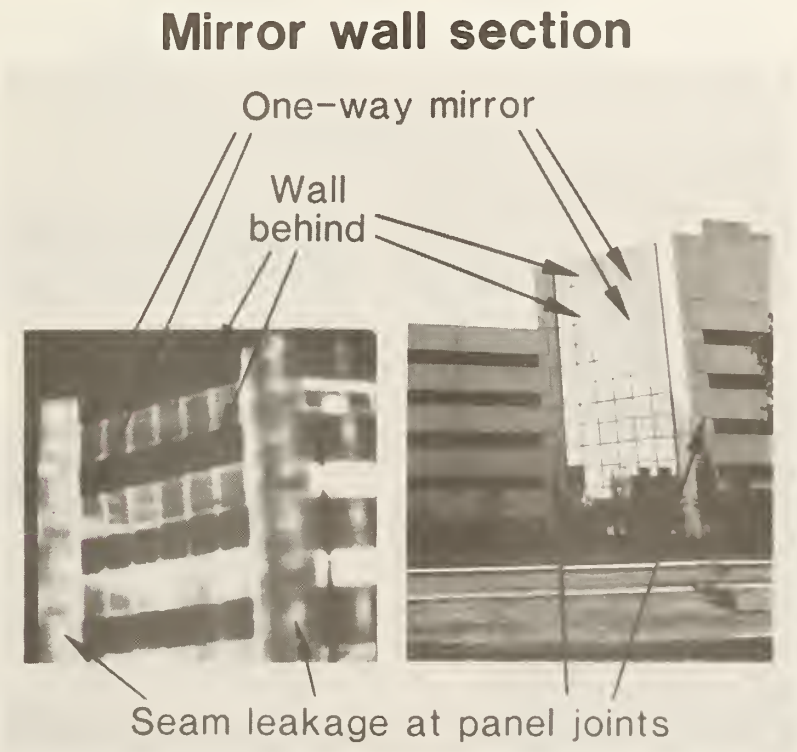

Figure 3.1 Sample Defects Observed in the Anchorage Federal Building

Figure 3.2 Thermal Defects Observed in the Anchorage Building

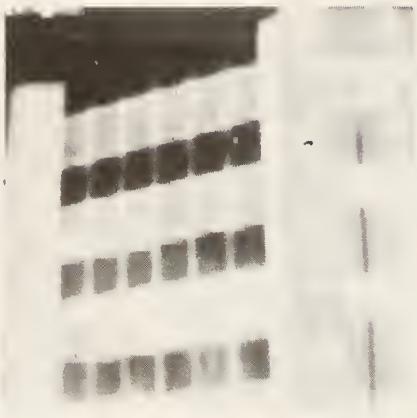

3.2-1
Mirror wall section

3.2-2
SW corner of
A module

3.2-3
SE corner of E wall,
upper floor F module

3.2-4
West face of the
A module

3.2.2 Description of Thermal Defects Observed in the Ann Arbor Federal Building

The federal building in Ann Arbor has many types of thermal anomalies, but the predominant defect is the lack of insulation in large rectangular sections in the east and west walls. Note the large heat loss areas in figures 3.3, 3.4. There are similar voids in the insulation in the wall outcroppings that face east in the top center of the building as seen in figure 3.4-6. Leakage in the seams is also a distinct problem in the building, as is evident in the thermograms of the adjoining panels in figures 3.4-1 and 3.4-2. The wall-floor joints are sources of heat loss as well and are found in nearly all exterior wall areas. The strong flaring in the close-up of the east wall at the south end, shown in figure 3.4-3, is indicative of serious thermal defects due to air leakage in the top seams. Note the cross-brace in the thermogram of the Post Office in figure 3.4-5 and some incompletely or unevenly insulated walls in figures 3.4-2 and 3.4-6, which the irregular voids indicate.

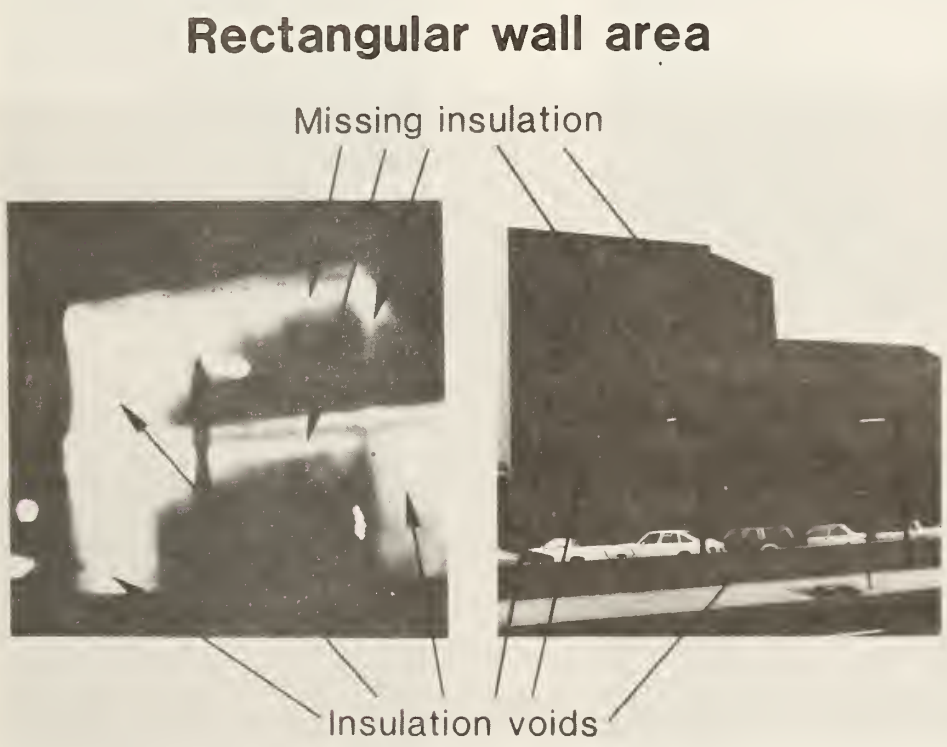

Figure 3.3 Sample Defects Observed in the Ann Arbor Federal Building

Figure 3.4 Thermal Defects Observed in the Ann Arbor Building

3.4-1
Middle two floors
of SW corner

3.4-2
Top floors of the
W wall at the S end

3.4-3
E wall at the
S end

3.4-4
E wall at the
S end

3.4-5
E wall at the N
end, first floor
Post Office

3.4-6
N face above and to
the left of the front
entrance

3.2.3 Description of Thermal Defects in the Columbia Federal Building

The thermal anomalies observed in the federal building in Columbia, SC consists primarily of leakage through defects in the window panels and voids in the insulation at the panel seams (figures 3.5 and 3.6). The thermograms shown in figures 3.6-1 and 3.6-2 made by interior inspections illustrate some of the thermal defects, such as poor insulation, missing insulation, and compression of insulation around the window areas of this building. Figures 3.6-3 and 3.6-4 indicate the compression and voids in the insulation in the north wall of the fourth floor by interior and exterior thermograms, respectively. Similar defects over the entire building are the main contributors to the high percentage, 17% of wall area subjected to thermal anomalies. Note the seam leakage in the panels that make up the solid edges in figure 3.6-4. The heat loss depicted in figure 3.6-5, which rises up the west edge of the south wall and across the top edge of the building, is due to the perimeter zone HVAC system ducts. The thermal integrity of the courthouse adjacent to the tower is also imperfect. Figure 3.6-6 shows the leakage that occurs at the NW corner indent of the courthouse, which is typical of the leakage at those seams.

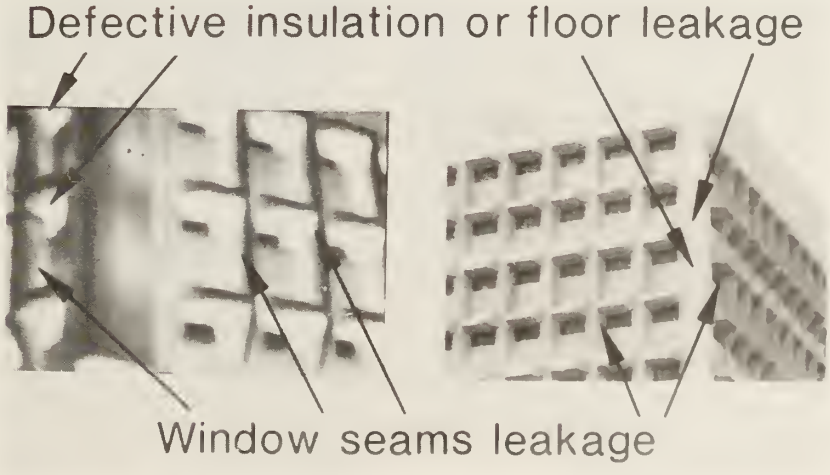

Figure 3.5 Sample Defects Observed in the Columbia Federal Building

Figure 3.6 Thermal Defects Observed in the Columbia Building

3.6-1
N wall on the fourth floor of the tower (interior)

3.6-2
N wall on the fourth floor of the tower (interior)

3.6-3
SE corner of the fourth floor of the tower (interior)

3.6-4
Lower west face of the tower at the N end

3.6-5
S face of W end

3.6-6
NW corner indent of the courthouse

3.2.4 Description of Thermal Defects Observed in the Fayetteville Federal Building

Of all the federal buildings inspected, the wall areas of the Fayetteville building are observed to be relatively uniformly insulated, however, this is actually due to a lack of insulation in the exterior wall envelope (figure 3.7 and 3.8). This indicates the limitation placed on infrared methods when applied to uninsulated walls. The leakage of the wall-floor seams are the predominant defects. Examples are the seams of the elevator towers as shown in figures 3.8-1 and 3.8-2. This type of thermal defect is also evident in the east and west walls below the overhangs where the roof of the overhanging section appears to be a source of heat loss as seen by the flaring against the tower in figure 3.8-1. Note that the heat loss through the floor of the overhangs could be due to the corner seams, for the defect is well-defined along the edges of the overhanging floor. There are relatively few insulation voids which helps account for the low, 6%, thermal defects of the total wall area.

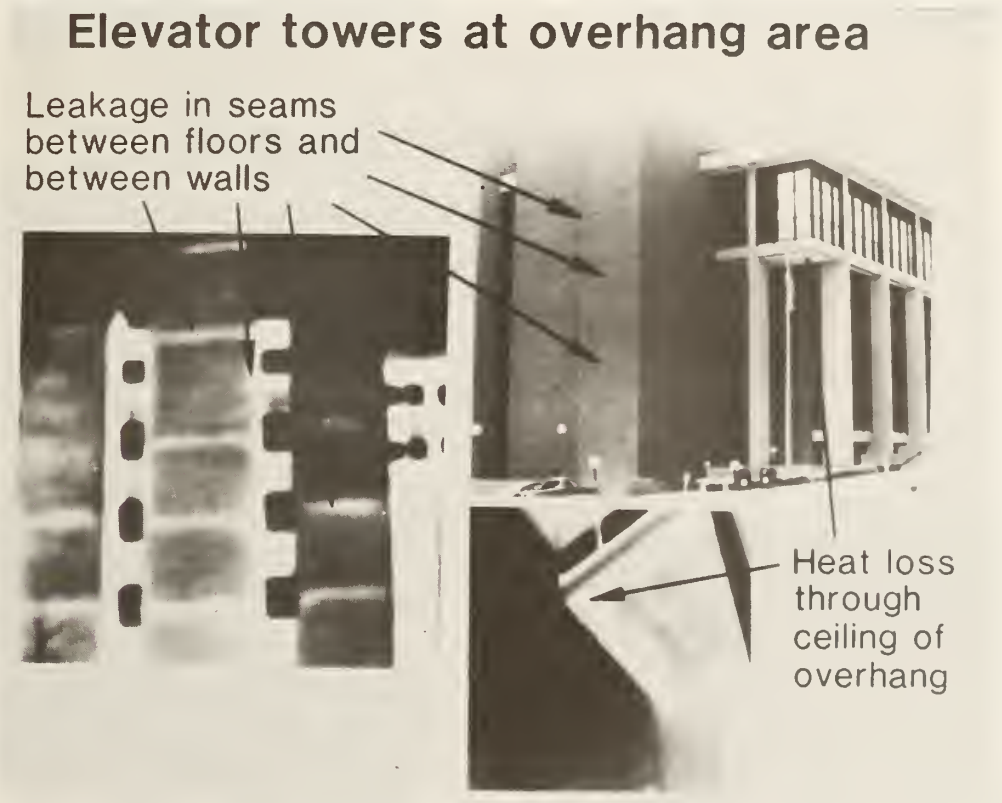

Figure 3.7 Sample Defects Observed in the Fayetteville Building

Figure 3.8 Thermal Defects Observed in the Fayetteville Building

3.8-1
NE corner with one
east face tower

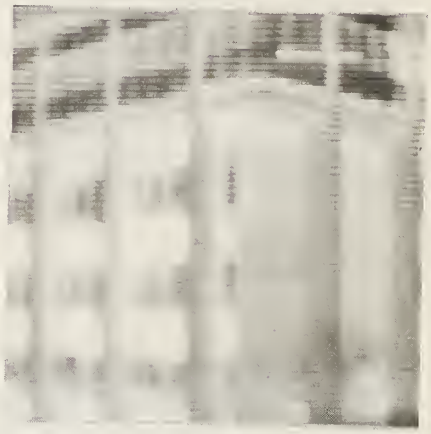

3.8-2
NW corner with west
wall under overhang

3.8-3
E end with three
elevator towers

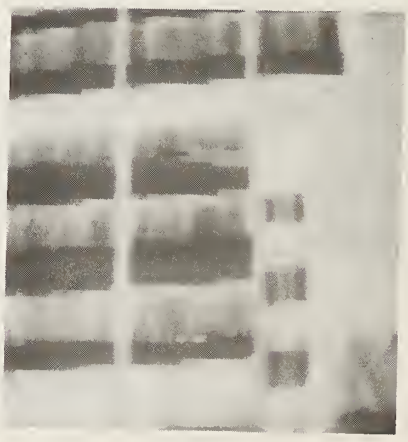

3.8-4
NW corner above N entrance
with view up to overhang

3.2.5 Description of Thermal Defects Observed in the Huron Federal Building

The federal building in Huron, SD is relatively sound with respect to thermal integrity (figures 3.9 and 3.10). The 9% thermal defects in wall area are primarily due to leakage through seams between floors and thermal bridges at intersections of walls, floors, and beams, as seen in figure 3.10-3. There is also flaring around and above the windows shown in figures 3.10-1 and 3.10-3. Note how the seams appear to be more defective as they approach the windows, especially as seen in figure 3.10-3. The brightness in the leftmost side of figure 3.10-4 is due to the windows near the front entrance in the background. Figure 3.10-4 is an interior thermogram of the fourth floor indicating a beam which conducts cold air in on the right hand side. Figure 3.10-4 also depicts some shrinkage in the insulation in the third and fifth sections of the wall, as well as air leakage at the top and the bottom of the wall where it intersects the floor and ceiling.

Figure 3.9 Sample Defect Observed in the Huron Federal Building

Figure 3.10 Thermal Defects Observed in the Huron Building

3.10-1
E wall with NE
entrance off to right

3.10-2
N face with NE
entrance on left

3.10-3
Close-up of middle
section on E wall as
shown in 5-2

3.10-4
Fourth floor interior
N wall of the E wing

3.2.6 Description of Thermal Defects in the Norfolk Federal Building

The thermal anomalies observed in the federal building in Norfolk, VA consist of two basic kinds, the leakage at the wall-floor seams and the leakage at the exterior panel seams (figures 3.11 and 3.12). In figure 3.12-1, there is a great deal of heat loss shown at the panel seams in the middle of the east wall. The wall-to-post-to-floor seams are also sources of heat loss as illustrated in figures 3.12-2 through 3.12-5. Figure 3.12-2 shows an interior thermogram of the west wall at the south end. (The middle window does not have the blind pulled down and is not reflecting.) Note the vertical, darker area in the center of the picture, which is a beam conducting cold inwards. Figures 3.12-3, 3.12-4, and 3.12-5 show leakage between the windows and from the panel seams in the solid wall sections below, which correspond to the horizontal, long, white areas across the entire length of the building. Other thermal defects observed include the floors of the third floor and second floor overhangs, as evidenced by the voids in insulation and leakage at the seams identified in figures 3.12-5 and 3.12-6.

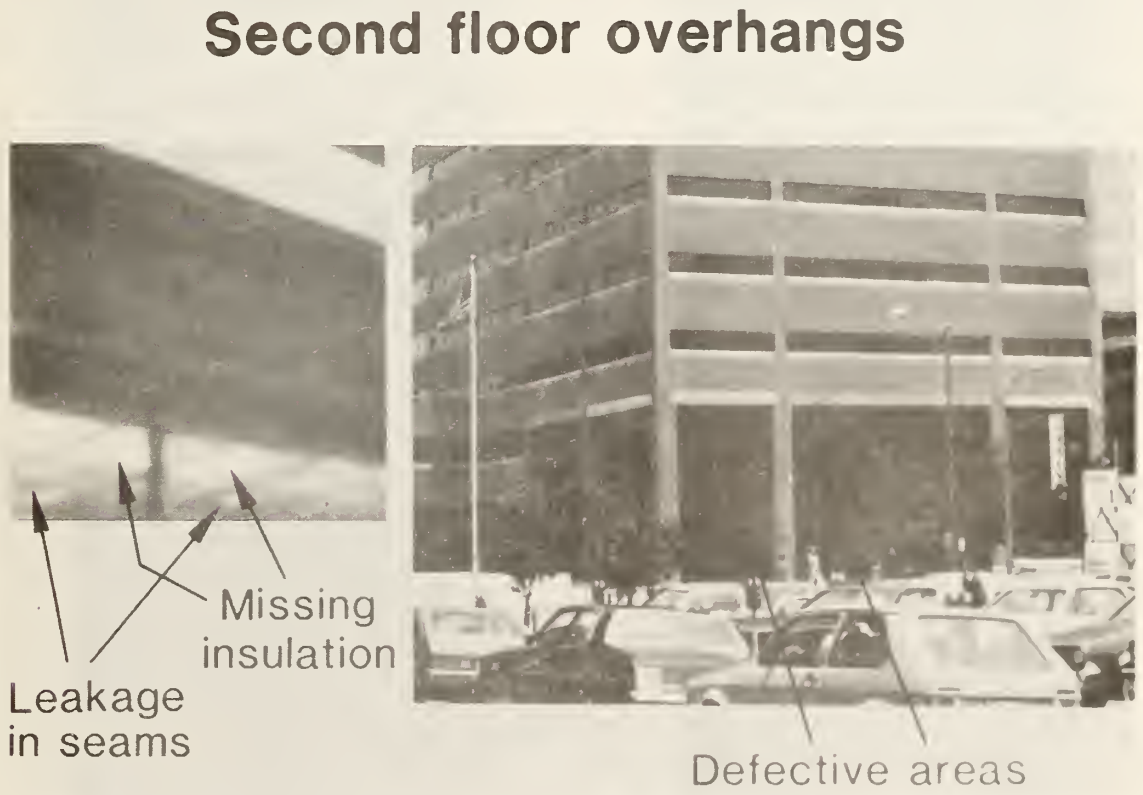

Figure 3.11 Sample Defects Observed in the Norfolk Federal Building

Figure 3.12 Thermal Defects Observed in the Norfolk Building

3.12-1
Lower wall section
of E wall

3.12-2
W wall at S end of
the third floor

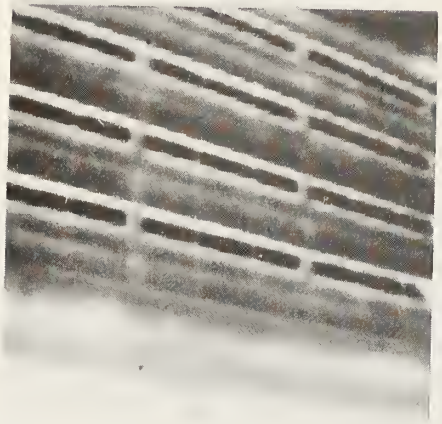

3.12-3
W face at the N
end

3.12-4
E wall at the
SE corner

3.12-5
Third floor overhang
of the N wall at the
W end

3.12-6
NE overhang of second
floor over garage

3.2.7 Description of Thermal Defects Observed in the Pittsfield Federal Building

The thermal integrity of the federal building in Pittsfield, MA can be characterized by a large number of poorly defined voids in the insulation (figures 3.13 and 3.14). Many sections have insulation that is distributed unevenly, and there are areas where a whole section of wall is lacking insulation as shown in figure 3.14-2, where the top third of the wall next to the front entrance is distinctly warmer. The large percentage, 18%, of defective wall observed in the Pittsfield building is due largely to these large rectangular voids, but there are problems with all types of seams. In figure 3.14-1 for example, note the leakage from the seam below the second floor windows and the wall-wall seam in the upper right-hand corner. The posts running through the walls also cause heat loss as shown in figures 3.14-4 and 3.14-6. These two thermograms are characteristic of those for every wall-post seam in the building. At each corner there is an indentation in which there is leakage as illustrated by the thermograms in figures 3.14-3 and 3.14-4, where the exterior and the interior of the NW corner on the first floor are shown. The dark line in figure 3.14-4, indicating the penetration of cold, corresponds to the bright white regions in figure 3.14-3 which indicate heat loss to the outside. Other defects observed in this building include the possibility of a damaged pipe inside the north wall as shown in figure 3.14-5, where a flaring warm area near the top is detected.

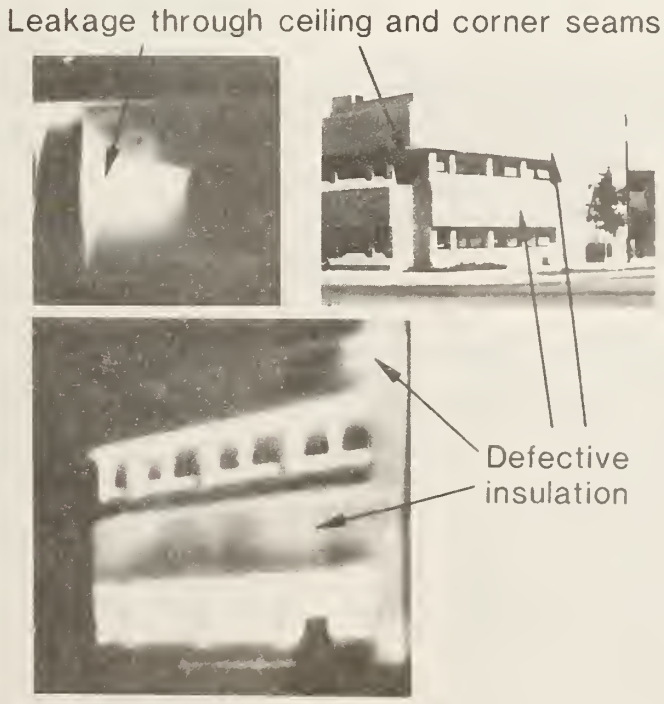

Figure 3.13 Sample Defects Observed in the Pittsfield Federal Building

Figure 3.14 Thermal Defects Observed in the Pittsfield Building

3.14-1
S end of E wall
(exterior)

3.14-2
The front entrance
on E wall (exterior)

3.14-3
NW corner with N
wall section and
indent (exterior)

3.14-4
NW corner with W
window and
indent (interior)

3.14-5
Center of N wall
(exterior)

3.14-6
Wall-post seams on E
wall first floor
(interior)

3.2.8 Description of Thermal Defects in the Springfield Federal Building

The Springfield federal building has a relatively low percentage, 7%, of wall area subject to thermal anomalies (figures 3.15 and 3.16). The main defects are the post-wall joints as seen in figures 3.16-1 through 3.16-6. Note the consistent pattern of the defect in figures 3.16-1 and 3.16-3. An exterior close-up of the post-wall seam is shown in figure 3.16-2 at the SW corner with an interior view in figure 3.16-4. The dimensions of the columns are defined in figures 3.16-1 and 3.16-2 by the heat loss that occurs at the edges as the column rises up the side of the building. The interior view shows the cold penetrating to the interior at the sides of the pillar at a single floor. The heat loss from the joints is also consistently evident at the corners, where there are small insulation voids above the windows as well, which can be observed in figure 3.16-3 and 3.16-5. There is also a great deal of heat loss from the glass windows on the first floor and from the atrium which rises up the center of the east face of the building, as shown in figures 3.16-5 and 3.16-6.

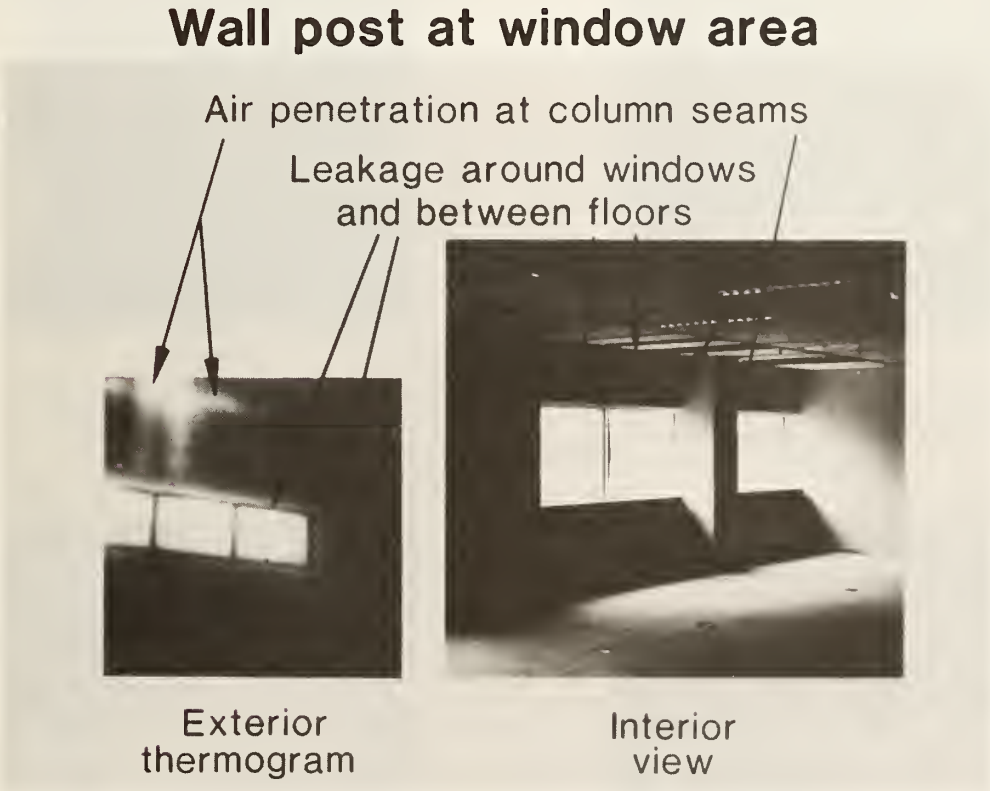

Figure 3.15 Sample Defects Observed in the Springfield Federal Building

Figure 3.16 Thermal Defects Observed in the Springfield Building

3.16-1
SE corner of
the N wing

3.16-2
Close-up of the floor-wall
post seam on the E face of
the N wing

3.16-3
SW corner showing seams
at the second and third
floors

3.16-4
Interior thermogram of
the wall-post seam

glass wall with metal
panel, W end

center of E face

3.3 Conclusions

Though seven of these eight federal office buildings were built to the new federal energy guidelines, thermographic inspection revealed serious defects in each building. Thermal defects in the insulation system were observed to be in the range of 6 to 18 percent of the wall areas of these buildings. Leakage around windows and seams were observed in all buildings. Other thermal anomalies found in these buildings included missing insulation in the wall, thermal bridges, defective ceiling and floor insulation, and convection within insulation. Buildings with overhangs and indentations appeared to have severe problems in those areas.

Thermographic inspections performed on commercial buildings are capable of determining the thermal integrity of the building envelopes and detecting defects in the mechanical system. For new buildings, thermography can be used for quality control during construction. Had such construction-stage inspections been done on these buildings, most of the observed defects could have been corrected at no cost to the building owner. After buildings are occupied, thermographic inspections can still identify degradation of materials and locations of poor performance of building envelopes. However, correction of these defects at this stage are costly and only justified in extreme cases.

4. Aerial Infrared Thermographic Inspections

4.1 Introduction

Aerial infrared thermography is an imaging process which produces an apparent radiance temperature map of the inspected terrain. An aerial thermography survey can be conducted using either infrared imaging equipment in a helicopter or a line scanner in an aircraft [1]. The technique is effective in identifying uninsulated roofs, defective roof insulation or wet insulation regions on built-up roofs. Variations in the thermal resistance produced by the roof defects cause differences in apparent radiance temperatures in the roofs displayed in an aerial infrared image. Flights are most often conducted at altitudes between 1000 and 2000 ft (305 and 610 m). The instantaneous field of view of the infrared scanner varies with the particular system but will generally range between 1 and 2.5 milli-radians.

Variations in roof emittance, local wind speed and outdoor temperature produce differences in radiance temperature which are larger than those between built-up roofs having 2 and 4 inches of insulation. If all the built-up roofs displayed in an aerial infrared thermogram are well insulated, then variations in parameters such as roof emittance, local wind speed, and local outdoor temperature may cause particular roofs to appear warmer than other roofs, which may be incorrectly interpreted as the absence of roof insulation without knowledge of building design. A potential problem with built-up roofs is that the exterior membrane ruptures, permitting water to penetrate the roof system and wet the insulation. Regions having wet insulation will conduct more heat and will appear warmer than regions having dry insulation. The merit of such a survey technique is that defective regions can be located, permitting repairs to be carried out instead of replacing the whole roof system.

4.2 Procurement of Aerial Thermographic Services

The aerial infrared thermographic inspections were performed by private contractors. A two-step process was undertaken which determined the availability of specialized representative services from competitive organizations, followed by negotiations based upon submitted proposals. Contractor costs, equipment, exceptions to requirements, diversity of geographical locations, and period for performance were sought. Compilations for contractor services responding organizations with interest, experience and background specific to building investigations, and staff capabilities were established from a "sources sought" solicitation in the Commerce Business Daily. Competitive proposals for building inspections were negotiated for contract awards. (See Appendix B for specification of services.)

The solicitation resulted in 25 responses for the aerial thermography contractor services. The respondees included companies with building experience, universities, and others with specialized infrared (IR) capabilities for military or forest fire surveillance.

The responses to proposal bid requests for aerial thermographic surveys are indicated below (bids for more than one building are included). Contracts for the three buildings were awarded.

Federal Building	Bids Received	Declined bids	Returned with no response
Anchorage, AK	2	-	-
Springfield, MA	4	1*	2
Columbia, SC	3	1*	1

* Letters indicated that walk-on roof inspection with IR and other equipment is required.

Comments from potential contractors expressed concern that aerial surveys may not be useful (particularly for a single building) and walk-on roof inspections are essential using IR and other equipment (e.g., core-sampling). Core-sampling was not allowed by GSA due to concern for long term durability of the repaired (removed) section.

4.3 Evaluation of Roof Systems by Aerial Thermography

From the responses of the potential contractors and other investigations [2], it appears that using flyover infrared surveys to identify defects in building roof systems is not sufficient. Walk-on thermographic inspection as well as visual investigation must be performed to detect thermal anomalies accurately. The roof systems of the Anchorage, Columbia and Springfield office buildings were evaluated by three different contractors. Summaries of their reports [3, 4, 5] follow.

Figure 4.1 is a thermogram from the aerial thermographic survey performed on the Springfield building. After the walk-on infrared inspection, no major thermal anomalies or water damage insulation were found. The analysis of potential locations of heat loss regions shown in figure 4.1 were explained by equipment under the area (2)* warm air vents and roof drains (4), metal hatch covers and "corner effects" (7). The extended bright area at (7), corresponds to vented warm air from wall louvers of the penthouse (adjacent to the courthouse roof) which may obscure actual roof surface conditions. One unexplained area (1) in figure 4.1, was the only potential location which required further study. It should be noted that the roof of an older building adjacent to the federal building showed extensive damaged areas (9)-(10).

After the flyover infrared survey was performed on the Columbia building, the anomalies in the IR images were explained by roof surface conditions caused by vents, skylights, drains and hatches. Only two locations required further investigation. One was found to be a build up of gravel and bitumen, the other produced an IR pattern common to divisions between wet and dry fiberous insulation board. The areas are shown in figures 4.2

---

* Numbers in the parenthesis refer to roof areas noted on figure 4.1.

(aerial) and 4.3 (walk-on). The source of water intrusion was presumed to be due to channeling precipitation behind the flashing (from grooves in the precast exterior wall panels). Since no core samples were taken from the roof, no further investigation was made to determine the composition of roof materials, deterioration, and moisture content.

The roof systems for Springfield and Columbia have built-up roofs. The Anchorage building has an inverted membrane roof with blocks of polystyrene thermal insulation covered by concrete blocks. An aerial thermographic inspection and walk-on infrared survey performed on the six modules of the building did not reveal any areas with thermal deficiencies, except some locations with explainable conditions, such as air vents. However, by walking the roof, several problems due to "sunken" surfaces could be seen. Removal of the concrete blocks in a few areas showed large gaps between the insulation boards. These areas were heavily laden with water and deteriorated, as shown in figure 4.4. Thermography is not a useful diagnostic tool for the inverted membrane roof since the thermal problems are masked by the thermally massive concrete blocks. The extent of damage to the entire roof surface was not determined, since the IR study was the only contracted service.

4.4 Conclusions

The quality of the aerial thermographic surveys produced by the three private contractors indicated that aerial thermographic surveys can yield information from which roof damage can be assessed. For detection of roof anomalies on single buildings, the economic benefits of aerial thermography have not been determined. For the multi-building complex or large areas, aerial surveys have shown that many buildings can be evaluated by flyovers. Since it is necessary to follow-up with walk-on inspections, the cost factors for also conducting the aerial survey may not be justifiable. On the other hand, the demonstration that all thermal roof problems on a building can be detected without an aerial survey should be undertaken. If proven, cost savings by elimination of the aerial study may then be realized.

Roof anomalies revealed through aerial infrared surveys are often not related to deficiencies resulting from the roofing system. Instead, they are attributable to building system components or equipment. The analysis of such sources requires building and roof inspections by experienced and/or trained staff.

Roof-top level inspections with infrared equipment was required to define potential deficiencies. Other testing, such as core-sampling or water content measurements in thermal insulation by destructive means, was recommended by contractors for evaluation of the extent of deterioration.

Thermography did not prove to be a useful tool for inspecting the inverted membrane roof of the Anchorage federal building. It helped to detect the beginning of water damage to a section of the roof of the federal building in Columbia, SC. The repair of this area before extensive damage is done would prevent the need for replacement of the roof system at a later date.

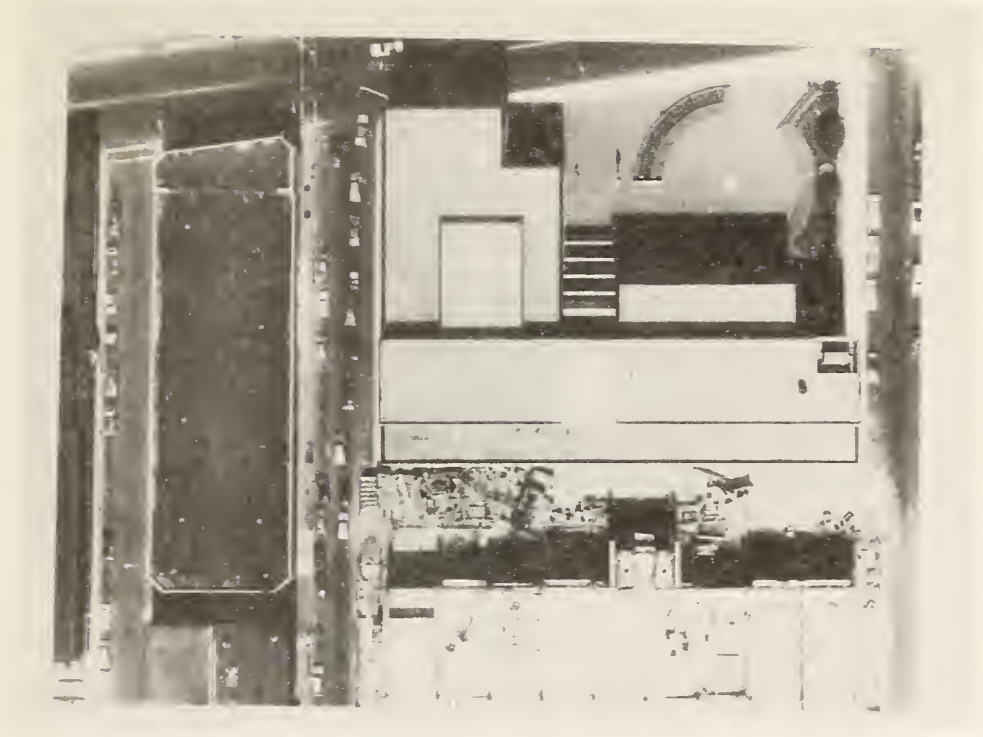

Aerial Photograph

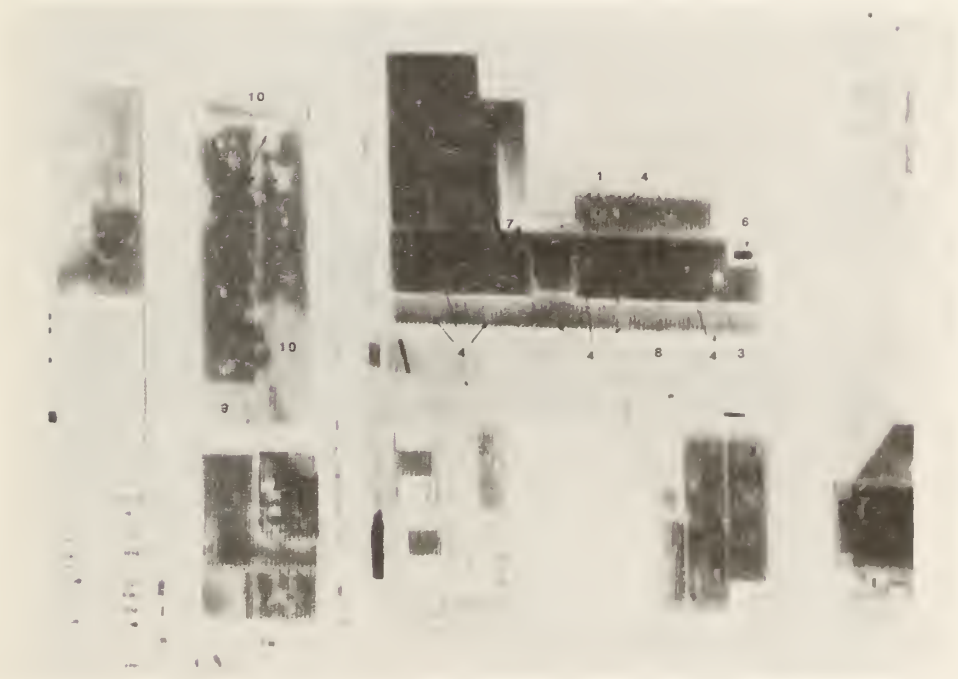

Thermogram

Figure 4.1 Heat loss areas of the Springfield roof system observed by aerial thermography

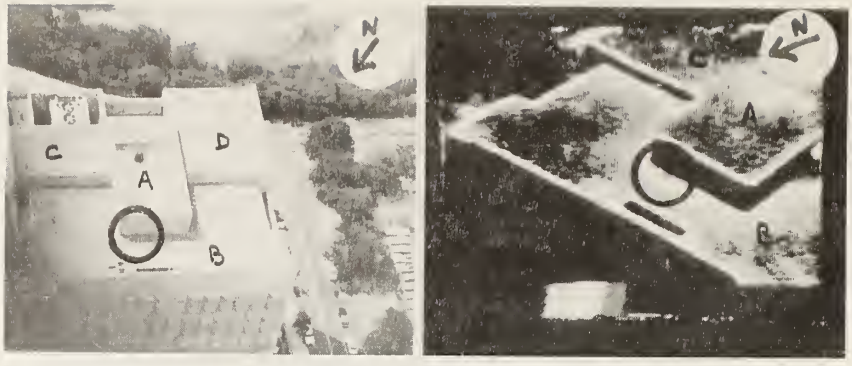

(a) (b)

Figure 4.2 (a) Aerial photograph and (b) aerial thermogram of the Columbia building roof system (area of anomaly circled)

(a) (b)

Figure 4.3 (a) Photograph and (b) thermogram from walk-on infrared survey of the Columbia building roof system (lines enclose area of concern)

(a)

(b)

Figure 4.4 (a) Wet polystyrene insulation and (b) deterioration of the Anchorage building roof system.

5.0 Audits Using Spot Radiometers

5.1 Introduction

The spot radiometer is a hand-held device used to radiometrically measure the equivalent blackbody temperature of a relatively small area of a surface [1]. Spot radiometers are calibrated by pointing at a surface of known temperature and making adjustments such that it determines the correct temperature of the reference surface (manufacturers frequently provide reference surfaces). A spot radiometer is used to measure the inside surface temperature of a building component and the inside air temperature. Another measuring device is used to measure the coincident air temperature at the exterior surface. From the three measured temperatures an estimate of the apparent thermal resistance of the component can be made. A suitable application is to determine qualitatively whether a wall is insulated or if insulation voids or other thermal defects are present.

In performing the measurement, the instrument is pointed at a surface area of interest and senses the total infrared radiation over a particular wavelength band emanating from the surface, including both the self-emitted surface radiation and reflected radiation from surrounding surfaces. The device is calibrated to read out the apparent radiance temperature on either a digital or meter display. The apparent radiance temperature is defined as the temperature of a black surface that would radiate the same amount of thermal radiation as a real surface at the same temperature and having a surface emittance different from unity. Typical specifications for spot radiometers include a temperature measurement resolution within $\pm$ 0.5 ^{o}F ($\pm$ 0.3 ^{o}C). Spot radiometers with a resolution of within $\pm$ 0.1^{o}F ($\pm$0.05^{o}C) are also commercially availble. Spot radiometers generally have their principal spectral response in the range of 10 microns, and a response tiee of less than 2 seconds.

5.2 Thermal Resistance Measurements by Spot Radiometer

The spot radiometer is a non-imaging infrared instrument designed to measure the net radiative heat-flow from the surface, which includes the emitted and reflected radiation. At steady state conditions, thermal resistance of an exterior surface of a building can be established from eq. 5.1.

$$R = \frac{T_i - T_o}{h_i(T_i - T_{is})} \qquad (5.1)$$

where R is the thermal resistance, hr·ft^{2}·^{o}F/Btu(m^{2}·K/W)

T_i is the interior air temperature, R(K)

T_o is the exterior air temperature, R(K)

T_{is} is the inside surface temperature, R(K)

h_i is the inside surface heat transfer coefficient, Btu/hr·ft^{2}·^{o}F(W/m^{2}·K)

The inside surface heat transfer coefficient, h_i, can be expressed in eq. 5.2, which includes thermal radiation and convection.

$$h_i = \sigma \cdot E \cdot [T_i^4 - T_{is}^4]/(T_i - T_{is}) + 0.19\ (T_i - T_{is})0.33 \qquad (5.2)$$

where σ is the Stefan-Baltzmann constant,

$$0.1714 \times 10^{-8}\ \text{Btu/hr}\cdot\text{ft}^2\cdot\text{R}^4 (5.67 \times 10^{-8}\ \text{W/m}^2\cdot\text{K}^4)$$

E is an emissivity factor which is determined from

$$\frac{1}{E} = \frac{1}{E_1} + \frac{1}{E_2}^{-1} \qquad (5.3)$$

where E_1 and E_2 are the emissivities of the subject surface and other room enclosure surfaces, respectively.

Therefore, thermal resistance of an exterior surface can be calculated from eqs. 5.1, 5.2 and 5.3 with temperature measurements and estimated emissivities.

Both the Huron and Ann Arbor buildings were inspected with a general purpose, dual-range spot radiometer with an indoor scale of 50°F (10°C) to 100°F (38°C) and an outdoor scale of -20°F (-29°C) to 150°F (66°C) [6, 7]. The instrument was equipped with a red filter of 8 to 14 microns to eliminate the effects of humidity, color, and other emissivity conditions that would affect the surface temperature readings. Calibration of the spot radiometer is accomplished by adjusting its zero control to match its output temperature to the attached surface thermometer of a factory-supplied reference block. The survey at each building was conducted three hours after sunset and one-half hour after the heating system was turned off. It was found that the spot radiometer should be left in the "on" position throughout the inspection to avoid calibration drifts. The temperatures of the inside and outside air were recorded with a digital thermometer with a range of -31°F (-14°C) to 122°F (50°C). The accuracy of both the spot radiometer and the digital thermometer is $\pm$ 0.5°F ($\pm$ 0.3°C). Temperature data were collected at certain regions of several surfaces. The thermal resistance (R-value) of the region was calculated by assuming 0.9 as the surface emissivity. Several spots were inspected on each surface, their R-values were determined and the average of these R-values was used to represent the thermal resistance of the surface.

From the architectural design of these two buildings, the R-value of each building surface component was also calculated following the methodology specified in the ASHRAE Handbook of Fundamentals [8].

5.3 Results of the Inspection of the Huron and Ann Arbor Federal Building

Tables 5.1 and 5.2 are summaries of measured and design R-values of the Huron and Ann Arbor buildings, respectively. In general, the measured thermal resistances of wall areas are lower than the design values and R-values of windows and doors are relatively close to the design values in these two buildings. The discrepancies between the measured and design R-values may be due to measurement errors, method of calculation, and deficiency in construction. Based on the accuracy of the spot radiometer

and the digital thermometer (both $\pm$ 0.5°F ($\pm$ 0.3°C)), the percentage variation of measurement versus the temperature difference between inside air and surface is illustrated in figure 5.1. According to eq. 5.1, the temperature measurements corresponding to surface components of large R-values will have a lower temperature difference between inside air and surface, and thus a higher percentage variation in the measurements as shown in figure 5.1. On the other hand, for surface components with low R-values, such as windows and doors, the air to surface temperature differences are expected to be high and the percentage variation in the measurements are relatively low. Hence, the measured and design R-values of these surfaces are much closer to each other (also shown in Table 5.1). In addition, the equations used to calculate the thermal resistance from temperature measurements are based on steady state conditions without considering transient effects of thermal storage in construction materials, and these effects may cause errors in computing heat transfer across the building envelope.

Table 5.1 indicates that the measured R-values of office and lobby walls in the Huron building are much lower than the design values. However, thermal conductance measurements on the north wall of the south wing using heat flow meters and calorimeters give much higher R-values of 20.41 and 11.98 $hr \cdot ft^{2} \cdot {}^{o}F/Btu$, respectively (see Chapter 8), as compared with 4.54 $hr \cdot ft^{2} \cdot {}^{o}F/Btu$ from spot radiometer inspections and 15.75 $hr \cdot ft^{2} \cdot {}^{o}F/Btu$ from design. The large discrepancy between the measured R-values and the design values of wall areas are suspected to be due to errors in the spot radiometer measurement caused by either equipment limitations or the non-steady state response of the building envelope (see Chapter 8).

The Ann Arbor building was designed such that various wall sections had different R-values. The measured thermal resistance of surface components in this building are relatively close to the design values, as given in Table 5.2. The thermal resistances measured by heat flow meter and calorimeter of the west wall are 11.53 and 11.05 $hr \cdot ft^{2} \cdot {}^{o}F/Btu$, respectively (see Chapter 8), compared with 7.85 $hr \cdot ft^{2} \cdot {}^{o}F/Btu$, the design values. In addition, the Ann Arbor building is not considered to be energy efficient, with a design R-value of less than 10 $hr \cdot ft^{2} \cdot {}^{o}F/Btu$ for all wall areas. The measured thermal resistances of surface components by spot radiometer survey appear to be reasonably accurate.

The utilization of spot radiometers for thermal property measurements has the advantage of portability, speed, and simple operation. However, laboratory evaluation of a low-resolution ($\pm$ 0.5°F or $\pm$ 0.3°C) spot radiometers to determine thermal resistance of building walls have shown that measurements are not accurate [9]. Results from data reduction of measurements by spot radiometer for both the Huron and Ann Arbor buildings show discrepancies between the measured R-values and the designed R-values. Figures 5.2 and 5.3 illustrate the distributions of these R-values as well as the regression lines based on fits of the entire dataset using least squares techniques for the Huron and Ann Arbor buildings.

Another field investigation using a high resolution ($\pm$ .1°F or $\pm$ 0.05°C) spot radiometer and a radiant flow radiometer (where thermal radiation is measured without conversion to temperatures) to determine thermal resistance of test house walls revealed that systematic errors were related to the heat capacity of wall materials [10].

5.4 Procurement of Audits Using Spot Radiometers

The inspection of the small buildings using spot radiometers was procured by a process similar to that described in Chapter 4 for aerial thermographic inspection. Appendix C contains the specifications used for procurement.

Responses from 12 companies were received to conduct energy audit inspections with hand held spot radiometers. The summary of responses to the solicitation to conduct energy audits with a spot radiometer is shown below (with bids for more than one building). Contracts for three buildings were awarded. Due to the lack of cold weather conditions the Pittsfield study was not performed.

Federal Building	Bids Received	Declined Bids	Returned with No Response
Pittsfield, MA	3	1*	2
Ann Arbor, MI	3	1*	2
Huron, SD	3	1*	2

* Letter indicated spot radiometers not useful for the intended purpose.

5.5 Conclusions

Results from spot radiometer inspections performed on two office buildings indicated there were larger discrepancies in the results for surface components of high R-values than those of low R-values. This may be due to the sensitivity of the instrument as well as inappropriateness of the steady state assumption used to derive the equations used for calculations. However, the thermal resistance values of building exterior surfaces provided qualitative indications of the surface's thermal performance, though the absolute measurements lacked accuracy. Due to the simplicity and portability of the spot radiometer, it can be used to qualitatively evaluate regions of building envelope components.

Table 5.1
Comparison of Thermal Resistance Measured by Spot Radiometer with Design Values in the Huron Building

	Average Measured R-Values $hr \cdot ft^2 \cdot {}^oF/Btu$ ($m^2 - {}^oC/W$)							Design R-values $hr \cdot ft^2 \cdot {}^oF/Btu$ ($m^2 - {}^oC/W$)
			North Wing		South Wing			
	West	South	North	East	North	East	Lobby	
Office wall	6.18	6.35	5.44	5.86	4.54	6.10	-	15.75
	(1.09)	(1.12)	(0.96)	(1.03)	(0.80)	(1.07)	-	(2.77)
Walls under windows	3.28	3.46	2.69	4.03	-	4.07	3.12	12.15
	(0.58)	(0.61)	(0.47)	(0.71)	-	(0.72)	(0.55)	(2.14)
Stairway walls	-	-	-	4.03	4.72	-	-	7.47
	-	-	-	(0.71)	(0.88)	-	-	(1.32)
Garage wall	-	1.73	-	-	-	-	-	2.35
	-	(0.30)	-	-	-	-	-	(0.41)
Garage roof	-	1.65	-	-	-	-	-	5.47
	-	(0.29)	-	-	-	-	-	(0.96)
Column walls	-	-	3.54	-	-	-	5.10	-
	-	-	(0.62)	-	-	-	(0.90)	-
Doors	1.50	-	-	-	-	-	-	1.69
	(0.26)	-	-	-	-	-	-	(0.30)
	-	-	-	-	-	-	1.26	0.90
	-	-	-	-	-	-	(0.22)	(0.16)
Windows with curtains	3.40	3.19	3.18	-	-	3.65	2.14	-
	(0.60)	(0.56)	(0.56)	-	-	(0.64)	(0.38)	-
windows without curtains	-	-	-	-	-	1.79	-	2.04
	-	-	-	-	-	(0.32)	-	(0.36)
Lobby wall	-	-	-	-	-	-	4.06	14.50
	-	-	-	-	-	-	(0.71)	(2.55)

Table 5.2
Comparison of Thermal Resistance Measured by
Spot Radiometer with Design Values in the Ann Arbor Building

	Average Measured R-Values $hr \cdot ft^2 \cdot {}^oF/Btu$ ($m^2 \cdot {}^oC/W$)					Design R-values $hr \cdot ft^2 \cdot {}^oF/Btu$ ($m^2 \cdot {}^oC/W$)
	West	South	East	North	Lobby	
Office Walls						
Type 1	7.85 (1.38)	-	-	9.19 (1.62)	8.53 (1.50)	8.40 (1.48)
Type 2	5.71 (1.01)	6.71 (1.18)	-	-	-	8.77 (1.54)
Type 3	-	4.42 (0.78)	5.71 (1.01)	-	-	9.04 (1.59)
Type 4	-	4.42 (0.78)	3.15 (0.55)	6.08 (1.07)	5.65 (0.99)	4.54 (0.80)
Lobby Walls						
Type 1	-	-	-	-	3.40 (0.60)	4.62 (0.81)
Type 2	-	-	-	-	2.67 (0.47)	2.12 (0.37)
Windows						
Vertical	-	-	1.22 (0.21)	1.53 (0.27)	-	2.04 (0.36)
Horizontal	-	-	1.27 (0.22)	1.38 (0.24)	-	1.69 (0.30)
Bay	-	1.09 (0.19)	-	0.94 (0.17)	-	0.90 (0.16)
Doors	-	-	-	1.52 (0.26)	-	1.69 (0.30)

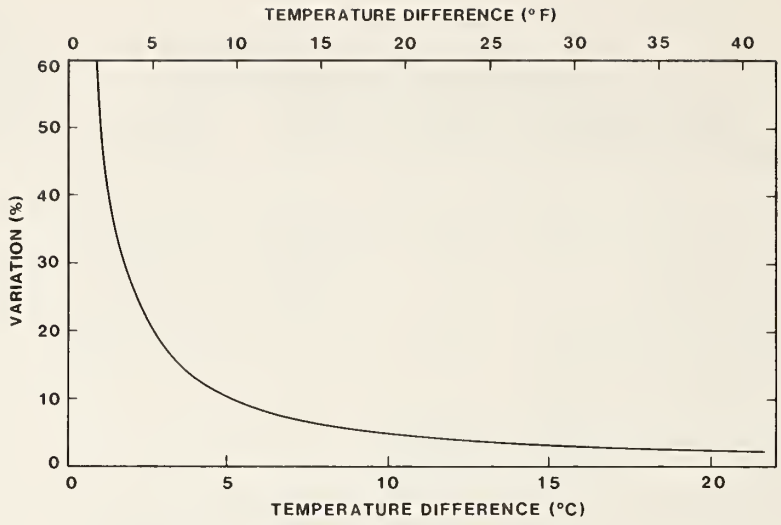

Figure 5.1 Percentage variation of measured R-values from spot radiometer versus temperature difference of inside air and surface

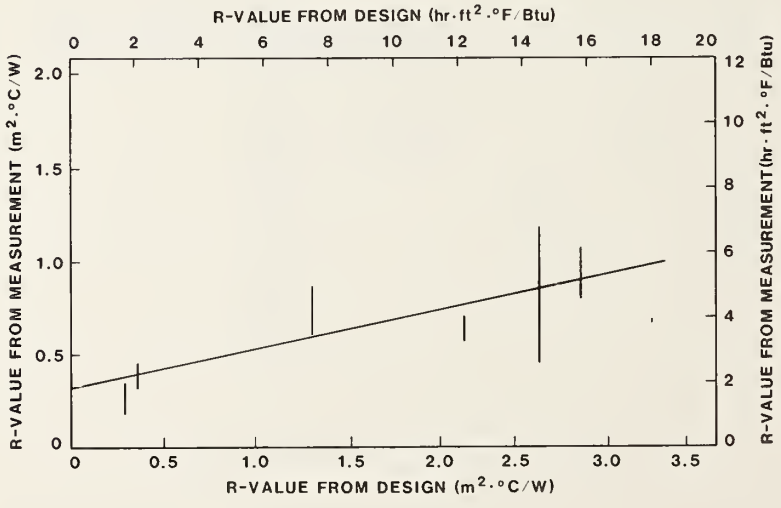

Figure 5.2 Thermal resistance (R-value) of spot radiometer measurement versus design for the Huron building.

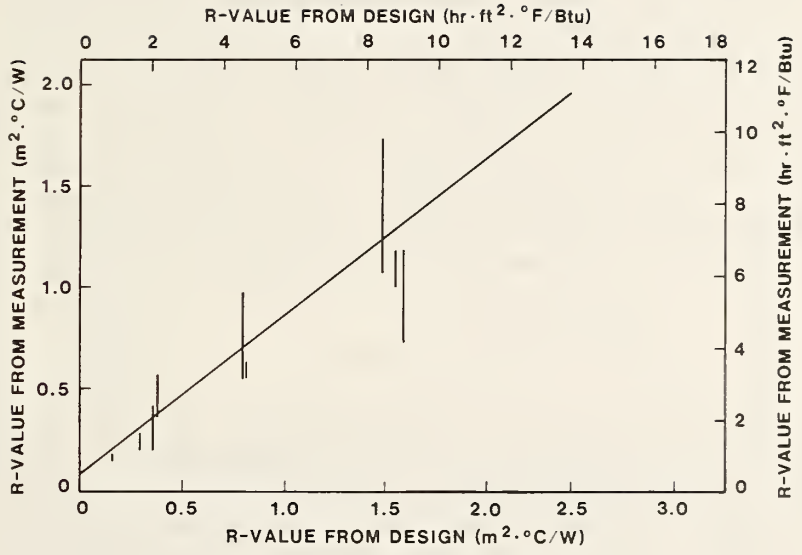

Figure 5.3 Thermal resistance (R-value) of spot radiometer measurement versus design of the Ann Arbor building.

6. Air Infiltration and Ventilation Rate Measurements

6.1 Introduction

The air infiltration and ventilation rates of the eight federal office buildings were tested using tracer gas techniques [1]. The measurement employed the tracer gas decay method using sulfur hexafluoride (SF_6) as the tracer. This test was designed for each building to produce a measure of the total air infiltration rate of the building and the rates of the major zones of the building. Sample and injection tubing was installed in each zone along with wiring for measuring interior temperatures, the status of the building's HVAC fans and exterior weather conditions (wind speed, wind direction and exterior temperature). The automatic air infiltration system previously designed by NBS for large buildings was installed in each building for a period of about a week during the fall, winter and spring (three automated air infiltration systems were used on this project). Tests were performed both during periods of occupancy and non-occupancy, with the outside air intake dampers operated normally and closed, respectively. Tracer gas measurements were made for a total of about 200 hours in each building. The air sample locations for these tests are given in Table 6.1, and shown in the building schematics in figures 2.2 through 2.8.

6.2 Results of the Air Infiltration Tests

The summary of the infiltration measurement results in Table 6.2 show average infiltration rates under winter conditions, neglecting extremely high wind speeds. These measurements are made with all outside air intake and exhaust dampers closed. These results indicate that the buildings in Huron and Anchorage are experiencing relatively low natural leakage rates. The buildings with the highest natural rates are Ann Arbor, Norfolk and Springfield. By using the results of these tests it is possible to estimate the contribution of air infiltration to the design load of the buildings. These estimates are also included in Table 6.2. As can be seen, the air infiltration contributed from 23% to 61% of the building heating load. Tables 6.3 through 6.7 show examples of typical one-hour decay tests for the buildings in Anchorage, Springfield, Norfolk, Huron and Columbia. These tables indicate the extent of tracer gas mixing obtained in these tests, with good mixing being a requirement for accurate results. They also show zones of the building which exhibit high air exchange rates compared to the rest of the building - the lobby in Springfield, the 1st floor in Norfolk, and the lobby in Columbia. Similarly high rates can also be shown for the 1st floor in Fayetteville and the lobby and post office in Ann Arbor. The lobbies generally exhibit larger exchange rates due to the exterior doors in these zones and the people moving in and out of the building. The post office in Ann Arbor has a large amount of such pedestrian traffic, and large, leaky doors for loading and unloading mail.

The data of the form shown in Tables 6.3 to 6.7 were checked for accuracy and then stored in separate files according to the condition of the vents and occupancy of the building. Tables 6.8 and 6.9 show data from these files for the Ann Arbor building. Note the large ventilation rates in Table 6.9. These rates were measured during the spring season when the outdoor air is cool enough to condition the building without running the chillers.

Table 6.1 Tracer Gas Sampling Locations

Anchorage
1. Module A
2. Module B
3. Module C
4. Module D
5. Module E
6. Module F
7. 5th Floor Module C
8. 3rd Floor Module C
9. 1st Floor Module C

Springfield
1. North Return
2. South Return
3. Atrium/Lobby
4. 5th Floor - North
5. 4th Floor - North
6. 3rd Floor - North
7. 2nd Floor - North
8. 1st Floor - North
9. 4th Floor - South
10. 2nd Floor - South

Ann Arbor
1. HVAC Return
2. 4th Floor Return
3. 3rd Floor Return
4. 1st & 2nd Floor Return
5. Lobby
6. Post office

Huron
1. North Return
2. East Return
3. 4th Floor - North
4. 3rd Floor - North
5. 2nd Floor - North
6. 1st Floor - North
7. 4th Floor - East
8. 3rd Floor - East
9. 2nd Floor - East
10. 1st Floor - East

Columbia
1. HVAC Return
2. 13th Floor
3. 11th Floor
4. 9th Floor
5. 7th Floor
6. 5th Floor
7. 3rd Floor
8. 1st Floor & Basement
9. Lobby
10. Courthouse

Norfolk
1. HVAC Return
2. 8th Floor
3. 7th Floor
4. 6th Floor
5. 5th Floor
6. 4th Floor
7. 3rd Floor
8. 2nd Floor
9. 1st Floor

Fayetteville
1. 1st Floor
2. 2nd Floor
3. 3rd Floor
4. 4th Floor
5. 5th Floor
6. Courtroom - 5th Floor

Pittsfield
1. 1st Floor Return
2. 2nd Floor Return

Table 6.2

Average Air Infiltration Rates of Each Federal Building

	Changes per Hour	Percent of Design Heat Load
Anchorage	0.28	55%
Ann Arbor	0.70	48%
Columbia	0.40	52%
Fayetteville	0.33	23%
Huron	0.20	30%
Norfolk	0.52	52%
Pittsfield	0.32	30%
Springfield	0.52	61%

Table 6.3

Typical One-Hour Decay Test for Anchorage

FEDERAL BLDG. - ANCHORAGE 1/ 7/83 12

MAX CURRENT = 1750 MIN CURRENT = 1708

EXTERIOR TEMP. = -18.2 C WIND SPEED = 3.9 M/S WIND DIR. = 135. DEG.

+/- .1 C +/- .8 M/S

INTERIOR TEMPERATURES

	MOD A	MOD B	MOD C	MOD D	MOD E	MOD F	1ST C	3RD C	5TH C	
	22.5	22.3	0.0	0.0	23.3	23.5	22.6	22.7	22.7	C
+/-	.7	.1	0.0	0.0	0.0	0.0	.4	0.0	0.0	C

HVAC FAN OPERATION

MOD A	MOD B	MOD C	MOD D	MOD E	MOD F	
3599	3599	3599	3599	3599	3599	SEC

TRACER CONCENTRATIONS

	MOD A	MOD B	MOD C	MOD D	MOD E	MOD F	1ST C	3RD C	5TH C	
12:00	114.6	108.9	101.1	91.8	78.2	81.4	68.2	86.5	103.3	ppb
12:10	105.0	98.2	99.9	88.2	76.1	77.7	62.3	78.6	97.4	ppb
12:20	102.6	96.6	92.4	83.2	73.7	74.6	49.9	76.6	97.6	ppb
12:30	93.9	90.1	89.3	82.2	69.2	69.2	46.3	72.8	130.3	ppb
12:40	91.2	84.3	79.0	76.8	65.1	64.1	48.9	66.1	80.9	ppb
INFIL	.31	.32	.44	.26	.32	.39	.48	.34	.16	/HR

Table 6.4

Typical One-Hour Decay Test for Springfield

FEDERAL BLDG. - SPRINGFIELD, M 12/ 2/82 0

MAX CURRENT = 1862 MIN CURRENT = 1810

EXTERIOR TEMP. = 12.1 C WIND SPEED = 1.3 M/S WIND DIR. = 247. DEG.

+/- .1 C +/- .6 M/S

INTERIOR TEMPERATURES

	NORTH	SOUTH	LOBBY	N 5TH	N 4TH	N 3RD	N 2ND	N 1ST	S 4TH	S 2ND	
	23.4	24.3	27.8	24.7	23.7	23.4	23.0	24.3	24.5	24.3	C
+/-	.2	.1	0.0	.1	.1	.1	.1	.1	.1	0.0	C

HVAC FAN OPERATION

NORTH	SOUTH	ATRIUM	
0	0	0	SEC

TRACER CONCENTRATIONS

	NORTH	SOUTH	LOBBY	N 5TH	N 4TH	N 3RD	N 2ND	N 1ST	S 4TH	S 2ND	
0:00	176.3	220.0	177.0	161.2	156.7	155.9	159.9	135.4	215.6	203.1	ppb
0:10	144.5	195.5	149.9	148.0	149.8	148.0	146.1	128.6	206.1	192.8	ppb
0:20	138.4	179.2	140.8	142.3	138.7	141.5	133.1	121.4	196.1	177.0	ppb
0:30	130.2	175.0	126.0	136.2	132.1	134.1	131.3	109.9	185.4	176.3	ppb
0:40	127.6	164.6	119.9	123.9	121.9	129.6	126.1	109.4	173.8	166.9	ppb
INFIL	.26	.32	.47	.35	.40	.27	.27	.35	.34	.26	/HR

Table 6.5

Typical One-Hour Decay Test for Norfolk

FEDERAL BUILDING - NORFOLK, VA 10/21/82 0

MAX CURRENT = 1665 MIN CURRENT = 1621

EXTERIOR TEMP. = 17.5 C WIND SPEED = 2.0 M/S WIND DIR. = 135. DEG.

+/- 0.0 C +/- .6 M/S

INTERIOR TEMPERATURES

	RET	8TH F	7TH F	6TH F	5TH F	4TH F	3RD F	2ND F	1ST F	
	25.7	25.7	25.4	24.6	24.7	24.7	24.8	24.4	23.5	C
+/-	.1	0.0	.2	0.0	0.0	0.0	0.0	0.0	0.0	C

HVAC FAN OPERATION

M HVAC	1ST FL	
0	0	SEC

TRACER CONCENTRATIONS

	RET	8TH F	7TH F	6TH F	5TH F	4TH F	3RD F	2ND F	1ST F	
0:00	137.9	107.2	128.5	126.4	119.0	120.9	127.4	114.9	68.0	ppb
0:10	126.9	95.6	116.0	118.1	111.1	113.7	118.7	106.6	51.9	ppb
0:20	117.1	90.1	111.7	112.1	106.5	106.6	112.7	93.8	49.3	ppb
0:30	111.1	84.1	101.7	106.9	96.9	97.1	105.7	86.4	36.5	ppb
0:40	101.7	77.3	97.9	98.0	92.7	88.2	98.4	79.7	30.0	ppb
INFIL	.43	.42	.36	.36	.38	.51	.38	.57	1.17	/HR

Table 6.6

Typical One-Hour Decay Test for Huron

FEDERAL BUILDING - HURON, S.D. 10/ 8/82 11

MAX CURRENT = 659 MIN CURRENT = 611

EXTERIOR TEMP. = 10.2 C WIND SPEED = 1.5 M/S WIND DIR. = 135. DEG.

+/- .6 C +/- .9 M/S

INTERIOR TEMPERATURES

	N RET	E RET	N 4TH	N 3RD	N 2ND	N 1ST	
	26.0	24.4	25.9	27.0	26.0	24.6	C
+/-	.6	0.0	.1	.3	.1	0.0	C

HVAC FAN OPERATION

ZONE 1	ZONE 2	
594	595	SEC

TRACER CONCENTRATIONS

	N RET	E RET	N 4TH	N 3RD	N 2ND	N 1ST	
11:00	99.8	121.4	99.5	95.2	96.9	93.1	ppb
11:10	89.8	88.8	89.9	87.9	86.0	86.9	ppb
11:20	82.7	77.6	83.5	84.8	82.9	84.4	ppb
11:30	82.1	76.1	82.1	81.3	82.4	81.6	ppb
11:40	78.6	75.1	81.4	80.9	80.8	78.3	ppb
INFIL	.24	.31	.19	.17	.12	.21	/HR

Table 6.7

Typical One-Hour Decay Test for Columbia

FEDERAL BUILDING - COLUMBIA 11/19/82 0

MAX CURRENT = 1708 MIN CURRENT = 1660

EXTERIOR TEMP. = 14.6 C WIND SPEED = 1.0 M/S WIND DIR. = 157. DEG.

+/- .1 C +/- .6 M/S

INTERIOR TEMPERATURES

	M RET	13 FL	11 FL	9 FL	7 FL	5 FL	3 FL	1ST-B	LOBBY	COURT	
	27.6	27.7	27.2	27.5	27.2	26.6	26.3	22.2	21.7	24.3	C
+/-	.4	0.0	0.0	0.0	0.0	.1	0.0	0.0	.1	0.0	C

HVAC FAN OPERATION

TOWER	1ST-BAS	COURT	
0	0	0	SEC

TRACER CONCENTRATIONS

	M RET	13 FL	11 FL	9 FL	7 FL	5 FL	3 FL	1ST-B	LOBBY	COURT	
0:00	96.1	94.4	85.6	91.3	85.0	84.9	92.2	32.9	33.3	44.9	ppb
0:10	86.3	89.8	80.5	88.0	84.6	80.5	91.0	28.1	29.0	42.3	ppb
0:20	82.0	86.5	78.2	85.5	79.4	78.3	89.2	27.8	26.4	39.8	ppb
0:30	78.4	83.6	74.0	80.8	78.6	75.7	84.2	24.5	25.0	37.6	ppb
0:40	75.5	80.5	70.6	77.2	72.0	69.8	79.7	23.8	22.4	35.8	ppb
INFIL	.27	.22	.27	.27	.30	.28	.27	.37	.50	.34	/HR

Table 6.8

Data Files for Ann Arbor Building with No Outside Air Intake

CITY AND BUILDING : FEDERAL BUILDING - ANNARBOR

CONDITION : 0% OUTSIDE AIR
CONDITION : VENTS UNSEALED
CONDITION : WIND DATA

DATE	HOUR	W.SPEED	W.DIR	T.OUT	T.IN	T.DIFF	AI.AVE
2/ 4/83	18	1.4	270.0	1.4	22.9	21.5	.86

HVAC	.47
4TH F	.71
3RD F	.39
1&2 F	.57
LOB.	.76
P.O.	2.28

DATE	HOUR	W.SPEED	W.DIR	T.OUT	T.IN	T.DIFF	AI.AVE
2/ 4/83	19	1.1	270.0	1.8	22.7	20.9	.95

HVAC	1.24
4TH F	1.01
3RD F	.54
1&2 F	.52
LOB.	.97
P.O.	1.43

DATE	HOUR	W.SPEED	W.DIR	T.OUT	T.IN	T.DIFF	AI.AVE
2/ 4/83	20	1.0	270.0	1.5	22.5	21.0	.81

HVAC	.62
4TH F	.42
3RD F	.62
1&2 F	.58
LOB.	1.22
P.O.	1.37

DATE	HOUR	W.SPEED	W.DIR	T.OUT	T.IN	T.DIFF	AI.AVE
2/ 4/83	21	1.0	270.0	.8	22.3	20.8	.93

HVAC	.54
3RD F	.64
1&2 F	.66
LOB.	1.53
P.O.	1.26

DATE	HOUR	W.SPEED	W.DIR	T.OUT	T.IN	T.DIFF	AI.AVE
2/ 4/83	22	.8	270.0	1.4	22.1	20.7	.82

HVAC	.61
4TH F	.57
3RD F	.64
1&2 F	.62
LOB.	1.27
P.O.	1.23

Table 6.9

Data Files for Ann Arbor Building with Outside Air Intake

CITY AND BUILDING : FEDERAL BUILDING - ANN ARBOR

CONDITION : AIR INTAKE
CONDITION : VENTS UNSEALED
CONDITION : WIND DATA

DATE	HOUR	W.SPEED	W.DIR	T.OUT	T.IN	T.DIFF	AI.AVE
5/25/83	8	1.8	157.5	15.0	24.0	9.0	3.22

HVAC = 3.19
4TH F = 3.90
3RD F = 3.38
2ND F = 3.98
1ST F = 2.94
LOB. = 1.90

DATE	HOUR	W.SPEED	W.DIR	T.OUT	T.IN	T.DIFF	AI.AVE
5/25/83	9	1.5	247.5	14.3	23.8	9.5	2.11

HVAC = 2.51
4TH F = 1.82
3RD F = 2.58
2ND F = 2.51
1ST F = 1.25
LOB. = 1.97

DATE	HOUR	W.SPEED	W.DIR	T.OUT	T.IN	T.DIFF	AI.AVE
5/25/83	10	2.0	270.0	13.8	23.6	9.8	2.32

HVAC = 3.00
4TH F = 2.96
3RD F = 2.78
2ND F = 2.85
1ST F = .51
LOB. = 1.83

DATE	HOUR	W.SPEED	W.DIR	T.OUT	T.IN	T.DIFF	AI.AVE
5/25/83	11	1.9	270.0	13.8	23.6	9.8	2.58

HVAC = 3.24
4TH F = 2.52
3RD F = 3.00
2ND F = 2.71
1ST F = 1.86
LOB. = 2.17

DATE	HOUR	W.SPEED	W.DIR	T.OUT	T.IN	T.DIFF	AI.AVE
5/25/83	12	1.9	270.0	14.2	23.5	9.3	2.73

HVAC = 2.78
4TH F = 3.34
3RD F = 3.10
2ND F = 3.71
1ST F = 1.65
LOB. = 1.79

The air infiltration rates for each building are plotted against inside-outside temperature difference ΔT in figure 6.1. Among the eight buildings there are varying degrees of dependence of infiltration on temperature difference. The most noticeable dependence occurs in the cases of Ann Arbor, Huron, Norfolk and Springfield. These buildings, with the exception of Huron, are also the leakiest. The lines shown in figure 6.1 are based on linear regressions of infiltration against temperature difference for positive values of ΔT. The equations of these lines for the eight cities are given by:

Anchorage: $I = 0.164 + 0.0019\ \Delta T\ (^{o}F)$; $r^2 = .180$; $s = .071$
$(0.0034\ \Delta T\ (^{o}C))$

Ann Arbor: $I = 0.444 + 0.0062\ \Delta T\ (^{o}F)$; $r^2 = .352$; $s = .112$
$(0.0111\ \Delta T\ (^{o}C))$

Columbia: $I = 0.333 + 0.0026\ \Delta T\ (^{o}F)$; $r^2 = .052$; $s = .117$
$(0.0047\ \Delta T\ (^{o}C))$

Fayetteville: $I = 0.243 + 0.0023\ \Delta T\ (^{o}F)$; $r^2 = .151$; $s = .062$
$(0.0042\ \Delta T\ (^{o}C))$

Huron: $I = 0.107 + 0.0026\ \Delta T\ (^{o}F)$; $r^2 = .255$; $s = .055$
$(0.0046\ \Delta T\ (^{o}C))$

Norfolk: $I = 0.464 + 0.0035\ \Delta T\ (^{o}F)$; $r^2 = .287$; $s = .082$
$(0.0064\ \Delta T\ (^{o}C))$

Pittsfield: $I = 0.351 - 0.0016\ \Delta T\ (^{o}F)$; $r^2 = .021$; $s = .113$
$(0.0029\ \Delta T\ (^{o}C))$

Springfield: $I = 0.167 + 0.0094\ \Delta T\ (^{o}F)$; $r^2 = .275$; $s = .121$
$(0.0169\ \Delta T\ (^{o}C))$

s is the standard error of the estimate. Some of the buildings' infiltration rates also exhibited a dependence on wind speed u. Figure 6.2 shows several plots of infiltration versus u, with regression lines drawn in. The equations of these lines are given by the following:

Ann Arbor: ΔT from 68 to 77°F (20 to 25°C):
$I = 0.399 + 0.051u\ (mph)\ (0.113u\ (m/s))$; $r^2 = .414$; $s = .145$

Fayetteville: ΔT from 32 to 41°F (0 to 5°C):
$I = -0.174 + 0.102u\ (mph)\ (0.228u\ (m/s))$; $r^2 = .672$; $s = .206$

Huron: ΔT from 68 to 77°F (20 to 25°C):
$I = 0.225 + 0.0046u\ (mph)\ (0.0102u\ (m/s))$; $r^2 = .221$; $s = .024$

Huron: ΔT from 77 to 86°F (25 to 30°C):
$I = 0.205 + 0.0081u\ (mph)\ (0.0181u\ (m/s))$; $r^2 = .131$; $s = .054$

Tables 6.10 through 6.17 give mean measured infiltration rates for each building within various ranges of temperature difference. Means are given for wind speeds less than 4.5 mph (2.0 m/s) and greater than 4.5 mph (2.0 m/s).

Temperature Difference Bin		Wind < 4.5 mph (2.0 m/s)	Wind > 4.5 mph (2.0 m/s)
°F	(°C)	(X/HR)	(X/HR)
0, 18	(0, 10)	0.19	-
18, 36	(10, 20)	0.20	0.23
36, 54	(20, 30)	0.38	0.24
54, 72	(30, 40)	0.25	0.31

Table 6.10 Average Air Exchange Rates in Various Temperature Difference Bins During Unoccupied Periods with Dampers Closed - Anchorage, AK

Temperature Difference Bin		Wind < 4.5 mph (2.0 m/s)	Wind > 4.5 mph (2.0 m/s)
°F	(°C)	(X/HR)	(X/HR)
-18, 0	(-10, 0)	0.40	0.40
0, 18	(0, 10)	0.37	0.33
18,36	(10, 20)	0.41	0.38
36, 54	(20, 30)	0.34	0.51

Table 6.11 Average Air Exchange Rates in Various Temperature Difference Bins During Unoccupied periods with Dampers Closed - Columbia, SC

Temperature Difference Bin		Wind < 4.5 mph (2.0 m/s)	Wind > 4.5 mph (2.0 m/s)
°F	(°C)	(X/HR)	(X/HR)
-36, -18	(-20, -10)	0.56	-
-18, 0	(-10, 0)	0.56	0.55
0, 18	(0, 10)	0.50	0.50
18, 36	(10, 20)	0.49	0.54

Table 6.12 Average Air Exchange Rates in Various Temperature Difference Bins During Unoccupied periods with Dampers Closed - Norfolk, VA

Temperature Difference Bin		Wind < 4.5 mph (2.0 m/s)	Wind > 4.5 mph (2.0 m/s)
°F	(°C)	(X/HR)	(X/HR)
-18, 0	(-10, 0)	0.38	0.35
0, 18	(0, 10)	0.44	-
18, 36	(10, 20)	0.43	0.56
36, 54	(20, 30)	0.55	0.53

Table 6.13 Average Air Exchange Rates in Various Temperature Difference Bins During Unoccupied periods with Dampers Closed - Springfield, MA

Temperature Difference Bin		Wind < 4.5 mph (2.0 m/s)	Wind > 4.5 mph (2.0 m/s)
°F	(°C)	(X/HR)	(X/HR)
-18, 0	(-10, 0)	0.25	-
0, 18	(,0 10)	0.29	0.37
18, 36	(10, 20)	0.36	0.31
36, 54	(20, 30)	0.26	-

Table 6.14 Average Air Exchange Rates in Various Temperature Difference Bins During Unoccupied periods with Dampers Closed - Pittsfield, MA

Temperature Difference Bin		Wind < 4.5 mph (2.0 m/s)	Wind > 4.5 mph (2.0 m/s)
°F	(°C)	(X/HR)	(X/HR)
0, 18	(0, 10)	0.13	0.14
18, 36	(10, 20)	0.10	0.11
36, 54	(20, 30)	0.23	0.26
54, 72	(30, 40)	0.26	0.26
72, 90	(40, 50)	0.26	-

Table 6.15 Average Air Exchange Rates in Various Temperature Difference Bins During Unoccupied periods with Dampers Closed - Huron, SD

Temperature Difference Bin		Wind < 4.5 mph (2.0 m/s)	Wind > 4.5 mph (2.0 m/s)
°F	(°C)	(X/HR)	(X/HR)
-18, 0	(-10, 0)		.370
0, 18	(0, 10)	0.28	0.50
18, 36	(10, 20)	0.29	0.35
36, 54	(20, 30)	0.39	0.35

Table 6.16 Average Air Exchange Rates in Various Temperature Difference Bins During Unoccupied periods with Dampers Closed - Fayettevile, AR

Temperature Difference Bin		Wind < 4.5 mph (2.0 m/s)	Wind > 4.5 mph (2.0 m/s)
°F	(°C)	(X/HR)	(X/HR)
0, 18	(0, 10)	0.53	0.52
18,36	(10, 20)	0.59	0.64
36, 54	(20, 30)	0.61	0.73

Table 6.17 Average Air Exchange Rates in Various Temperature Difference Bins During Unoccupied periods with Dampers Closed - Ann Arbor, MI

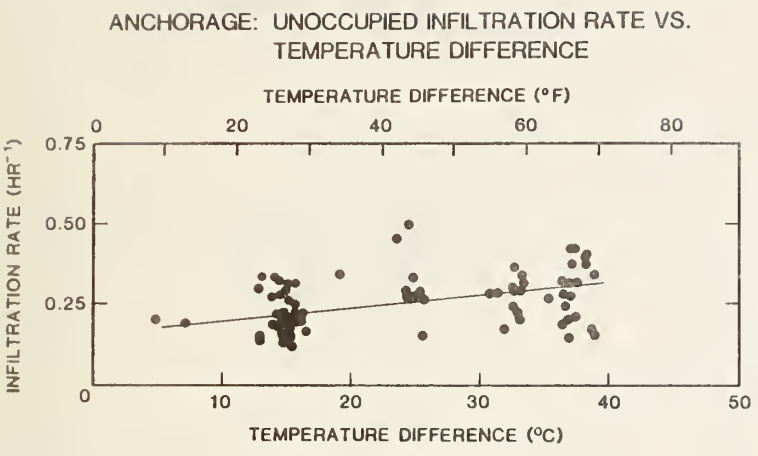

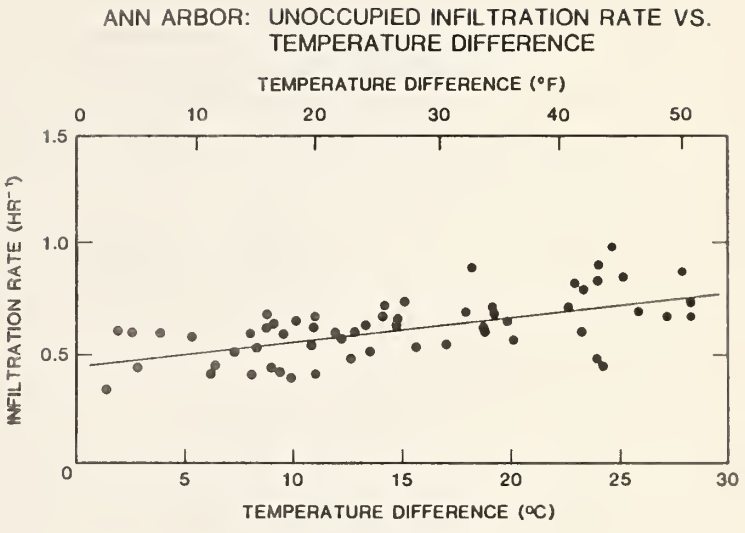

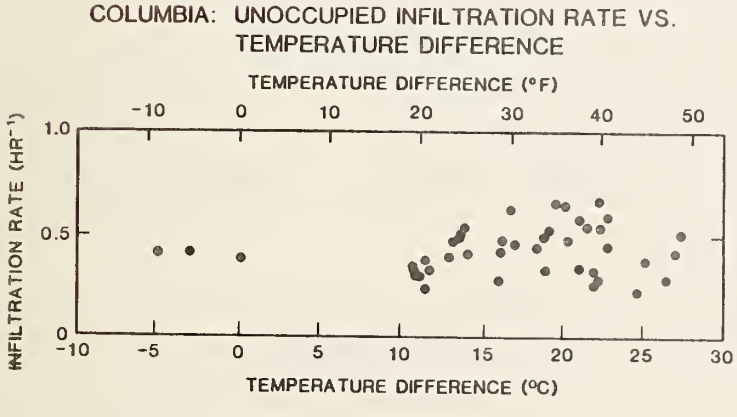

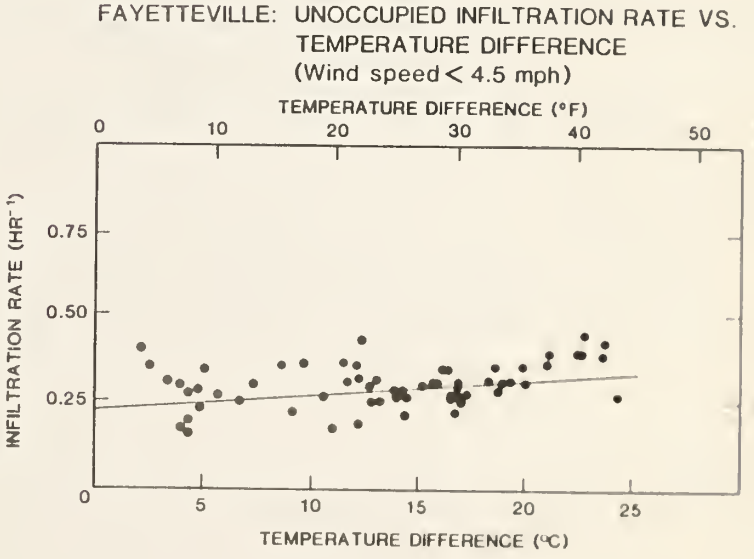

Figure 6.1 Infiltration Rate Versus Temperature Difference

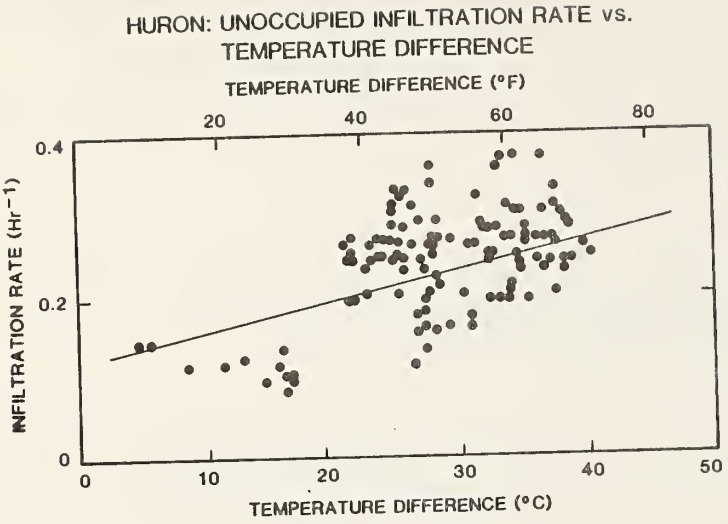

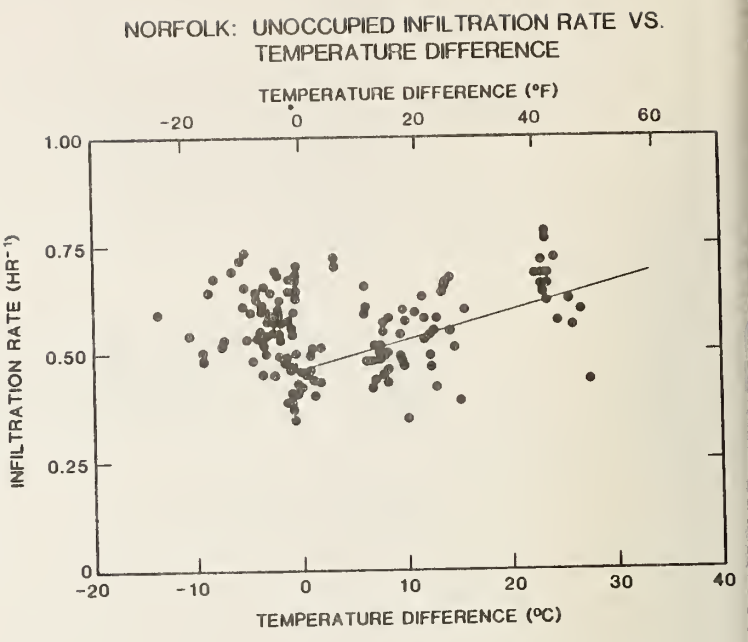

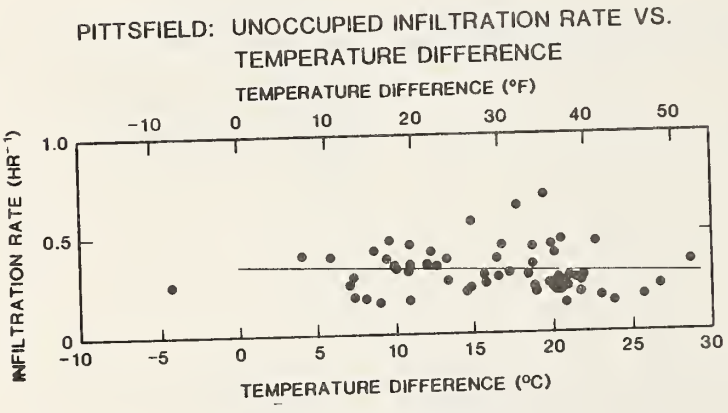

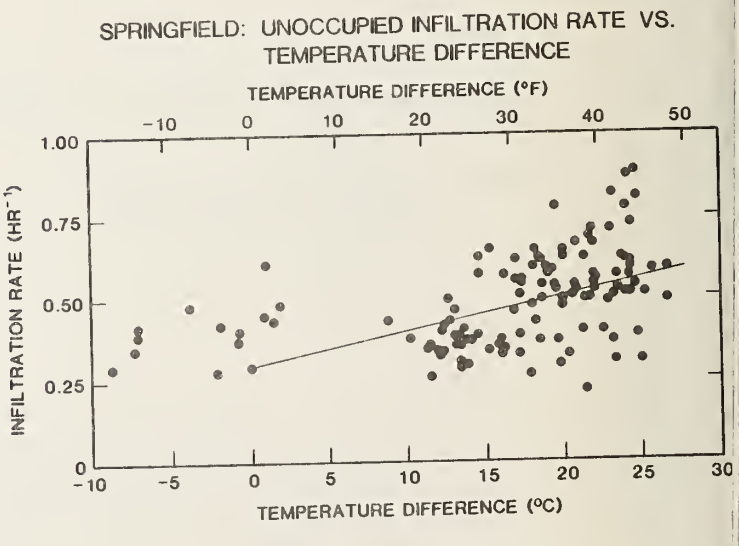

Figure 6.1 (continued) Infiltration Rates Versus Temperature Difference

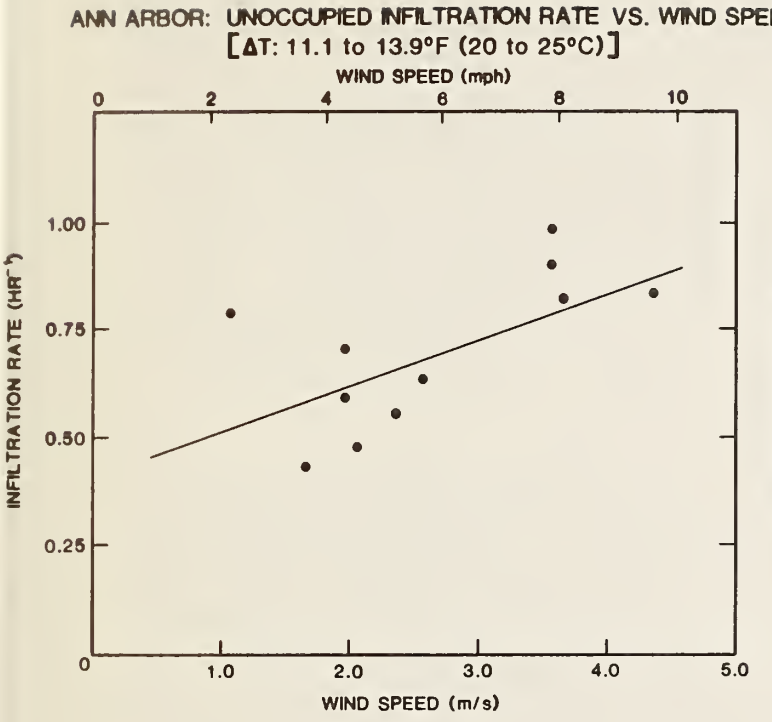

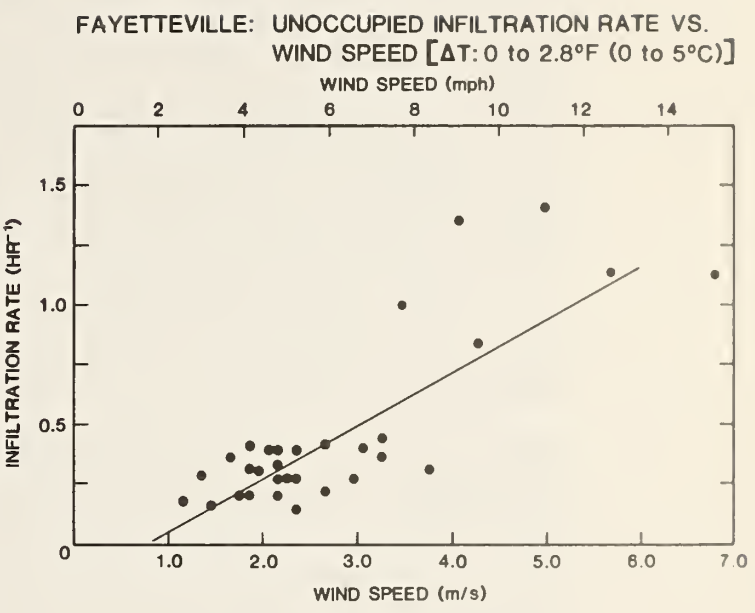

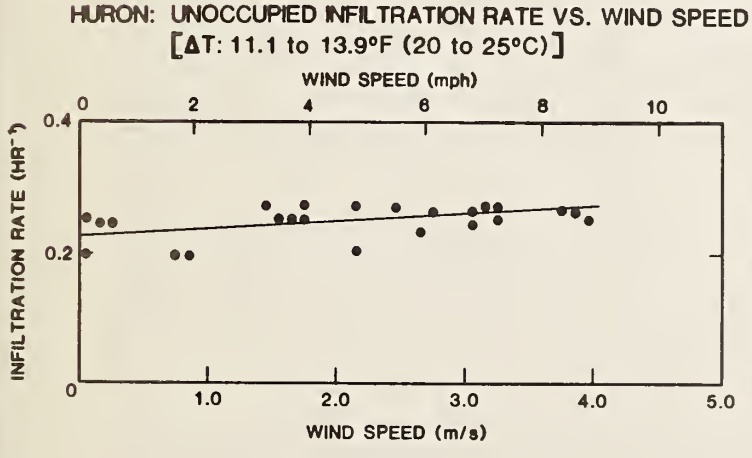

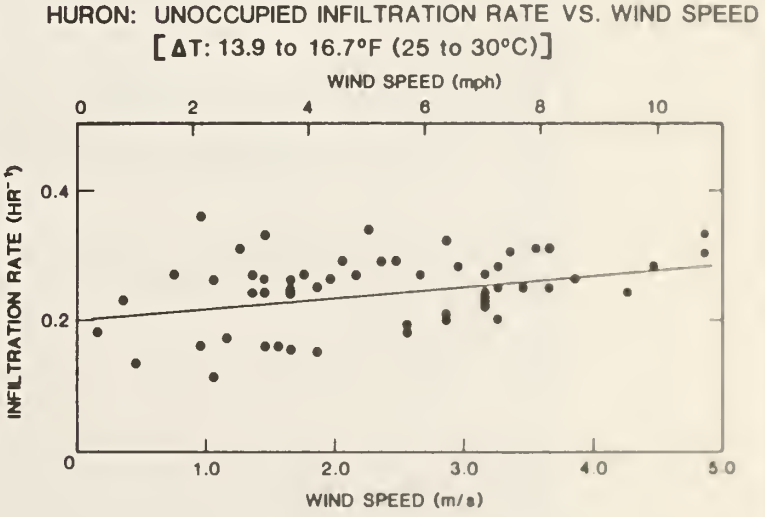

Figure 6.2 Infiltration Rates Versus Wind Speed

6.3 Measured Ventilation Rates

In most of the buildings the measured ventilation rates exhibit a seasonal dependence such that the lowest ventilation rates occur during maximum heating and cooling loads. This can be seen in the ventilation rate versus inside-outside temperature difference plots for each federal building shown in figure 6.3. Table 6.18 shows mean ventilation rates, along with the standard deviations of these means, for 9°F (5°C) intervals of temperature difference for all eight buildings. The mean ventilation rates can be somewhat misleading for mild temperature conditions. Buildings with enthalpy control are operated at low or high ventilation rates at the same outside temperature because of differences in outside humidity. This variation in ventilation rate at the same outside temperature also occurs in buildings with other types of control systems. Also, as discussed below, the ventilation rate at a given temperature can be affected by weather conditions in buildings for which weather induced infiltration is a significant portion of the total ventilation rate.

Figure 6.3 shows the ventilation rate in the Anchorage federal building as a function of temperature difference. There are low ventilation rates, about 0.25 to 0.50 exchanges per hour, during cold outside conditions and higher ventilation rates for temperature differences below 36°F (20°C). None of the measurements in Anchorage were made under conditions which were warm enough for the building's air conditioning system to be used for cooling and for the ventilation rate to again be minimized.

Figure 6.3 also shows the ventilation rate of the Ann Arbor federal building plotted against temperature difference. These data exhibit a large amount of scatter due in part to some very high ventilation rates induced by high wind speeds. This implies that the infiltration rate of the Ann Arbor building was strongly dependent on wind speed and that infiltration became a significant portion of the net ventilation rate under windy conditions. Figure 6.4 includes a plot of these ventilation rates versus wind speed for a limited range of temperature difference, and indeed a strong dependence is evident. A similar dependence of infiltration on wind speed was noted earlier in figure 6.2. These large, wind induced rates were not considered in calculating the Ann Arbor mean ventilation rates in table 6.18. Under cold outside conditions, $\Delta T > 36°F$ (20°C), this building was operated at about 0.5 exchanges per hour. For milder temperatures, outside air was used to cool the building with ventilation rates as large as 3.0 exchanges per hour. When the temperature difference was close to zero, the ventilation rates did return to 0.5 exchanges per hour. Thus, in the Ann Arbor building, the summer and winter ventilation rates were similar.

The Columbia building's ventilation rates cover a wide range of warm temperature conditions (ΔT from -18 to 9°F (-10 to 5°C)), but there is no clear dependence of ventilation rate on temperature difference for the summer. If the weather dependent natural ventilation, or infiltration, is a large fraction of the net ventilation rate which was measured, then the data may show a dependence on temperature difference. Such a dependence would tend to imply that infiltration is similar in magnitude to the intentional ventilation.

When the Fayetteville building is being heated or cooled, the ventilation rate is about 0.35 exchanges per hour. Under mild temperature conditions, T from 0 to 9°F (0 to 5°C), the ventilation rate varies between 0.35 and 1.5 exchanges per hour. The ten high ventilation rates between 1.0 and 1.5 exchanges per hour were measured under very windy conditions and probably were due to a dominance of natural ventilation or infiltration, as in the Ann Arbor building. Attempts to pressure test this building using its own supply fans, while successful in the other seven federal buildings, were unsuccessful in Fayetteville because the ventilation system could not bring in enough outside air to raise the internal pressure significantly. Thus, the ventilation rates of 1.0 exchanges per hour and higher are probably not due to mechanical ventilation alone and contain a large component of natural ventilation induced by the high wind speeds during these measurements. The wind speed dependence of infiltration for this building is evident in figure 6.4.

The Huron building has the lowest ventilation rates of all the buildings examined. Under hot and cold outside temperature conditions, ventilation rates of 0.2 exchanges per hour and less were measured. The cold weather ventilation measurements exhibit a dependence on both wind speed and temperature difference. This is the only building which showed a significant dependence of measured ventilation rate on temperature difference.

Figure 6.1 shows the dependence of infiltration on ΔT for this building, which also appears in the ventilation data. The Huron ventilation rates in figure 6.3 exhibit additional scatter due to wind effects. Figure 6.4 contains two plots of ventilation versus wind speed in the Huron building for two different ranges of temperature difference. Plots of infiltration versus wind speed, shown in figure 6.2, for the same building also show some dependence, though not as strong as for ventilation. It is possible that the wind effects are enhanced when the outside air intake dampers are open.

In the Norfolk building the winter and summer ventilation rates are comparable, both around 0.6 to 0.7 exchanges per hour. In the Pittsfield building, the minimum ventilation rates during cold weather are lower than the warm weather ventilation rates.

The Springfield building ventilation rates exhibit an unusual pattern. The ventilation rates under warm conditions, $\Delta T < 18°F$ (10°C) are relatively constant at about 0.6 exchanges per hour. For temperature differences greater than about 27°F (15°C), the ventilation rate varies from a minimum of 0.6 to a maximum of about 1.25 exchanges per hour. It is not clear if the high ventilation rates are due to intentional outside air intake, or to a strong dependence of infiltration on temperature difference. The outside air intake is controlled to maintain the supply air temperature at about 55°F (13°C). This is indeed the temperature difference at which the ventilation rate is seen to increase. Measurements of infiltration made with the outside air dampers closed show a similar, but less extreme, dependence on temperature difference (see figure 6.1). Thus the dependence of the net measured ventilation on ΔT appears to be a combination of the outside air intake control strategy and a significant portion of temperature dependent infiltration.

6.4 Minimum Ventilation Requirements

The measurements of actual ventilation rates in occupied office buildings are compared to ventilation standards and design specifications of minimum fresh air intake. A certain minimum ventilation rate must be maintained to remove pollutants generated inside a building. These minimum ventilation rates are determined by the building occupancy level (number of people per 1,000 ft^2 (100 m^2) of floor area) and the extent and nature of the activities within the building (smoking, painting and other pollutant generating activities). In some of the buildings, the mechanical equipment specifications give a minimum outside air intake level in units of volumetric air flow. Another commonly accepted minimum ventilation rate is equal to 10% of the HVAC system's total airflow rate. The American Society of Heating, Refrigerating, and Air-Conditioning Engineers (ASHRAE) has established minimum recommended building ventilation rates which are a function of occupancy levels, building type (e.g., office, store, hotel) and room type (e.g. kitchen, office, conference room) [12].

Table 6.19 lists the minimum ventilation rates, in units of exchanges per hour, based on 10% of total air for all the buildings. The minimum ventilation rates based on ASHRAE standard 62-81 [12] are also included for the cases of both smoking and non-smoking occupants in office buildings. In order to determine the recommended ventilation rate from the ASHRAE standard one needs to know the floor areas of each type of room in the building and the occupancy levels in each room. Since the occupancy levels in the buildings are not known, seven persons per 1,000 ft^2 (100 m^2) of floor area was used, which ASHRAE recommends when design or actual occupancy is not known. All the floor area was assumed to be office space, neglecting the fact that there are kitchens, bathrooms, conference rooms and waiting areas. At the estimated occupancy level for office space, ASHRAE recommends 20 cfm per person (10 L/s·person) when the occupants smoke and 5 cfm (2.5 L/s) when they do not smoke. When smoking is permitted, ASHRAE recommends using the ventilation rate for smoking conditions. Finally, the table lists a representative value for the minimum measured ventilation rate in each building.

In all the buildings, except Fayetteville, the 10% total air rate is less than the ASHRAE recommendation for smoking conditions. In Anchorage and Norfolk, the smoking rate is twice the 10% ventilation rate. The ASHRAE non-smoking value is less than all the 10% rates. Since smoking is permitted in all the buildings, the non-smoking recommendation is not relevant to the operation of the buildings.

Rather than compare the different ventilation standards to each other, it is more important to compare them to the ventilation rates measured in the buildings. The ASHRAE smoking recommendation is used for these comparisons. In Anchorage and Huron, the minimum ventilation rates when the buildings are heated or cooled are about one-third of the smoking rate. In fact, these measured ventilation rates are close to the ASHRAE non-smoking rates. In all the other buildings, the lowest measured ventilation rates are very close to, and at times lower than, the smoking ventilation rates. Thus, all of the buildings are at times being operated at ventilation rates which are lower than may be desirable for the maintainance of indoor air quality. As will be discussed below, local

variations in air distribution may lead to ventilation rates in specific zones which are very low.

The question of the adequacy of outside air intake is primarily an issue during hot and cold weather when outside air intake is at a minimum. This minimum outside air intake is supposedly assured by having a minimum outside air damper position or by keeping a certain portion of the outside air dampers open at all times. In other cases the outside air dampers are closed completely and it is assumed that leakage through the building envelope will fulfill the minimum outside air requirements.

It is interesting to compare the measured ventilation rates under conditions of minimum outside air intake to measurements of building infiltration made with the dampers totally closed and the HVAC fans running. These so-called infiltration rates provide a measure of the tightness of the building shell and of any leakage in the HVAC system. The measurements are not strictly a measure of the shell tightness because ventilation systems are often designed to pressurize a building which will lead to more air leakage than that induced by the weather alone. The daytime ventilation rates during periods of minimum outside air intake and the 0% outside air infiltration rates are compared for similar weather conditions. This comparison provides an indication of how much additional air is really brought in through the outside air intake to meet ventilation requirements and how much of the outside air intake results from uncontrolled air leakage. In Pittsfield and Springfield, the ventilation rates are about 0.2 exchanges per hour higher during occupied periods than the exchange rates when the building outside air dampers are closed tightly. In Anchorage, Columbia, Fayetteville, and Norfolk the difference is only 0.1 exchanges per hour, and in Huron and Ann Arbor the difference is insignificant. Thus, during times of minimum outside air intake, little of the outside air enters the Huron and Ann Arbor buildings through the outside air intake vents. In the rest of the buildings, the amount of air brought in through the vents is comparable to the ASHRAE nonsmoking ventilation recommendation. Thus, either the minimum outside air damper settings are much too low or the building designers are relying on residual air leakage or infiltration to meet outside air ventilation requirments.

Table 6.20 shows the monthly average ventilation rates for all nine buildings based on monthly average outside temperatures for the cities or nearby cities and an assumed inside temperature of 73°F (23 °C). The ventilation rate for each month is based on the averages in table 6.18 or visual inspection of the plots of ventilation versus temperature difference (figure 6.3) when the mean ventilation rate is not representative of the data. Again there are some very low monthly average ventilation rates in some of the buildings. In some cases, the monthly average ventilation rate is lower than the ASHRAE recommendation. Even when the monthly average is not below the recommendation, there will be periods during the month when the ventilation rate is lower.

6.5 Ventilation Efficiency

In measuring the ventilation rates in the eight office buildings it has been found that when the mechanical systems are bringing in minimum amounts of outside air, these rates are close to or below suggested ventilation levels. In addition, these measured rates are averages over an entire

building, and there are local variations in ventilation and in the uniformity of air distribution among zones, floors, rooms and parts of rooms. These local variations lead to lower effective ventilation rates in specific areas than for the whole building. Some of these variations are evident during the ventilation measurements after the injection of the SF_6 tracer when the SF_6 concentration on some of the floors does not increase at the same rate as the rest of the building. There are many ways to define ventilation efficiency, but they generally quantify the departure from uniform mixing of the supply air flowing into a space with the air in that space. In addition to a floor not receiving its proper portion of supply air flow, there can also be distribution problems on a floor. Individual rooms may not receive the appropriate amount of supply air even though the floor or zone is properly ventilated. This can happen when partitions are installed in a room and obstruct the intended airflow through the space. Finally, even within a well ventilated room the supply air may be removed through exhaust or return ducts before it mixes with the rest of the interior air. Occurrences of such "short-circuiting" further reduce the effective ventilation rate in the occupied spaces of a building. Thus, low ventilation efficiency can reduce an already low ventilation rate to a lower effective ventilation rate for the occupants of a building. The extent of such air distribution problems in buildings is not well known and needs to be investigated. Tracer gas techniques can be used to study air distribution and measure ventilation efficiency on a large scale (floors and zones) and on a small scale (within a room).

6.6 Conclusions

The average natural air infiltration rates measured in these buildings varied from 0.2 air changes per hour for the Huron federal building to 0.70 air changes per hour for the Ann Arbor federal building. The component of the design heating load from these buildings ranged from 23% for the uninsulated Fayetteville federal building to 61% for the new Springfield federal building. In four of the buildings air infiltration contributed to over 50% of the heating loads. Two of the federal buildings, Anchorage and Huron, have low air infiltration rates (0.28 and 0.20 air changes per hour). However, even for these buildings air infiltration was a very important part of the heating load.

Ventilation rates under occupied conditions were also measured in the eight buildings. It was found that for hot and cold outside temperatures, the buildings are operated at minimum ventilation levels to reduce space conditioning loads. At mild temperatures, outside air is used to cool the buildings and the ventilation rates increase significantly. The minimum ventilation rates show little temperature dependence in most of the buildings, but some of the buildings exhibit a dependence on wind speed. When the miniumum ventilation rates vary with weather conditions, this implies that uncontrolled air leakage or weather induced infiltration is a significant portion of the net ventilation rate. In most of the buildings, the summer and winter minimum ventilation rates are similar, but in some buildings there is a notable difference between the two minimum ventilation rates. The minimum ventilation rates were compared to minimum outside air intake levels suggested by ASHRAE, and it was found that most of the buildings were operated very close to or below the ASHRAE recommendation. Two of the buildings were operated well below this recommended ventilation rate. Local variations in air distribution and problems of ventilation

efficiency can lead to effective ventilation rates in specific areas of the building which are significantly lower than the average rate for the building. Three of the buildings, Springfield, Ann Arbor and Columbia, had minimum ventilation rates from 20 to 50% more than required, thus wasting energy during periods of extreme weather.

Table 6.18 Average Ventilation Rates in the Buildings

Temp Diff °F	(°C)	Anchorage	Ann Arbor*	Columbia	Fayetteville
-18,-9	(-10,-5)	--	--	0.68/0.18	--
-9,0	(-5,0)	--	--	0.68/0.21	0.36/0.12
0,9	(0,5)	--	0.94/0.95	0.69/0.32	0.65/0.39
9,18	(5,10)	1.34/0.36	1.94/0.42	1.10/0.90	0.35/0.07
18,27	(10,15)	1.22/0.25	1.96/0.97	1.09/0.56	0.35/0.01
27,36	(15,20)	1.10/0.23	0.86/0.20	0.64/0.26	0.32/0.02
36,45	(20,25)	--	0.47/0.07	0.62/0.24	--
45,54	(25,30)	0.46/0.14	--	--	--
54,63	(30,35)	0.24/0.04	--	--	--
63,72	(35,40)	0.36/0.10	--	--	--
72,81	(40,45)	0.26/0.02	--	--	--

Temp Diff °F	(°C)	Huron Mean/SD**	Norfolk	Pittsfield	Springfield
-27,-18	(-15,-10)	--	0.73/0.09	--	--
-18,-9	(-10,-5)	0.19/0.00	0.62/0.11	0.49/0.09	0.55/0.09
-9,0	(-5,0)	0.16/0.04	0.58/0.07	0.43/0.09	--
0,9	(0,5)	0.53/0.43	0.75/0.19	1.19/0.73	0.59/0.08
9,18	(5,10)	0.52/0.00	1.00/0.32	1.25/1.15	0.62/0.08
18,27	(10,15)	0.13/0.04	1.05/0.37	0.67/0.48	0.76/0.20
27,36	(15,20)	0.14/0.06	--	0.84/0.47	0.96/0.20
36,45	(20,25)	0.32/0.14	0.70/0.09	0.38/0.14	0.95/0.22
45,54	(25,30)	0.25/0.05	0.66/0.06	--	--
54,63	(30,35)	0.26/0.07	--	--	--
63,72	(35,40)	0.29/0.04	--	--	--
72,81	(40,45)	0.31/0.06	--	--	--

All the ventilation rates are in units of exchanges per hour.

---

* Calculations neglect some very high, wind induced ventilation rates.

** Standard deviation of the mean ventilation rate.

Table 6.19 Recommended Minimum Ventilation Rates in the Buildings

Building	10% Total Air	ASHRAE 62-81 Smoking	ASHRAE 62-81 Non Smoking	Measured Building Minimum	Measured Minimum as Percent of Requirement*
Anchorage	0.28	0.67	0.17	0.26	39%
Ann Arbor	0.36	0.38	0.09	0.47	124%
Columbia	0.28	0.41	0.10	0.62	151%
Fayetteville	0.57	0.41	0.10	0.32	78%
Huron	0.31	0.49	0.12	0.13	26%
Norfolk	0.25	0.69	0.17	0.62	90%
Pittsfield	0.32	0.42	0.10	0.38	90%
Springfield	0.44	0.46	0.12	0.55	120%

All the ventilation rates are in units of exchanges per hour.

* Based on ASHRAE 62-81 smoking requirement

Table 6.20 Monthly Average Ventilation Rates

Month	Anchorage[1]	Ann Arbor[2]	Columbia	Fayetteville[3]
January	0.46	0.47	0.64	0.32
February	0.46	0.47	1.09	0.32
March	0.46	0.47	1.09	0.35
April	0.75	1.96	1.10	0.35
May	1.10	1.94	0.69	0.65
June	1.22	0.94	0.68	0.36
July	1.22	0.50	0.68	0.36
August	1.22	0.50	0.68	0.36
September	1.22	1.94	0.68	0.36
October	0.75	1.96	1.10	0.35
November	0.46	0.86	1.09	0.35
December	0.46	0.47	0.64	0.32

	Huron	Norfolk	Pittsfield[4]	Springfield[4]
January	0.26	0.70	0.40	1.00
February	0.26	0.70	0.40	1.00
March	0.32	1.05	0.38	0.95
April	0.14	1.00	0.67	0.76
May	0.52	0.75	1.25	0.62
June	0.53	0.58	0.50	0.59
July	0.16	0.58	0.50	0.59
August	0.53	0.58	1.19	0.59
September	0.52	0.75	1.25	0.62
October	0.13	1.00	0.67	0.76
November	0.32	1.05	0.84	0.96
December	0.26	0.70	0.40	1.00

All the ventilation rates are in units of exchanges per hour.

1 Based on outside temperatures from Homer, AK.
2 Based on an average of outside temperatures from Flint and Detroit, MI.
3 Based on outside temperatures from Ft. Smith, AR.
4 Based on outside temperatures from Hartford, CT.

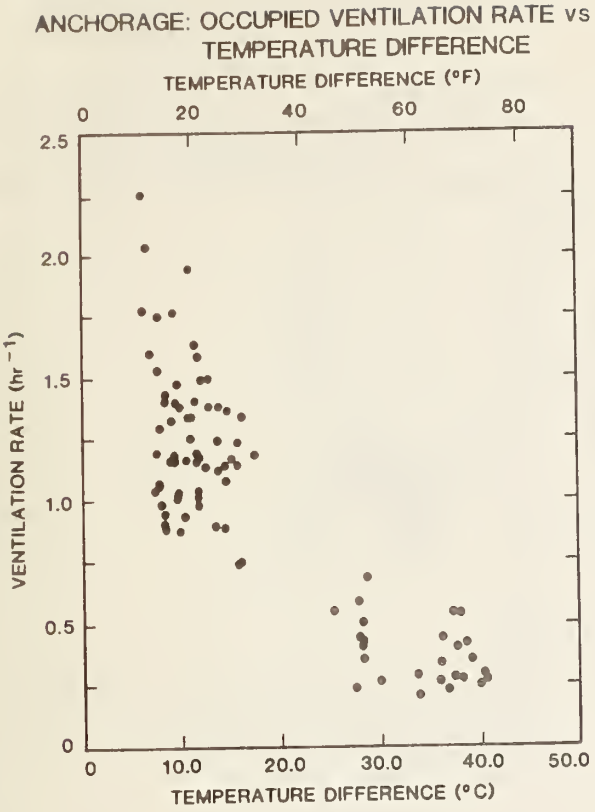

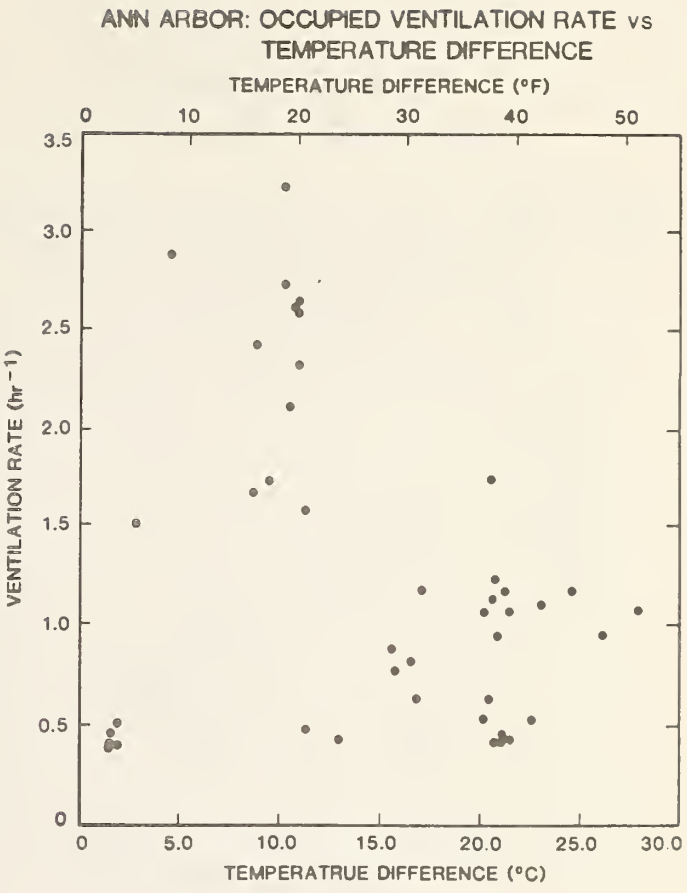

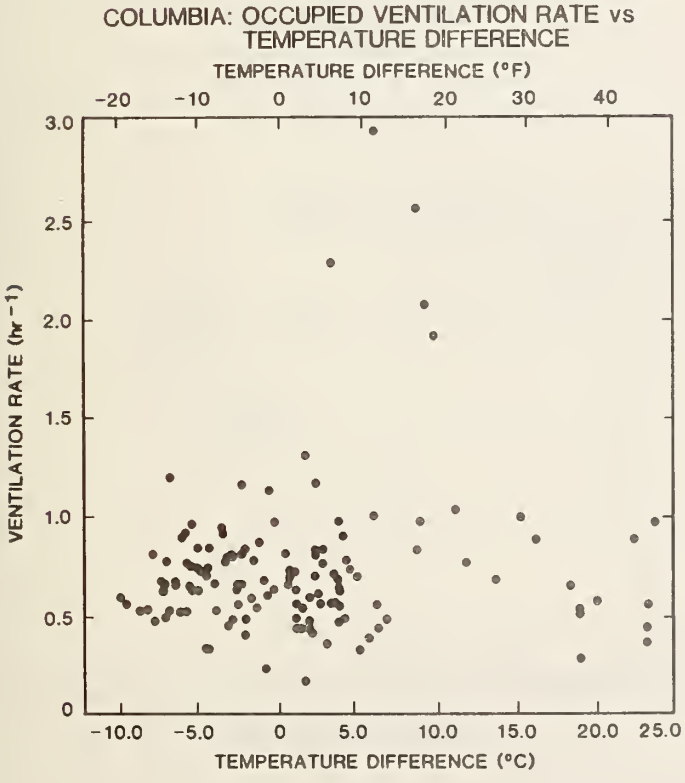

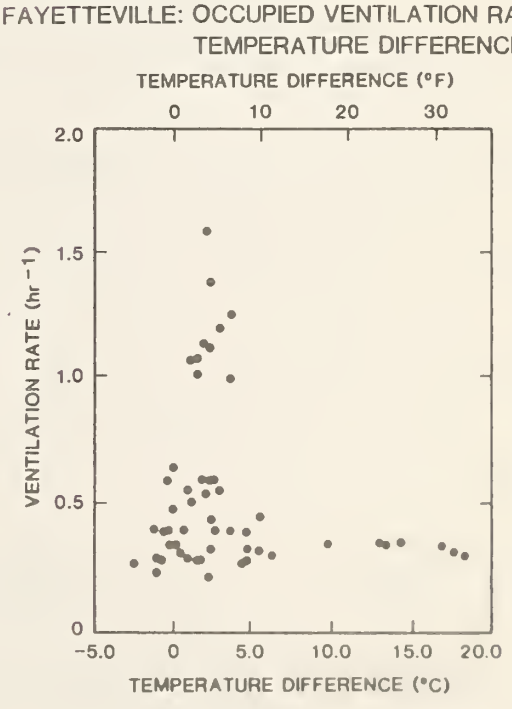

Figure 6.3 Ventilation Rate Versus Temperature Difference

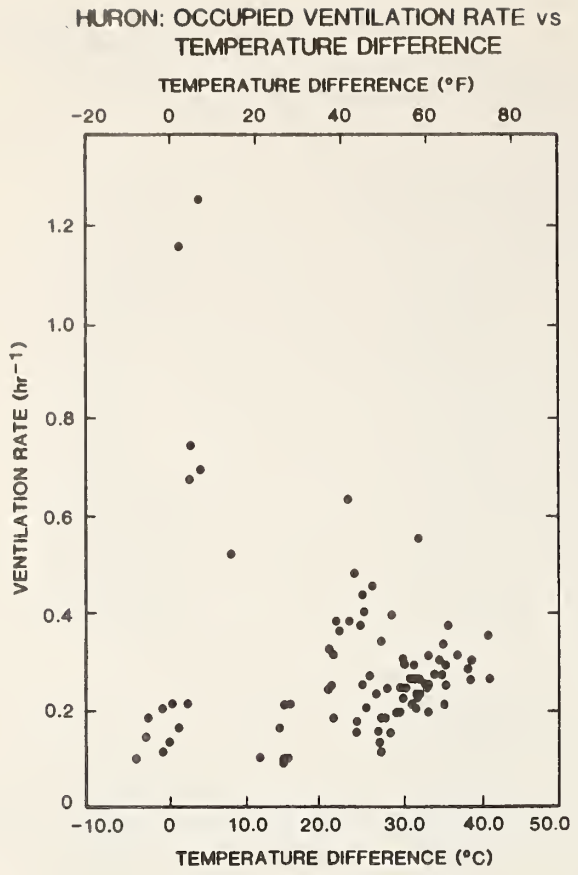

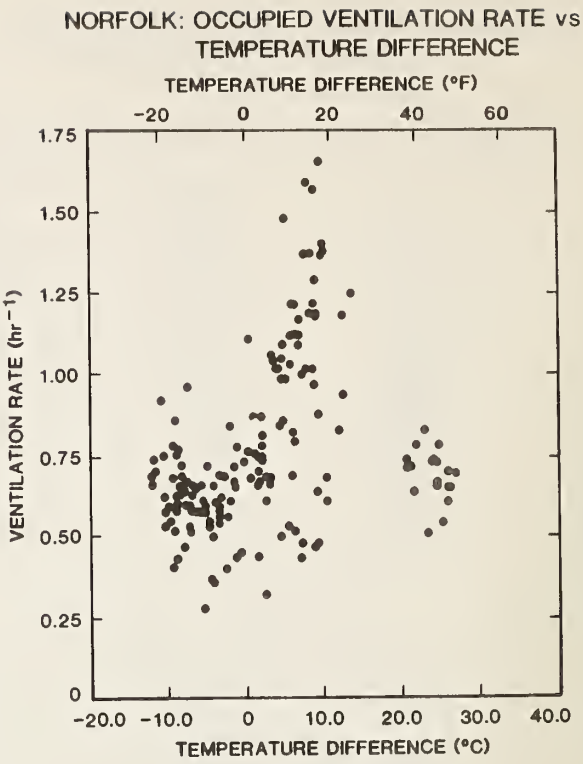

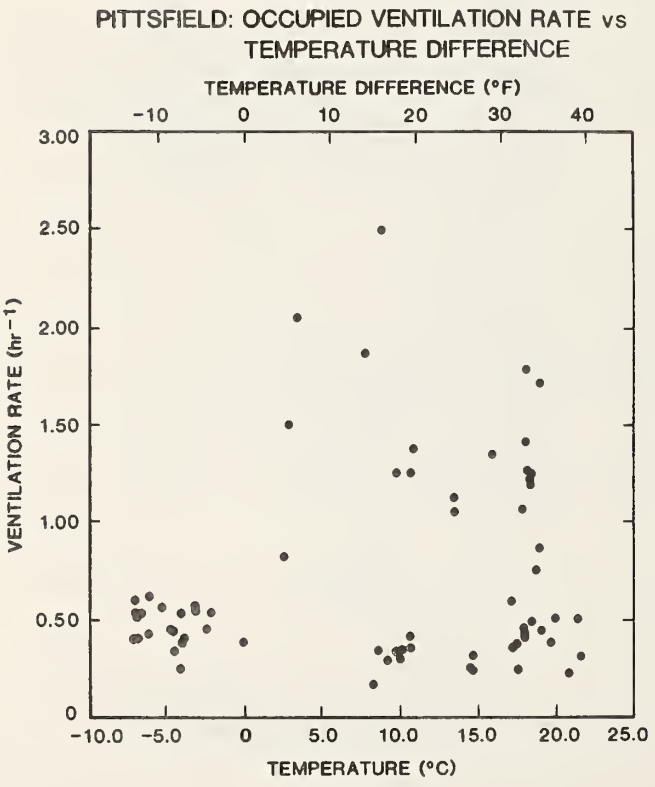

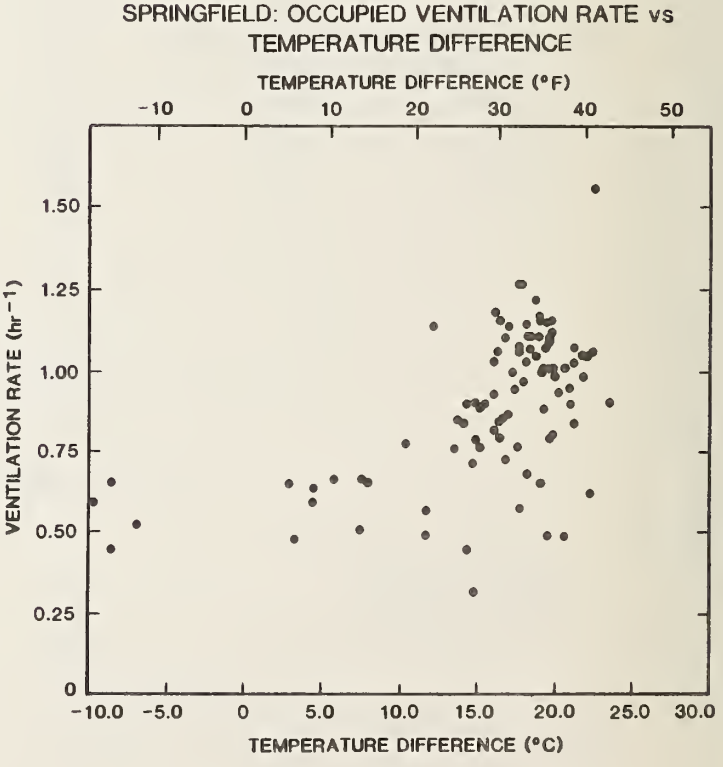

Figure 6.3 (continued) Ventilation Rate Versus Temperature Difference

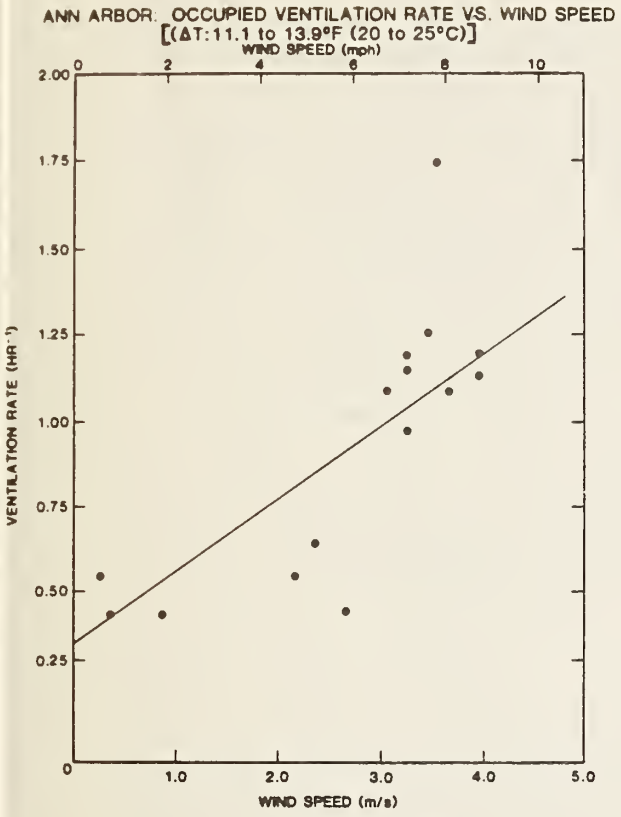

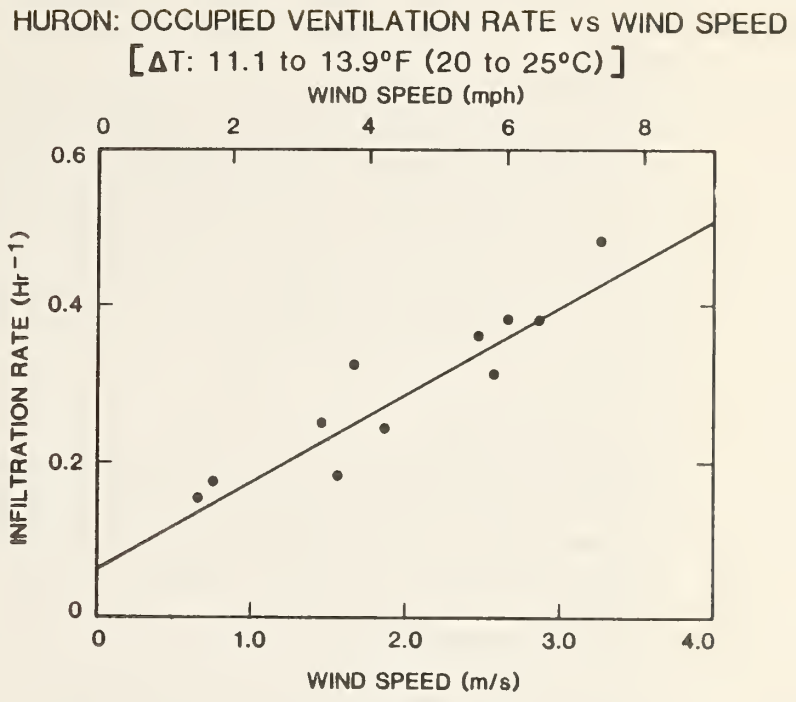

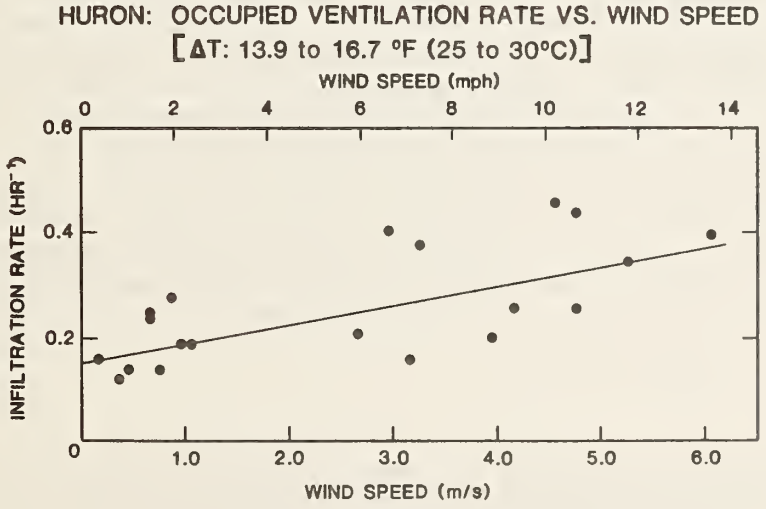

Figure 6.4 Ventilation Rate Versus Wind Speed

7. Building Tightness Testing Using Pressurization

7.1 Introduction

Whole building pressurization testing has been used for many years to evaluate the airtightness of single-family homes [13,14]. In this test method, a fan induces a large and uniform pressure difference across the building envelope, and the airflow rate required to induce a specific pressure difference between inside and outside serves as a measure of the airtightness of the building shell. Although the test conditions differ considerably from those which normally induce air exchange, pressurization testing provides a quick and quantitative measurement of building tightness. The technique has been used to evaluate the airtightness of a small number of large buildings [15,16]. Most of the previous pressurization measurements on large buildings involved bringing a high capacity fan to the building, as is done on a smaller scale for homes. The tests described below differ in that the existing HVAC equipment was used to pressure test the buildings. These tests employed a constant injection, tracer gas measurement technique to measure the airflow rate required to induce each inside-outside pressure difference. Seven of the eight federal buildings were subjected to whole building pressurization tests. Pressurization testing was also applied to individual windows to evaluate the airtightness of these components [17].

7.2 Test Methods

The buildings were pressure tested in a manner similar to that used in houses [7]. A large airflow into the building induced a large and constant pressure difference across the building envelope. Several different pressure differences were induced and the flow required to induce each pressure difference was measured. During the whole building pressurization tests the building ventilation system was arranged as shown in figure 7.1. The supply fans were operating while all return and exhaust fans were turned off. All return dampers were closed so that the supply air flowing into the building could only leave the interior through outside doors, windows and other leakage sites. The airflow through the supply fans was measured using a constant flow, tracer gas injection scheme [18]. Tracer gas (sulfur hexafluoride, SF_6) was injected at a constant and known rate into the airstream being brought into the building at a location close to the outside air intake vent. The tracer gas concentration was measured in the supply duct downstream from the injection point. Under conditions of good mixing of the tracer with the airflow, the flow rate can be determined from the SF_6 injection rate and the measured concentration according to

$$Q = i/c, \qquad (7.1)$$

where

Q = airflow rate
i = tracer gas injection rate
c = tracer gas concentration.

The airflow rate Q into the building was modulated either by adjusting the outside air intake dampers or the intake vanes on the centrifugal supply fans. In buildings with more than one large supply fan, individual fans

could be turned on or off to further adjust the flow. For each induced flow rate Q, the inside-outside pressure difference was measured at several locations as discussed below. All of the pressurization tests were conducted under relatively mild wind speed conditions (less than 4.5 mph (2 m/s)) and at outside temperatures between 50 and 68°F (10 and 20°C) in order to avoid weather induced pressure differences during the tests.

The component pressurization tests were conducted by measuring the airflow necessary to induce pressure differences across individual components [17]. A temporary enclosure was installed around the component being tested, from inside the building, and air was blown into this enclosure such that it could only leave through leaks in the window being tested. The airflow was induced with a large vacuum cleaner and measured with an electronic flowmeter. The airflow rate was modulated by diverting varying amounts of airflow out of the vacuum cleaner at a point upstream of the flowmeter.

7.3 Test Equipment

The equipment used in the whole building pressurization measurements includes flowmeters to measure the SF_6 injection rate, an electron capture detector gas chromatograph to determine the SF_6 concentration and magnetic linkage pressure gauges to determine the inside-outside pressure difference. The SF_6 flowmeters were variable-area float-type rotameters equipped with a control valve to adjust the SF_6 injection rate. Each flowmeter was individually calibrated for SF_6 by the manufacturer with an accuracy of $\pm$ 1% of full scale. The SF_6 concentration downstream of the injection was measured with the same system used in the tracer gas measurements of air infiltration rates of these buildings. The gas chromatograph/electron capture detector was calibrated with $\pm$ 5% in the range of 10 to 250 ppb. The inside-outside pressure differences induced during the pressurization tests were measured with magnetic linkage pressure gauges which were individually calibrated against an inclined manometer. The pressure gauges were accurate within roughly $\pm$ 0.0025 in H_2O (0.6 Pa). The induced pressure difference across the building shell was measured at several locations in each building. The same pressure gauges were used in the pressure tests of individual components. The flowmeters used in these tests were electronic devices utilizing hot-wire amemometer principles, with an accuracy of $\pm$ 2%.

7.4 Details of Whole Building Pressurization

The following section briefly outlines the details of the whole building pressurization measurement in each building, including location and number of pressure difference measurements, fan operation and pressure differences achieved.

Anchorage

The federal building in Anchorage is divided into six connected modules. The modules vary in height from two to six stories. The building has six supply fans of varying capacities, one for each module. All of the modules are open to each other, and the airflow from any of the six fans pressurizes the entire building. All six fans were used in the pressurization tests, and therefore SF_6 was injected in, and sampled from, six locations in the building. Four different inside-outside pressure

differences were induced in this building, ranging from 0.055 to 0.150 in H_2O (14 to 38 Pa). For the lowest pressure difference, only four of the six fans were operated. The next highest pressure difference employed five of the fans, and the other pressure differences were obtained using all six fan. The pressure differences were measured at two ends of the building on the ground floor, and at the fifth floor of one of the modules. The variation in pressure difference among these three locations was only $\pm$ 0.004 in H_2O (1 Pa).

Ann Arbor

The federal building in Ann Arbor is a four story building with a terraced roof construction, i.e. each story has less floor area than the story below. There is a post office in part of the lower two floors which has its own air handling system. The lobby also has a separate air handler. The rest of the building is served by a main air handler located on the third floor. This building was pressurized using only the main supply fan. Four inside-outside pressure differences were induced, ranging from about 0.040 to 0.240 in H_2O (10 to 60 Pa). The pressure differences were measured at two locations on the ground floor and on the third floor. The post office on the first floor, which occupies about 16% of the total building volume, is not served by the fan used in the pressurization test. Although there is not a great deal of communication between the main building volume and the post office, a significant pressure difference did develop between the post office and the outside during these tests. The post office-outside pressure difference was about one-half of the main volume-outside pressure difference. In analyzing the test data the total building volume (including the post office) was assumed to be involved in the test.

Columbia

The federal building in Columbia is a fifteen story building. It also has a two story courthouse attached through an underground passageway, but only the fifteen story tower was pressure tested. The building has two large air handling systems located in a mechanical room on the fifteenth floor. The first floor, basement and lobby are served by two air handlers located in the basement. Although, there are two large fans in this building, only one fan running at partial capacity was needed to induce inside-outside pressures from 0.104 to 0.240 in H_2O (17 to 50 Pa). The pressure difference was measured at the odd numbered floors from three to thirteen.

Huron

The federal building in Huron is a four story building. There are two main supply fans in a mechanical penthouse serving two zones which communicate freely. Both fans were used to pressurize the building for some of the data points, and only one for the others. The induced pressure differences ranged from 0.068 to 0.200 in H_2O (17 to 50 Pa) and were measured at two locations on each of the four floors.

Norfolk

The Norfolk federal building is an eight story building. The building has one large supply fan in the mechanical penthouse which was sufficient to

induce inside-outside pressure differences from 0.032 to 0.120 in H_2O (8 to 30 Pa). These pressure differences were measured on each floor of the building.

Pittsfield

This two story building has a separate fan for each story. The locations for communication between the floors include two stairways, an elevator shaft and other smaller leakage sites. Using both fans, identical inside-outside pressure differences were developed on each floor. These pressure differences were measured at two locations on each floor and ranged from 0.100 in H_2O (25 Pa) to almost 0.400 in H_2O (100 Pa).

Springfield

The Springfield federal building is a five story building. There are two large supply fans located in a penthouse which serve the north and south zones respectively. On the upper floors, the two zones are connected through passageways. On the first two floors, both zones open onto an atrium. During the pressurization test all doors between the zones and into the atrium were open. The north zone fan was used to obtain pressure differences of 0.040 and 0.056 in H_2O (10 and 14 Pa), while both fans were used to induce a 0.092 in H_2O (23 Pa) pressure difference. The inside-outside pressure differences were measured on all five floors of the north zone, and on the second and fourth floors of the south zone.

7.5 Whole Building Pressurization Results

The following section presents the results of the pressurization tests on the seven federal buildings and some analysis of these data. In addition, the airtightness values of these buildings are compared to measurements made in several Canadian office buildings.

The test data for each building is in the form of several combinations of airflow Q and inside-outside pressure difference Δp. For each building, the Q and Δp values are fit to a curve of the form

$$Q = C\Delta p^n \qquad (7.2)$$

Table 7.1 presents equations for the curve fits for each of the seven buildings and the range of pressure differences which were achieved. Five of the seven exponents n are, as expected, in the approximate range of one-half to one. The exponent for Springfield is quite large due to difficulties in maintaining the low flow rates at a constant level, however the flow at 0.092 in H_2O (23 Pa) was repeatable and is believed to be accurate. There are many ways to quantify the results of pressurization tests. The test results for homes are often presented in terms of the induced flow rate at an inside-outside pressure difference 0.20 H_2O (50 Pa). The ranges of measured pressure difference in table 7.1 are variable over the seven buildings, but they all have measurements at roughly 0.10 in H_2O (25 Pa). In addition, the measurements close to 0.10 in H_2O (25 Pa) were repeatable in the buildings which had flow exponents out of the range from one-half to one. Therefore, the flow at 0.10 in H_2O (25 Pa) as determined with equation 7.2 is used to compare the tightness of these buildings. By using the 0.10 in H_2O (25 Pa) flow rates we need not compare

values extrapolated out of the range of measurements.

The 0.10 in H_2O (25 Pa) flow rates in units of building volumes or exchanges per hour and cfm per ft^2 (m^3/hr per m^2) of building envelope (wall and roof) area are presented in table 7.2. Note that these flow rates are significantly larger than the infiltration rates induced by weather. The 0.20 in H_2O (50 Pa) exchange rates of the buildings are about 1.5 times the 0.10 in H_2O (25 Pa) flows shown in the table (assuming n=0.65 in equation 7.2), and are low compared to those measured in homes. U.S. homes generally range from about 5 exchanges per hour to greater than 20 exchanges per hour at 0.20 in H_2O (50 Pa). Swedish and Canadian homes are being built with 0.20 in H_2O (50 Pa) flow rates of less than 2 exchanges per hour [19]. Thus, the 0.20 H_2O (50 Pa) flow rates of these federal buildings correspond to very tight houses.

In comparing the pressurization test results of the federal buildings to each other and to residential buildings, the important factor of surface to volume ratio arises. Figure 7.2 shows the surface to volume ratios S/V in ft^2/ft^3 (m^2/m^3) for the federal buildings and two sample houses. The 1-story house is assumed to have a 1200 ft^2 (110 m^2) square floor area and 8 ft (2.5 m) ceilings. The 2-story home also has a square floor plan with roughly 1100 ft^2 (100 m^2) on each floor and a 16 ft (5 m) building height. It is seen in the figure that the large sizes of the federal buildings lead to values of S/V which are about one-third of those associated with homes.

Figure 7.3 shows the 0.10 in H_2O (25 Pa) flows listed in table 7.2. The vertical scale on the left shows the 0.10 in H_2O (25 Pa) flows in exchanges per hour for the seven federal buildings and the two sample houses shown in figure 7.2 (2.0 exchanges per hour at 0.20 in H_2O (50 Pa) very tight). The vertical scale on the right shows the 0.10 in H_2O (25 Pa) flows in cfm/ft^2 (m^3/hr-m^2) of envelope area. In moving from exchanges per hour to cfm/ft^2 (m^3/hr-m^2) the ranking of the buildings' tightness changes significantly. Also, the spread in the leakage values using the second measure is larger than the spread in exchanges per hour. The most significant change occurs for the sample houses which are almost the tightest in terms of cfm/ft^2 (m^3/hr-m^2) of envelope area. Thus, while the federal buildings appear to be quite tight in terms of exchanges per hour compared to houses, the airtightness per unit of envelope area is not as impressive.

The airtightness of the federal buildings in units of cfm/ft^2 (m^3/hr-m^2) is worse if one considers the fact that the roofs are of low-slope built-up design, constructed to be impervious to both water and air. Therefore, it might be more appropriate to normalize the 0.10 in H_2O (25 Pa) flows by the wall area alone instead of using the total envelope area including the roof. Normalizing the leakage rate with the wall area will lead to higher values of the 0.10 in H_2O (25 Pa) flows in cfm/ft^2 (m^3/hr-m^2).

These values of induced flow per unit envelope area may be compared to values obtained previously in Canada [15,20]. In the Canadian work, building leakage coefficients were determined for eight office buildings with construction dates ranging from 1964 to 1974 and heights from 9 to 25 storys. Seven of the eight Canadian buildings ranged from 0.13 to 0.34 cfm/ft^2 (2.4 to 6.2 m^3/hr-m^2) at 0.10 in H_2O (25 Pa) and one had a value of 0.60 cfm/ft^2 (11.0 m^3/hr-m^2). These Canadian values are flows per square meter of wall area as opposed to envelope area as used in table 7.2.

Comparing these values to those listed in table 7.2, we see that the federal buildings are comparable in tightness to these Canadian buildings.

7.6 Component Pressurization Results

Windows were individually pressure tested in six of the eight buildings. Because of the large variation in component size and frame arrangements, it was difficult to seal the test apparatus. For these reasons, only a small number of components were tested and the results should be considered preliminary. The results are expressed in units of cfm (L/s) of induced airflow at 0.30 in H_2O (75 Pa) per foot (meter) of crack length for windows, and include both frame and sash leakage. The ASHRAE Handbook of Fundamentals [8] lists a window leakage standard of 0.50 cfm/ft (0.77 L/s-m) (sash leakage only), varying somewhat with window type. Table 7.3 shows the results of the window pressurization tests for the six buildings tested. In addition, this table lists samples of window leakage measurements from the literature [15,21,22].

In table 7.3 there is a wide variation in the measured window leakage rates, even for the relatively small number of windows tested. The operable windows in the Columbia building are very leaky, along with some cracks around windows in the Fayetteville building through which daylight is visible. Most of the other windows tested are somewhat leakier than the standard of 0.50 cfm/ft (0.77 L/s-m). As mentioned earlier, the standard applies to sash leakage only, while these measurements include both sash and frame leakage. The field tests of many new residential windows yielded an average value very close to this standard [21]. The office building from reference 16, built in the mid-1960's, has very leaky windows. Several windows from Canadian supermarkets and shopping centers [17] had leakage values comparable to those in the office buildings discussed in this report. Most of the windows tested in the federal buildings and those in the literature are leakier than the 0.50 cfm/ft (0.77 L/s-m) standard.

Window leakage rates can be combined with the total window crack length to estimate the net window leakage in the buildings. These window leakage values are compared with the total building leakage from the whole building pressurization tests to determine the fraction of total building leakage associated with windows. This fraction is generally around 20% for houses [23]. Since only a small number of windows were tested in the buildings, the measured leakage values may not be representative of the building average. Therefore, in calculating the fraction of building leakage associated with windows, the standard of 0.50 cfm/ft (0.77 L/s-m) is used along with two and three times this value. In addition, the average of the measured values is used when available. Table 7.4 presents the results of these calculations of the fraction of total building leakage attributable to windows at 0.10 in H_2O (25 Pa). The total building leakage is based on the equations in table 7.1. Although it is not entirely clear as to which window leakage value is appropriate for each building, the windows account for about 10 to 20% of the total building leakage at 0.10 in H_2O (25 Pa). This percentage is similar to the fraction of leakage associated with windows in homes.

7.7 Relation of Pressurization Test Results to Infiltration Rates

While the pressurization tests are useful for comparing buildings to each other and to airtightness standards, the question remains of how the pressurization test results are related to air infiltration rates induced by weather. This question has been studied extensively in houses [23], and less so in large buildings [24,25]. The existence of both whole building pressurization test results and air infiltration measurement for the seven federal buildings allows a comparison of the two measurements. Figure 7.4 is a plot which compares tracer gas measurements of infiltration rates in the buildings to the 0.10 in H_2O (25 Pa) flow rates in exchanges per hour from the pressurization tests. The infiltration rates are measurements of the leakage induced by weather, and the rates for each building correspond to approximately the same weather conditions. The correlation between these two variables is as strong as it is for homes, but the slope of the infiltration rate versus pressurization flow is steeper for these large buildings than it is for houses. Such a simple relation between pressurization and infiltration neglects the dependence of infiltration on weather conditions. A more complex model of the pressurization/infiltration relation in large buildings which accounts for weather effects is discussed below.

Shaw and Tamura, of the National Research Council of Canada, have developed a model which predicts infiltration in large buildings [24]. This model consists of predictive equations for infiltration based on a computer model building and wind tunnel tests of a model of a 40-story building. The buildings considered in the work of Shaw and Tamura are generally taller than the federal buildings discussed in the report.

This large building model has separate predictive equations for wind and temperature induced infiltration. The wind induced infiltration Q_w is expressed as

$$Q_w = \alpha C' LH(\rho u^2 C_p/2)^n \qquad (7.3)$$

where is a factor to account for wind directions other than normal to the longest building wall, which is of length L. H is the building height. C' and n are the building flow coefficient and exponent from equation 7.2. The value of C' is the leakage coefficient of the walls, determined by dividing the value of C in equation 7.2 by the building wall area. ρ is the air density, u is the wind speed in m/s and C_p is the wind pressure coefficient for the windward wall. The stack induced infiltration is expressed as

$$Q_s = C'S[3464\,\gamma\,(\Delta T/T_{in}T_{out})]^n\ [(\beta H)^{n+1}/n+1] \qquad (7.4)$$

where S is the building perimeter and ΔT is the inside-outside temperature difference in ^oC. β is the height of the neutral pressure level divided by the building height. γ is a thermal draft coefficient which accounts for the extent of vertical communication in the building. A value of $\gamma = 0.0$ corresponds to no openings between floors and $\gamma = 1.0$ corresponds to a totally open interior. While there is no straightforward technique for determining the appropriate value of γ for an individual building, Shaw and Tamura suggest a value of 0.80 for office buildings, and this value was used for all the federal buildings with two exceptions. In Anchorage, all

the floors open onto a central lobby area, and therefore a value of 0.95 was used for the thermal draft coefficient. The Springfield building has a vertically open atrium on the front of the building and a value of 0.87 was used. The neutral pressure level is assumed to equal one-half the building height in all the buildings. The wind Q_w and temperature difference Q_s infiltration rates are combined to yield and net infiltration rate according to

$$Q_{ws} = \max(Q_w,Q_s)\ [1 + 0.24(\ (\min(Q_w,Q_s)/\max(Q_w,Q_s)\ )^{3.3}] \qquad (7.5)$$

The max and min functions correspond to the maximum or minimum value in the parentheses.

Table 7.5 compares the measurements of infiltration in the seven buildings to predicted rates from the Shaw-Tamura model. The predictions are made for the same weather conditions as the measurements, a wind speed of 4.5 mph (2 m/s) and an outside temperature of 45°F (7°C). In all buildings, the predictions are much lower than the measurements, especially in Ann Arbor and Springfield. The Springfield predictions are low because the curve fit to the building's pressurization data (equation 7.2) has a large value for the flow exponent (n=2.09) and a correspondingly low value for the flow coefficient. This low flow coefficient value leads to low predicted infiltration rates. If instead the exponent is assumed to be equal to 0.65 and the 0.10 in H_2O (25 Pa) flow rate is used to get a new flow coefficient, these predictions are more accurate. These second Springfield predictions correspond to the Springfield-adjusted values in table 7.5. This result of generally low predictions compared to measurements was also found by Hunt and Treado [25] in an eleven-story office building. They attributed the larger measured infiltration rates to toilet exhausts and other forced ventilation. However, in the seven federal buildings discussed here, all mechanical exhausts were off during the infiltration measurements.

It is not clear why the predicted infiltration rates are generally so much lower than the measurements. One potential explanation for the disagreement is the existence of open elevator shafts in the buildings, that are quite susceptible to stack induced infiltration. Another reason may have to do with the fact that during the infiltration measurement the HVAC system was running to keep the interior air well mixed. Even though the outside air supply and exhaust dampers were closed, they could have leaked. However, in Anchorage and Pittsfield, infiltration measurements were made with these dampers sealed with plastic sheets, and the measured rates were no different from the rates when the dampers were closed but not sealed. Another factor to consider is leakage due to local pressurization when the fans are running. All the buildings use ceiling plenums as return ducts, and leakage in the outside walls surrounding this plenum space will lead to the intake of outside air through these leaks and increased air exchange rates. Such plenum leaks were seen in Fayetteville and their existence is suspected in other buildings. However, it is difficult to estimate the contribution of such leakage to the net air exchange of the building. Another reason for the disagreement between the model predictions and the measurements may be that the model was developed for taller buildings (about 40-stories) than the federal buildings (from two to fifteen-stories). Another factor could be that the wind speed measurements

at the federal buildings were made roughly 16 ft (5 m) above the roof while the model calls for free stream wind speed at the building height. However, predicted infiltration rates for higher wind speeds do not exhibit significantly larger errors than the 4.5 mph (2 m/s) predictions shown in table 7.5, and therefore wind speed measurement error does not appear a likely source of the model error.

7.8 Conclusions

As part of this project to evaluate the thermal integrity of the building envelopes of eight federal buildings, the airtightness of the envelopes were evaluated using pressurization techniques. Seven of the buildings were subjected to whole building pressurization tests and were found to possess airtightness levels similar to tight houses in units of exchanges per hour at an induced pressure difference. The airtightness of the buildings in units of flow per envelope area were generally higher than for tight houses due to the low surface to volume ratios of the federal buildings. Therefore, the airtightness in exchanges per hour from the pressurization tests provides a misleading indication of the federal buildings' airtightness. A small number of windows in six of the buildings were pressure tested individually, and while a wide range of leakiness levels was evident, they were generally leakier than a common window tightness standard. The fraction of total building leakage associated with windows was calculated to be about 10 to 20%, a percentage similar to that found in houses. The large building infiltration model of Shaw and Tamura was applied to the seven buildings which were pressure tested, and the predictions were lower than the infiltration rates measured with tracer gas.

Table 7.1

Curve Fits to Pressurization Data
and Pressure Measurement Range

Building	Curve Fit		Range of Measured Pressure Difference	
	Q(cfm) Δp(in H_2O)	(Q(m^3/hr)) (Δp(Pa))	in H_2O	(Pa)
Anchorage	$Q = 3.66 \times 10^5 \Delta p^{.61}$	$(Q = 2.14 \times 10^4 \Delta p^{.61})$	.056-.152	(14-38)
Ann Arbor	$Q = 7.54 \times 10^4 \Delta p^{.67}$	$(Q = 3.17 \times 10^3 \Delta p^{.67})$	.044-.244	(11-61)
Columbia	$Q = 1.44 \times 10^5 \Delta p^{.47}$	$(Q = 1.83 \times 10^4 \Delta p^{.47})$	.104-.240	(26-60)
Huron	$Q = 3.18 \times 10^4 \Delta p^{.64}$	$(Q = 1.58 \times 10^3 \Delta p^{.64})$	.068-.200	(17-50)
Norfolk	$Q = 2.83 \times 10^5 \Delta p^{.74}$	$(Q = 8.08 \times 10^3 \Delta p^{.74})$	.032-.120	(8-30)
Pittsfield	$Q = 1.10 \times 10^4 \Delta p^{.36}$	$(Q = 2.55 \times 10^3 \Delta p^{.36})$	.100-.388	(25-97)
Springfield	$Q = 5.99 \times 10^6 \Delta p^{2.09}$	$(Q = 9.90 \times 10^1 \Delta p^{2.09})$	.040-.092	(10-23)

Table 7.2

Pressurization Test Results in Terms of 0.10 in H_2O Flow Rates

Building	Airflow rate at 0.10 in H_2O (25 Pa) (volumes/hr)	cfm/ft^2 of envelope area	$(m^3/hr\text{-}m^2)$
Anchorage	0.80	0.37	6.7
Ann Arbor	0.86	0.23	4.1
Columbia	0.67	0.33	6.0
Huron	0.45	0.10	1.9
Norfolk	1.45	0.40	7.2
Pittsfield	0.95	0.19	3.5
Springfield	1.43	0.51	9.2

Table 7.3

Results of Window Pressurization Tests

Building	Window	Air Flow Rates at 0.3 in H_2O (cfm/ft) (L/s-m)
Anchorage	Inoperable	2.08, 0.43, 0.70, 0.57, 0.63 (3.22, 0.67, 1.09, 0.89, 0.98)
Ann Arbor	Inoperable	0.59, 0.67 (0.91, 1.04)
Columbia	Operable	2.85, 3.59, 2.33, 2.08 (4.41, 5.56, 3.61, 3.22)
Fayetteville	Inoperable	0.28, 0.21 (0.44, 0.32)
	Window Cracks*	4.78, 3.85 (7.40, 5.96)
Norfolk	Inoperable	0.79, 1.01, 0.95 (1.23, 1.56, 1.47)
Pittsfield	Operable	0.84, 0.26 (1.30, 0.41)
Window Leakage Standard (Ref. 8)		0.50 (0.77)
Residential Windows (Ref. 21)		Mean Value of 0.52 (0.81)
Office Building (Ref. 22)		0.88, 2.29, 2.29, 2.30, 2.67, 3.21, 3.28, 6.98, 7.71, 10.36 (1.36, 3.54, 3.55, 3.56, 4.13, 4.97, 5.08, 10.81, 11.94, 16.04)
Supermarkets and Shopping Malls (Ref. 15)		0.13, 0.13, 0.36, 0.39, 0.71, 0.77, 1.55 (0.20, 0.20, 0.55, 0.60, 1.10, 1.20, 2.40)

*These are cracks around particularly leaky windows.

Table 7.4

Fraction of Total Building Leakage Associated with Windows

Building	Window Leakage at 0.10 in H_2O (25 Pa)* cfm/ft^2	(L/s-m)	Fraction of Building Leakage Associated with Windows
Anchorage	0.23	(0.36)	8.8%
	0.46	(0.72)	17.6%
	0.70	(1.08)	26.4%
Measured**	0.36	(0.55)	13.4%
Ann Arbor	0.23	(0.36)	6.2%
	0.46	(0.72)	12.4%
	0.70	(1.08)	18.6%
Measured	0.34	(0.53)	9.1%
Columbia	0.23	(0.36)	6.4%
	0.46	(0.72)	12.8%
	0.70	(1.08)	19.2%
Measured	1.12	(1.74)	30.9%
Huron	0.23	(0.36)	13.3%
	0.46	(0.72)	26.6%
	0.70	(1.08)	39.9%
Norfolk	0.23	(0.36)	6.4%
	0.46	(0.72)	12.8%
	0.70	(1.08)	19.2%
Measured	0.44	(0.68)	12.1%
Pittsfield	0.23	(0.36)	8.3%
	0.46	(0.72)	16.6%
	0.70	(1.08)	24.9%
Measured	0.28	(0.43)	10.0%
Springfield	0.23	(0.36)	7.1%
	0.46	(0.72)	14.2%
	0.70	(1.08)	21.3%

---

*0.23, 0.46 and 0.70 cfm/ft^2 (0.36, 0.72 and 1.08 L/s-m) correspond to 1, 2 and 3 times the standard of 0.50 cfm/ft^2 at 0.3 H_2O (0.77 L/s-m at 75 Pa).

**This value is the average for all the windows tested in this building.

Table 7.5

Predictions of the Shaw-Tamura Large Building Model

Building	Measured Infiltration* (exchanges/hour) Wind Speed < 4.5 mph (2 m/s) T_{out} ~ 45°F (7°C)	Predicted Infiltration (exchanges/hour) u = 4.5 mph (2 m/s) T_{out} = 45°F (7°C)
Anchorage	0.25	0.07
Ann Arbor	0.55	0.02
Columbia	0.35	0.13
Huron	0.15	0.03
Norfolk	0.50	0.15
Pittsfield	0.35	0.14
Springfield	0.40	0.01
Springfield-Adjusted		0.25

---

*Representative infiltration rate for specified weather conditions.

Figure 7.1

Building Pressurization Testing Set-Up

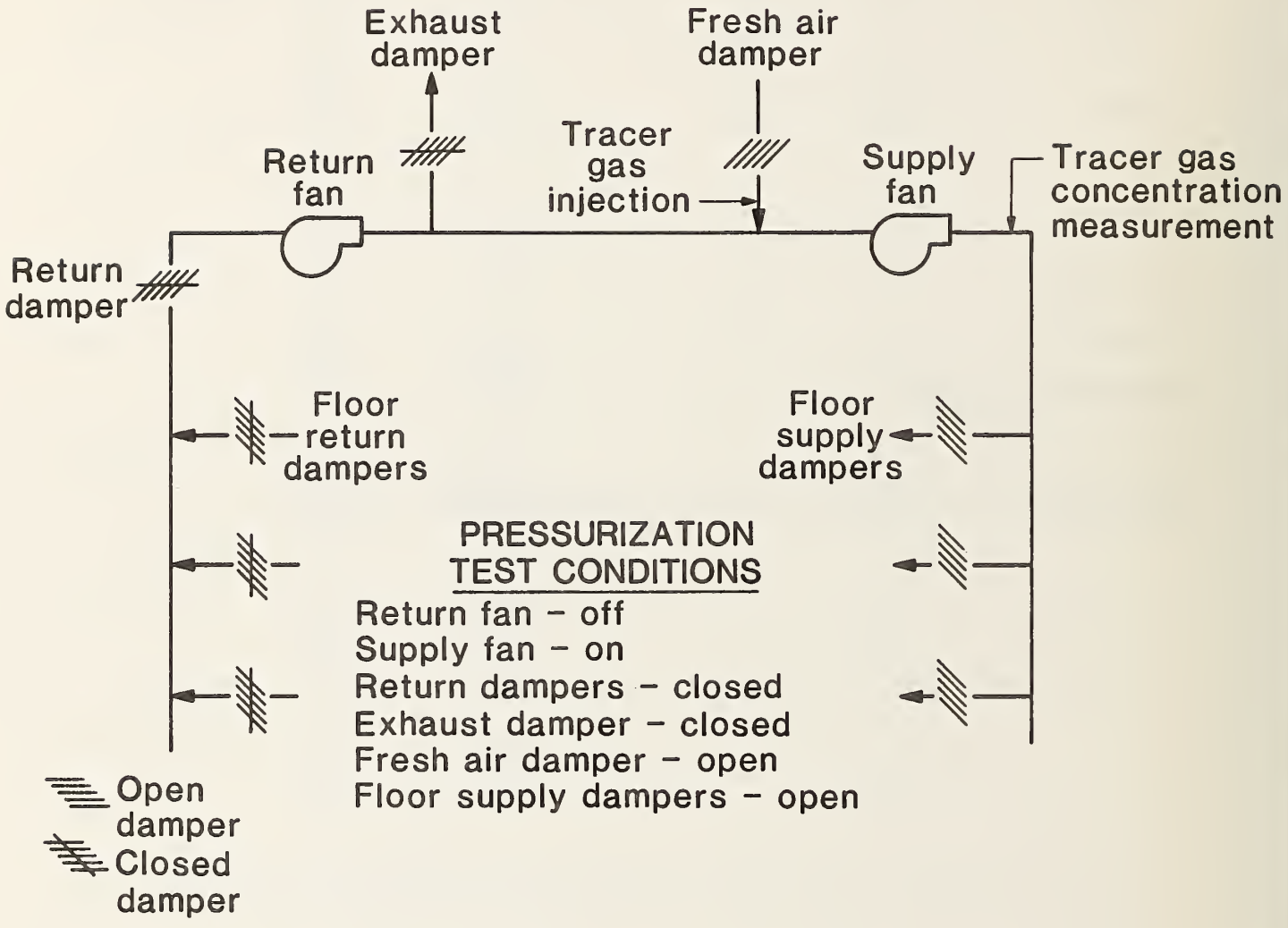

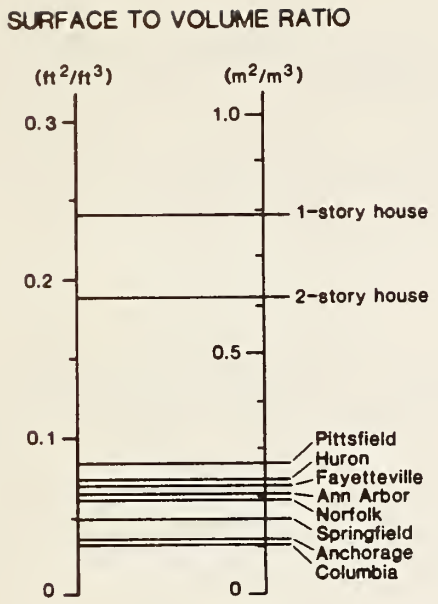

Figure 7.2 Surface to Volume Ratios of Federal Buildings and Houses

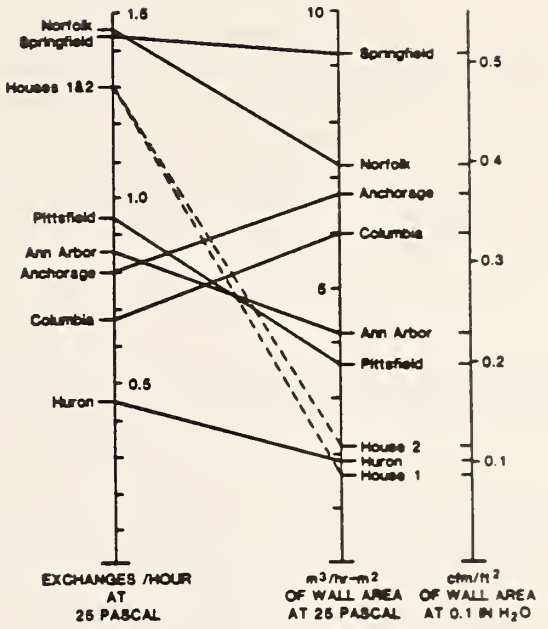

Figure 7.3 Pressurization Test Results

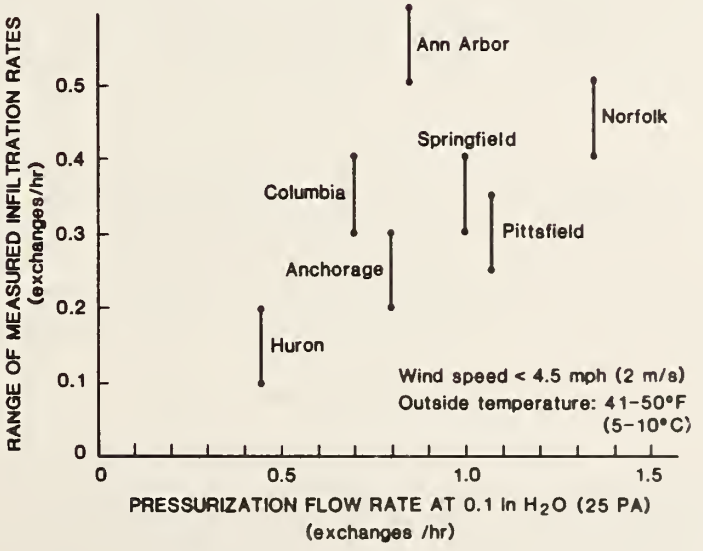

Figure 7.4 Weather Induced Infiltration Rates versus Pressurization Test Results

8.0 Measurement of the Thermal Resistance of the Buildings

8.1 Introduction

The in-situ measurements of the thermal resistance of sections of the building envelope were carried out between February and May of 1983 on seven of the eight federal buildings. These tests were performed using either heat flow meters or a portable calorimeter. It was also intended to use the Envelope Thermal Testing Unit (ETTU) developed by Lawrence Berkeley Laboratories, however, this device was not available to NBS in time for this demonstration.

8.2 Instrumentation and Procedures

The rates of heat flow through the building envelopes and major building components were measured with heat flow meters and a portable calorimeter. The heat flow meter used consisted of a 4-inch (102 mm) diameter, thin, circular, wafer-type sensor comprising the hot and cold junctions of an embedded thermopile attached to its flat surfaces. The voltage signals generated by the heat flow meter when exposed to a thermal field were proportional to the rate of heat flow through the meter.

Upon completion of a series of field tests, the heat flow meters were calibrated using a standard guarded hot plate apparatus described in references [26, 27]. The sensitivity of each heat flow meter was determined by exposing it to a range of uniform heat flux, at the temperature levels experienced during the field testing, after it had been placed between the insulations attached to the hot and cold plates of the apparatus. The accuracy of the calibration of the heat flow meters was about $\pm$ 1%.

During field measurements, the heat flow meters were taped on the inside surfaces of the exterior walls, structural columns and beams, and the roof deck and floor assemblies. A metal stud finder was used during the installation of the heat flow meters to ensure that the transducers were mounted over thermal insulation filled cavities between wall framing members.

In order to evaluate the thermal integrity of building envelopes of the selected office buildings, a portable calorimeter similar to that used by Brown and Schuyler [28, 29] was designed, fabricated and instrumented for field measurements of heat fluxes through the wall structures. The usefulness of portable calorimeters has been demonstrated by the Division of Building Research, National Research Council of Canada, in determining the effects of framing members on the overall thermal resistance and heat flow through frame walls of single-family dwellings [28, 29].

The calorimeter was a five sided box, 49x78x8 inches (1.24x1.98x0.2 m) deep, whose open face was attached to the interior wall surface to be measured. The calorimeter walls were constructed of two 2 inch (50 mm) thick layers of foil-faced, semi-rigid glass fiber insulation boards glued together with the foiled side exposed. The combined thermal resistance of the calorimeter walls was R 17.4 ft^2-h-^oF/Btu (3.06 m^2-K/W). All joints were staggered, filled with crumbs of glass fiber insulation mixed with glue, and covered with aluminum foil duct tape. The calorimeter box was

stiffened by framing its sides and corners with a 0.5 in. (13 mm) fir plywood board. A narrow rubber foam strip attached to a 1/32 in. (0.8 mm) thick aluminum angle frame was installed along the edges of the calorimeter box to provide an air-tight seal between the open face of the calorimeter and the wall surface under test. The calorimeter had a metering area of 46 in. (1.17 m) by 75 in. (1.91 m), and was designed to accommodate test structures with heat loss rates ranging from 0.3 to 19 Btu/h-ft^2 (0.9 to 60 W/m^2).

The portable calorimeter contained a 140 W electric resistance heater, which consisted of a bare B. & S. (Brown and Sharpe) gauge No. 27 nickel chromium wire with an electric resistance of 3.35 ohms per ft. (10.98 ohms per meter). The heating wire was secured through steel springs and hooks to ceramic stand-off insulators which were fastened to the plywood frame. The wire spacing was varied to provide more heat in the bottom portion of the calorimeter than the upper part. This was done to minimize the vertical temperature gradient produced by the buoyancy effect within the air space.

By maintaining no temperature difference between the interior and exterior wall surfaces of the calorimeter, the amount of heat loss through the calorimeter walls to the guarded room could be reduced. The temperature differentials across the back wall of the calorimeter were monitored by an eighteen-junction pair thermopile with the thermocouple junctions placed on both the inner and outer faces of the wall. There were no thermocouple junctions positioned on the side walls since the surface area of the sides constituted only about 12% of total surface area of the calorimeter. The thermocouples were constructed from B. & S. gauge No. 28 copper and constantan wires with 0.0126 in. (0.32 mm) diameter and solid nylon insulation. Figure 8.1 shows the construction details of the portable calorimeter.

Using the thermopile output as the feedback variable, a voltage controller was used to automatically control the operation of the electric heater and maintain a zero temperature differential across the back calorimeter wall. A safety thermostat with a sensing element installed inside the calorimeter was connected to the heater to provide control of air temperature within safe limits by opening the circuit at high temperature. The total electric energy consumption of the heater was measured by a watt-hour meter furnished with an optoelectronic device installed in the circuit. The device consisting of a light-emitting diode and a detector. An electric pulse was generated by the device each time 1.8 watt-hour of electricity was consumed. The pulses were totaled by an electronic counter. Figure 8.2 shows the wiring schematic of the measurement/control system for the calorimeter.

The temperature of the exterior and interior air in the vicinity of heat flow meters, and the air inside the calorimeter, were measured with thermistors. These temperature sensors were a thermistor-resistor network type and consisted primarily of a bead shaped thermistor and an external network with a fixed precision resistor. The sensor possessed a resistance-temperature function which was very nearly linear over a specific temperature range. With an applied voltage of 1.2 volts to the electric circuit, the thermistor produced an output voltage that was linear with temperatures over a temperature range between -22 to 122^{o}F (-30 to

50°C). Based on the data furnished by the manufacturer, measurement error for the thermistors used is within ± 0.5°F (0.3°C). The sensing element of each thermistor was installed at a distance of 6 in. (152 mm) for the exposed measurement surface. A micro-computer based data acquisition system was used to monitor the output signals from the heat flow meters, the portable calorimeter and the associated counter, and the thermistors. The channels of all transducers were scanned every 2 seconds. For each hour, the readings from each channel were averaged by the computer. At the end of each one hour interval, the computer recorded the hourly averages on a floppy disk for later analysis.

8.3 Test Results

The field measurements were performed in unoccupied rooms of selected floor levels of office buildings situated in Ann Arbor, MI, Columbia, SC, Springfield, MA, Huron, SD, Norfolk, VA, Pittsfield, MA and Anchorage, AK. Construction details of the exterior walls and major building components on which heat flow measurements were carried out are summarized in table 8.1

The time variations of indoor and outdoor air temperatures and air-to-air temperature difference across the external wall at the locations of a heat flow meter and the portable calorimeter for 3 daily cycles in the Huron building are plotted in the upper portion of figure 8.3. The heat flow meters were placed in the proximity of the calorimeter. At the bottom of this figure, the corresponding measured rates of heat flow through the metering area of the calorimeter and the wall area covered by the heat flow meter are depicted as a function of time. As shown, the outdoor temperature oscillated periodically around a mean level during a 24-hour time interval. However, the indoor temperature was found to be relatively constant. The surface heat flux changed in a periodic manner and lagged behind the temperature difference between the indoor and outdoor air. This thermal time lag was attributed to the heat storage in the wall and found to be approximately 6 hours from visual inspection of the curves. This time lag is the time required for the maximum heat flow to be reached after the maximum temperature difference across the wall was attained.

During the measurements, the average temperature of the air inside the calorimeter was about 2°F (1.1°C) lower than the indoor air temperature. The heat flow rates measured by the calorimeter exhibit a similar periodic variation as those determined by the heat flow meter. However, the heat flux values determined from data obtained by the calorimeter were approximately 30% greater than those by the heat flow meter. The calorimeter measurement included heat flow through the wall area containing both highly conductive metallic framing members and the insulation filled cavities between the framing, while the heat flow meter involved only heat transmission through the area between the framing members.

The time variations of the daily and cumulative thermal resistances of wall sections and major building components contained in the exterior wall of the Huron building during a fifteen day measurement period are shown in Figures 8.4 and 8.5. The thermal resistance R-value is defined as the ratio of the average air-to-air temperature difference across a section of the exterior wall to the average heat flow rate and is calculated from the relation:

$$R = \overline{\Delta T}/\overline{q} = \int_0^\tau (\Delta T)\, dt \;/\; \int_0^\tau Q\, dt \qquad (8.1)$$

where ΔT is interior-to-exterior air temperature difference, q is the heat flow rate, and τ is the measurement period or the period of integration.

Data were averaged over a 24-hour period in order to reduce the influence of the transient effects of the exterior wall associated with its large thermal inertia. The wall resistance values derived from the heat flow meter, as shown in Figure 8.4, were the average values of the data from eight heat flow meters placed on the interior wall surface below the suspended ceiling. As can be seen in the figure, the R-values measured with heat flow meter and the calorimeter varied over a 24-hour period. These changes were due to daily variations in the outdoor temperature as illustrated in the upper part of Figure 8.4, and the ambient airflow, which affected the thermal resistance of the air film at the outer surface of the exterior wall.

The cumulative averages of daily thermal resistance values for the wall, the upper wall located in the ceiling plenum, and structural beam and column are calculated by dividing the sum of the daily average thermal resistance by the elapsed days, and are plotted in Figures 8.4 and 8.5 for comparison. Based on the fifteen days of measurements using heat flow meters, the measured overall thermal resistances at the wall, the upper wall, and structural beam and column were found to be 20.4, 21.0, 10.4, and 9.5 ft^2-h-^oF/Btu (3.6, 3,7, 1.8, and 1.7 m^2-K/W) respectively. As shown in Figures 8.4 and 8.5, the cumulative average resistance values were generally within 5% of its final value after 2 days of measurements. The low thermal resistance of the structural beam and column shown in Figure 8.5 were attributed to highly conductive heat flow paths or thermal bridges contained in these sections of the building envelope.

The average wall resistance values as measured by heat flow meters, and by the portable calorimeter, are plotted in Figure 8.6 as a function of measurement period for the Huron building. Also plotted in the figure are the corresponding values of the standard deviation.

As stated earlier, the large thermal mass of the external wall, which was subject to a varying air temperature at the outer surface, caused the heat flow to lag behind the temperature difference driving force. A prolonged measurement period is required for the results of wall thermal resistance calculations to converge to a constant value. As shown in Figure 8.6, both the variation in the wall thermal resistances and its associated standard deviation generally decrease with an increase in the length of the measurement period. Thermal resistance values calculated from data obtained by the calorimeter were approximately 30% lower than values obtained with heat flow meters. As mentioned previously, this difference was attributable to the effect of wall framing members.

In Table 8.2, a comparison is made of the thermal resistance values, as measured using heat flow meters and the portable calorimeter, and the corresponding predicted steady-state values. Also presented in the table are heat flow rates, and the outdoor and indoor air temperatures. All the data tabulated in table 8.2 are averages obtained on 2 to 16 consecutive 24-hour cycles. The predicted steady-state thermal resistance values were

calculated using the series resistance method [8] and the published data include manufacturer's literature on thermal properties of the building materials involved. The thermal resistances of air films at the interior and exterior surfaces used in the calculations were 0.68 ft^2-h°F/Btu (0.12 m^2-K/W) and 0.17 ft^2-h-°F/Btu (0.03 m^2-k/W), respectively.

Inspection of table 8.2 shows that a fairly good correlation exists between the measured R-values and the predicted results. The significant disagreement between the measured and calculated results for the structural column in the Anchorage building may be due to the fact that the resistance calculations did not reflect multi-dimensional heat flow conditions. In general, the portable calorimeter gave lower wall resistance values than the heat flow meters. For these tests, the wall framing members and fasteners reduced the overall resistances by approximately 33% compared to the same walls without taking the framing effects into account. The significantly high wall resistance determined by the portable calorimeter for the Columbia building was probably attributable to the additional heat conducted laterally into the measured area from a nearby hot air duct.

The thermal resistance values of various building components measured with heat flow meters are plotted in figure 8.7 against the corresponding predicted steady-state values. It appears from this plot that the linear correlation between these two variables is fairly good because all the points fall around the line of best fit obtained from the least squares method. The standard error of estimate and the coefficient of correlation, which is a measure of the degree of linear association between the measured and predicted thermal resistance values, were found to be 3.61 ft^2-h°F/Btu (0.64 m^2-K/w) and 0.87, respectively. Some significant variations in resistance values were attributable to differences in construction workmanship, assembly techniques, defective insulation, aging building materials, difference between the actual material thermal properties and the handbook values, and the presence of moisture.

8.4 Conclusions

Reliable thermal resistance values of building envelopes can be derived from in situ measurements of indoor-outdoor air temperature differences and of heat flow across test structures provided that the measurements are carried out over a sufficiently long period. A measurement period of at least two days is recommended, but an entire week of data collection is advisable when possible. Both the heat flow meters and the portable calorimeter were found to be useful tools for measuring heat flow through large, non-homogeneous building assemblies in the field. Wall thermal resistances derived from data obtained using a portable calorimeter yield lower values than those obtained with heat flow meters. This difference is attributed to the additional heat flow through highly conductive framing members in the structure. The thermal resistance values of masonry exterior walls of seven office buildings situated in various climate zones have been found to vary widely from approximately 8 to 39 ft^2-h-°F/Btu (2 to 7 m^2-K/W). The measured thermal resistances deviated from the design thermal resistances by an average of 14%, the worst case being 45%.

Table 8.1
Construction Details of Building Components in Test Buildings

A. The Ann Arbor building

1. Wall located below the suspended ceiling:
0.5 in (13 mm) Quarry tile, 1 in (25 mm) metal lath and mortar bed, 10 in (254 mm) concrete masonry unit, 1.5 in (38 mm) semirigid glass fiber insulation board, and 0.63 in (16 mm) acoustic wall panel.

B. The Columbia building

1. Wall below the acoustic tile ceiling:
12 in (305 mm) precast concrete panel, 2 in (51 mm) glass fiber blanket insulation, 0.63 in (16 mm) gypsum wallboard on 2 in (51 mm) metal studs.

2. Wall above acoustic tile ceiling:
8 in (203 mm) precast concrete panel, 24 in (610 mm) air space inside concrete overhang, 3 in (76 mm) precast concrete panel, 2 in (51 mm) glass fiber blanket insulation, and 0.63 in (16 mm) gypsum wallboard on 2 in (51 mm) metal studs.

3. Concrete wall inside the ceiling plenum:
15 in (381 mm) precast concrete panel.

C. The Springfield building

1. Walls located below and above acoustical tile ceiling:
5.5 in (140 mm) precast concrete panel, 2.5 in (64 mm) semirigid glass fiber insulation board, and 0.5 in (13 mm) gypsum wallboard.

2. Structural column:
5.5 in (140 mm) precast concrete panel, 2.5 in (64 mm) semirigid glass fiber insulation board, fire-proof steel beam, and 0.5 in (13 mm) gypsum wallboard on 2.5 in (64 mm) metal studs as the column enclosure.

D. The Huron building

1. Wall below acoustical tile ceiling:
4 in (102 mm) face brick, 6 in (152 mm) light weight concrete masonry unit, 3 in (76 mm) semirigid glass fiber insulation board, and 0.63 in (16 mm) gypsum wallboard.

2. Wall inside the ceiling plenum:
Same as above.

Table 8.1 (continued)

E. The Norfolk building

1. Wall below acoustical tile ceiling:
4 in (102 mm) face brick, 0.75 in (19 mm) air space, 0.5 in (13 mm) gypsum board sheathing, 4 in (102 mm) glass fiber blanket insulation, and 0.5 in (13 mm) gypsum wallboard.

2. Structural column:
4 in (102 mm) face brick, 0.75 in (19 mm) air space, 0.5 in (13 mm) gypsum board sheathing, 4 in (102 mm) glass fiber blanket insulation, structural column with spray-on fire proofing, and 0.5 in (13 mm) gypsum board enclosure.

3. Structural beam inside the ceiling plenum:
4 in (102 mm) face brick. 0.75 in (19 mm) air space, 0.5 in (13 mm) gypsum wallboard, and structural beam with spray-on fire proofing.

F. The Pittsfield building

1. Wall below the suspended ceiling:
4 in (102 mm) face brick, 2 in (51 mm) semirigid glass fiber insulation board, 6 in (152 mm) solid masonry concrete block, and 4 in (102 mm) face brick.

2. Wall inside the ceiling plenum:
4 in (102 mm) face brick, 2 in (51 mm) semirigid glass fiber insulation board, 4 in (102 mm) face brick, 10 in (254 mm) airspace, and 4 in (102 mm) masonry concrete block.

3. Structural column:
4 in (102 mm) face brick, 0.5 in (13 mm) thick pre-molded expansion filler, 10 x 7 in (254 x 178 mm) steel column, and 1 in (25 mm) particle board with plastic laminated face.

G. The Anchorage building

1. Wall below the suspended ceiling:
5 in (127 mm) precast concrete panel, 3 in (76 mm) semirigid glass fiber insulation board, 4 in (102 mm) glass fiber batt insulation, and 0.63 in (16 mm) foil backed gypsum wallboard on metal studs.

2. Wall inside the ceiling plenum:
5 in (127 mm) precast concrete panel, and 3 in (76 mm) semirigid glass fiber insulation board with spray-on fireproofing.

3. Roof deck inside the ceiling plenum:
1 in (25 mm) concrete paver, 3 in (76 mm) semirigid glass fiber insulation board, and 6 in (152 mm) lightweight aggregate concrete roof slab on corrugated steel deck tied to wall structure.

Table 8.1 (continued)

4. Mirror wall:
0.25 in (6 mm) reflective tempered glass, 4 in (102 mm) glass fiber batt insulation, and 0.63 in (16 mm) foil backed gypsum wallboard on metal studs.

Table 8.2
Comparison of Wall Thermal Resistances Measured with a Portable Calorimeter (PC) and Heat Flow Meters (HFM) to Corresponding Design Values

Building	Building Component	Air Temp °F (°C) Hot Side	Air Temp °F (°C) Cold Side	Heat Flow Rate Btu/h-ft² (W/m²)	R-Value, ft²-h-°F/Btu (m²-K/W) Measured PC	Measured HFM	Predicted Value
Ann Arbor, MI	1. Wall	68.1 (20.1)	39.4 (4.1)	2.49 (7.85)	11.1 (1.95)	11.5 (2.03)	10.6
	2. Structural Beam	65.1 (18.4)	39.4 (4.1)	5.85 (18.4)		4.40 (0.77)	3.7 (0.66)
	3. Structural Column	68.9 (20.5)	39.4 (4.1)	2.22 (7.00)		13.3 (2.34)	8.8 (1.55)
Columbia, SC	1. Wall	70.3 (21.3)	47.9 (8.8)	2.08 (6.56)	15.1 (2.66)	10.8 (1.89)	11.2 (1.97)
	2. Upper Wall	69.1 (20.6)	47.9 (8.8)	2.76 (8.70)		7.7 (1.35)	9.4 (1.66)
	3. Concrete Wall	69.1 (20.6)	47.9 (8.8)	4.75 (15.0)		4.5 (0.79)	3.9 (0.68)
	4. Concrete Beam	69.1 (20.6)	47.9 (8.8)	3.64 (11.5)		5.8 (1.03)	4.5 (0.78)
Springfield, MA	1. Wall	69.5 (20.8)	41.9 (5.5)	2.20 (6.92)	6.8 (1.20)	12.6 (2.21)	13.0 (2.29)
	2. Upper Wall	69.9 (21.1)	41.9 (5.5)	2.50 (7.88)		11.2 (1.97)	13.0 (2.29)
	3. Structural Column	69.3 (20.7)	41.9 (5.5)	2.33 (7.35)		11.8 (2.07)	13.0 (2.29)
Huron, SD	1. Wall	66.9 (19.4)	37.9 (3.3)	1.42 (4.48)	12.0 (2.11)	20.4 (3.59)	16.9 (2.97)
	2. Upper Wall	63.8 (17.7)	37.9 (3.3)	1.23 (3.88)		21.0 (3.70)	16.9 (2.97)
	3. Structural Beam	63.8 (17.7)	37.9 (3.3)	2.49 (7.85)		10.4 (1.83)	15.6 (2.75)
	4. Structural Column	66.6 (19.2)	37.9 (3.3)	3.02 (9.52)		9.5 (1.67)	9.7 (1.71)

Table 8.2 (continued)

Building	Building Component	Air Temp °F (°C) Hot Side	Air Temp °F (°C) Cold Side	Heat Flow Rate Btu/h-ft² (W/m²)	R-Value, ft²-h-°F/Btu (m²-K/W) Measured PC	Measured HFM	Predicted Value
Norfolk, VA	1. Wall	77.2 (25.1)	48.4 (9.1)	3.36 (10.6)		8.6 (1.51)	15.7 (2.76)
	2. Structural Column	77.7 (25.4)	48.4 (9.1)	1.98 (6.24)		14.8 (2.61)	15.7 (2.76)
	3. Structural Beam	78.4 (25.8)	48.4 (9.1)	1.11 (3.48)		27.2 (4.78)	22.1 (3.88)
Pittsfield, MA	1. Wall	77.8 (25.4)	38.7 (3.7)	3.81 (12.0)		10.3 (1.81)	11.8 (2.07)
	2. Upper Wall	78.0 (25.6)	38.7 (3.7)	4.02 (12.7)		9.8 (1.72)	4.6 (1.93
	3. Structural Column	77.5 (25.3)	38.7 (3.7)	6.62 (20.9)		5.9 (1.03)	4.6 (0.81)
Anchorage, AK	1. Wall	73.2 (22.9)	50.6 (10.3)	0.70 (2.21)		32.0 (5.64)	29.9 (5.27)
	2. Upper Wall	69.2 (20.7)	50.6 (10.3)	0.85 (2.71)		21.7 (3.81)	14.6 (2.56)
	3. Structural Column	69.2 (20.7)	50.6 (10.3)	1.59 (5.01)		11.7 (2.06)	15.1 (2.66)
	4. Roof Deck-Webs						
	Lower	69.6 (20.9)	50.6 (10.3)	1.07 (3.37)		17.8 (3.13)	20.4 (3.59)
	Upper	69.6 (20.9)	50.6 (10.3)	0.64 (2.02)		29.6 (5.21)	
	5. Mirror Wall	73.8 (23.2)	50.6 (10.3)	0.87 (2.74)		26.7 (4.70)	17.1 (3.01)

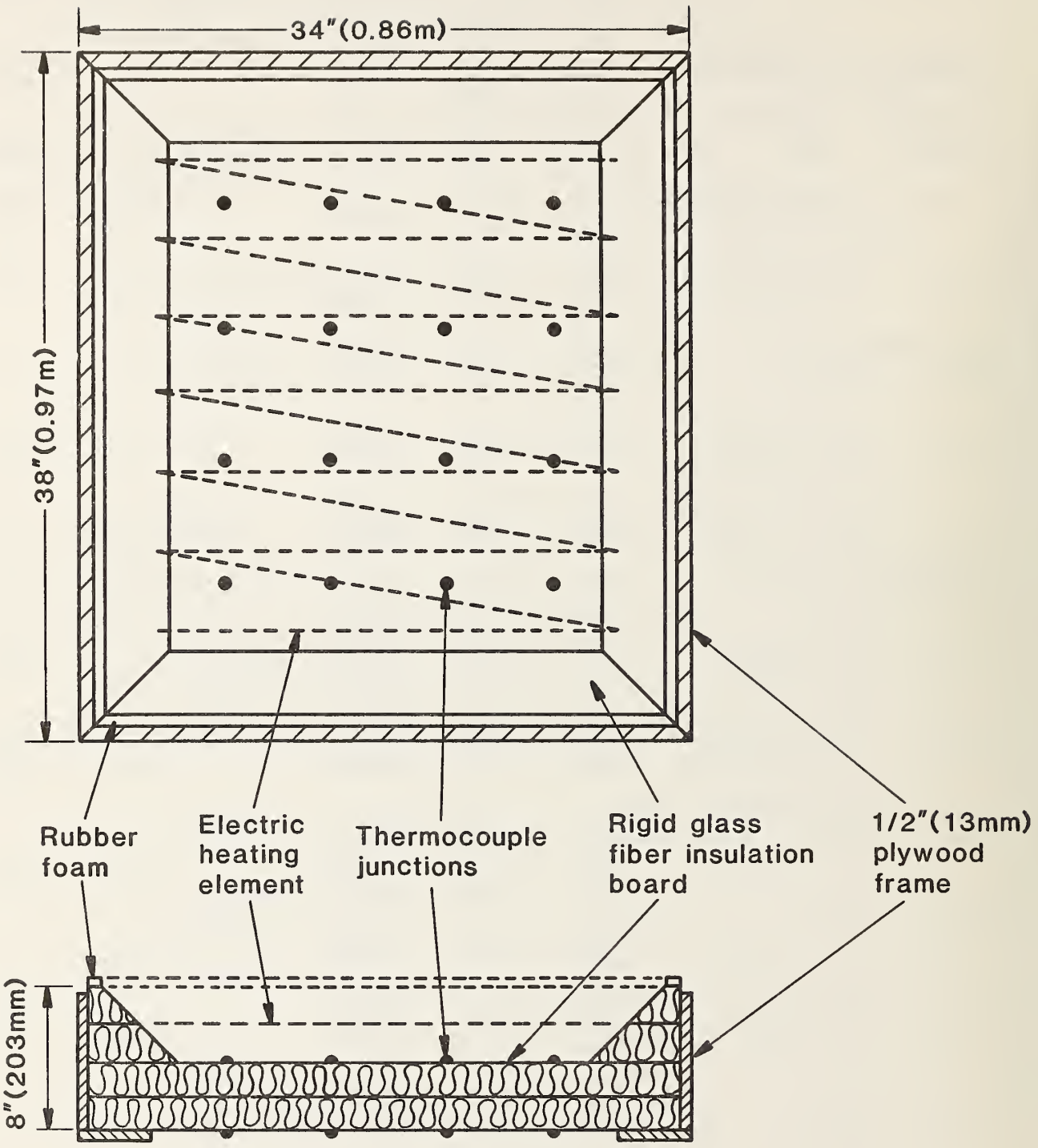

Figure 8.1 Construction Details of Portable Calorimeter

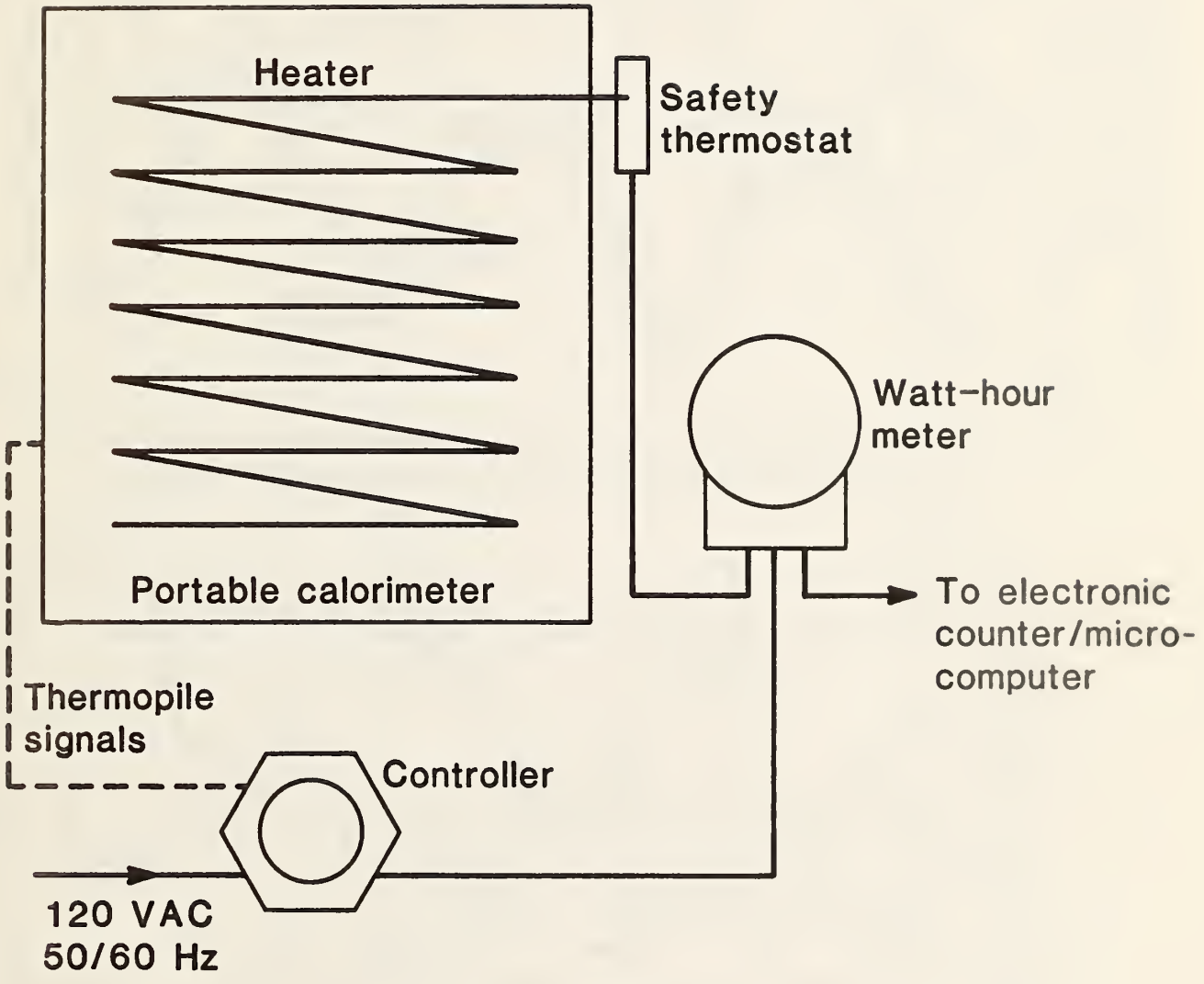

Figure 8.2 Schematic of the Measurement/Control System of the Portable Calorimeter

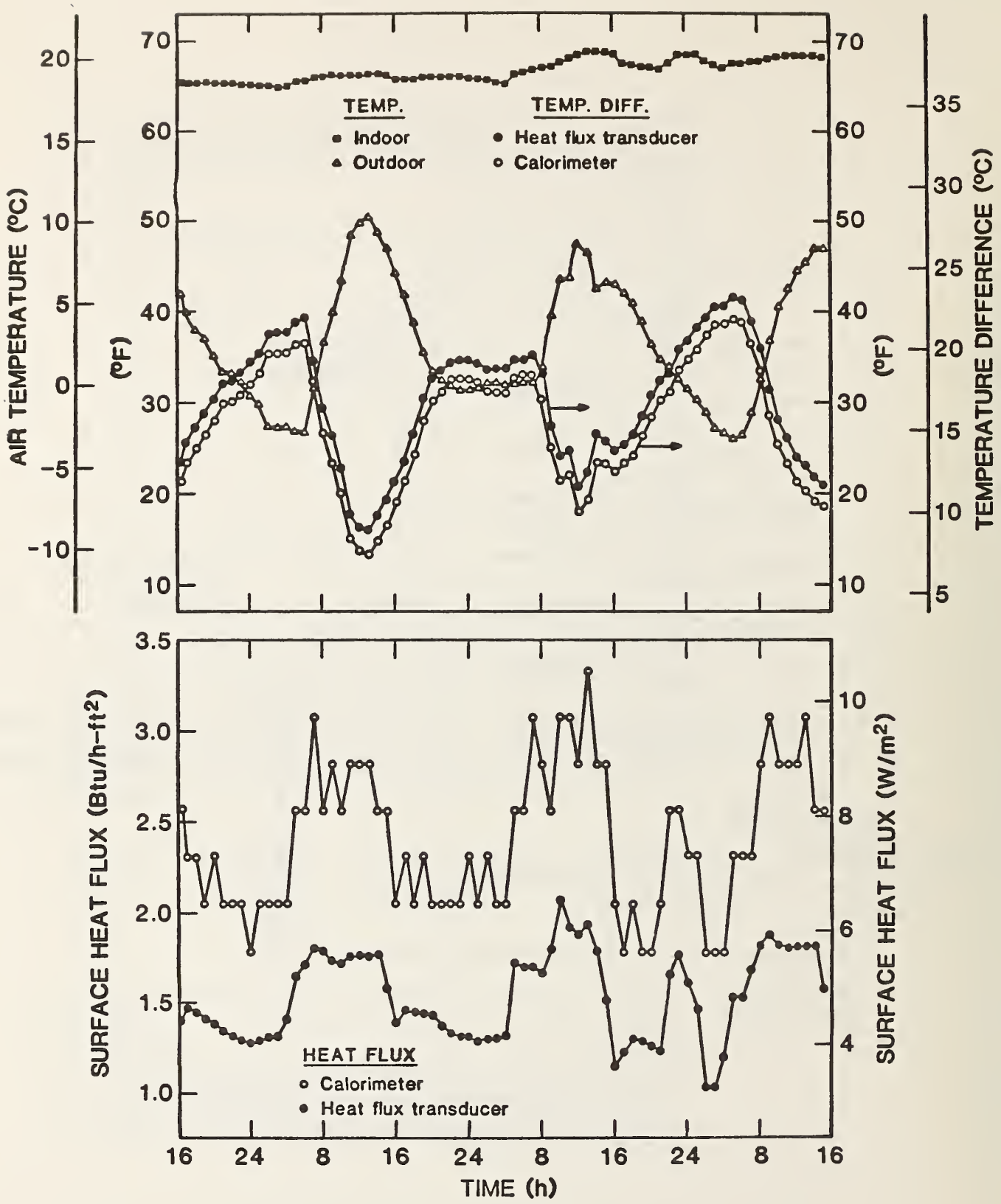

Figure 8.3 Indoor and Outdoor Temperatures, Temperature Difference Across Wall and Surface Heat Fluxes Measured with Heat Flux Transducers and the Calorimeter

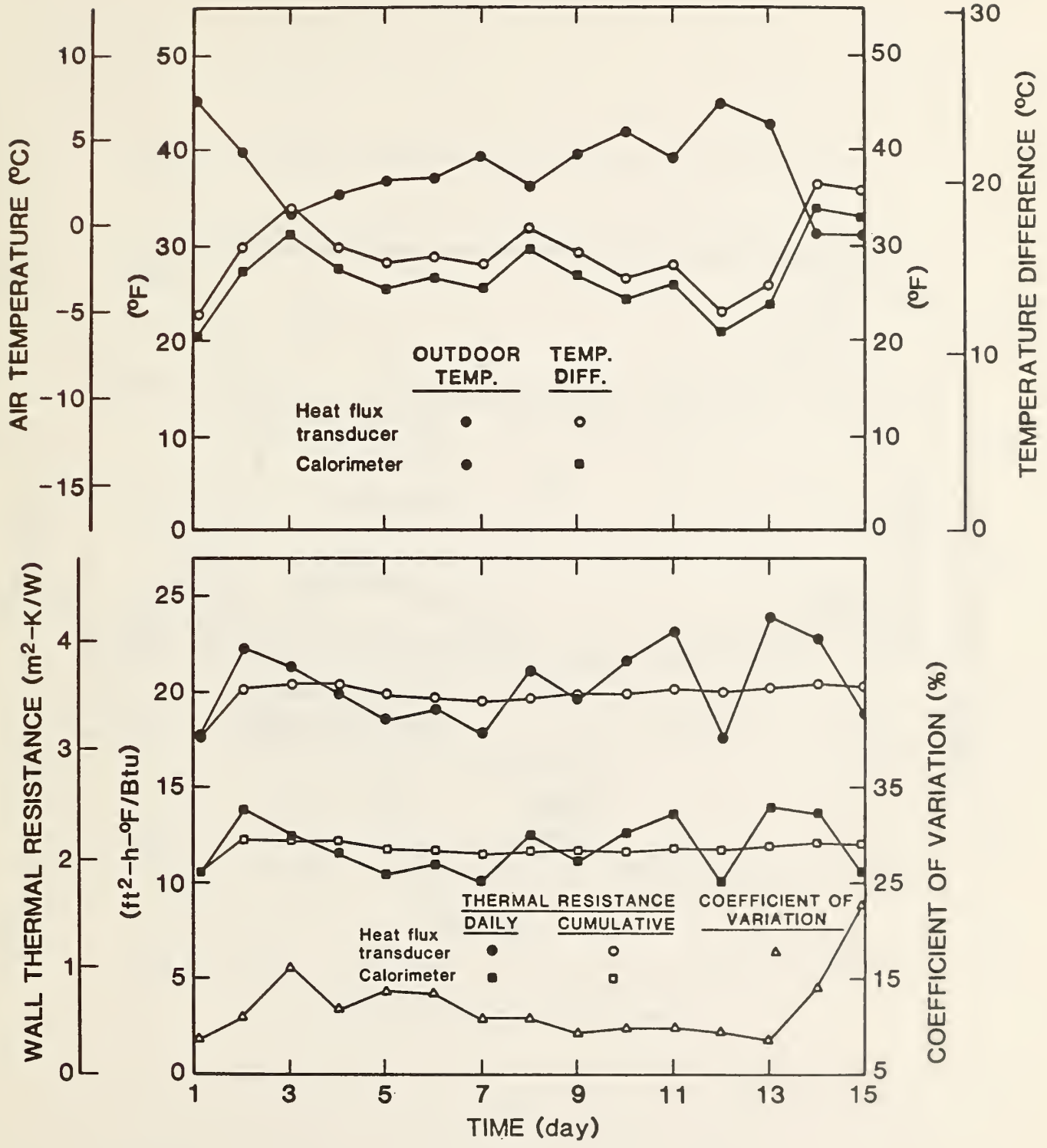

Figure 8.4 Long Term Variations in Heat Flux Transducer and Calorimeter Measurements of a Wall Section

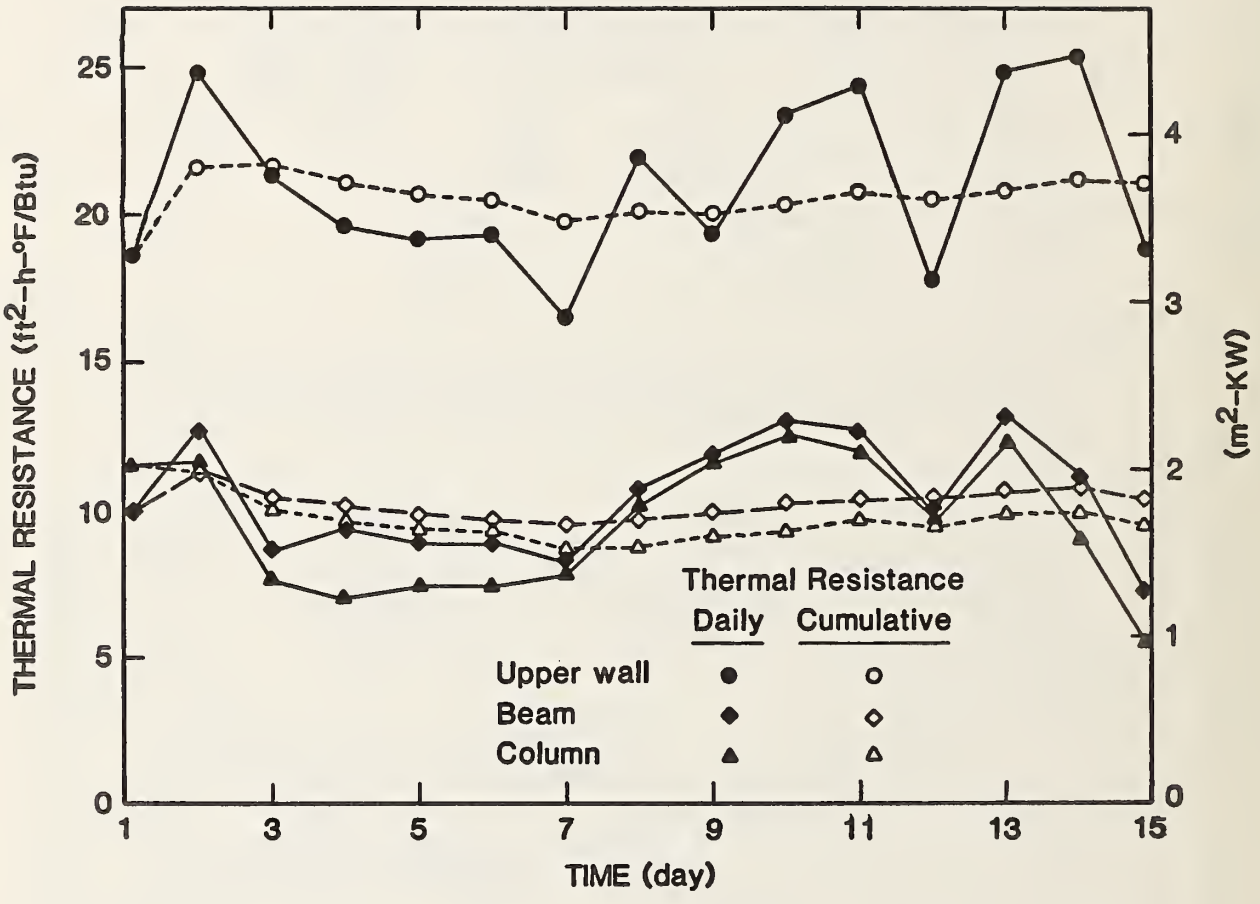

Figure 8.5 Long Term Variations of Thermal Resistance Measurement of the Upper Wall and Structural Beam and Column

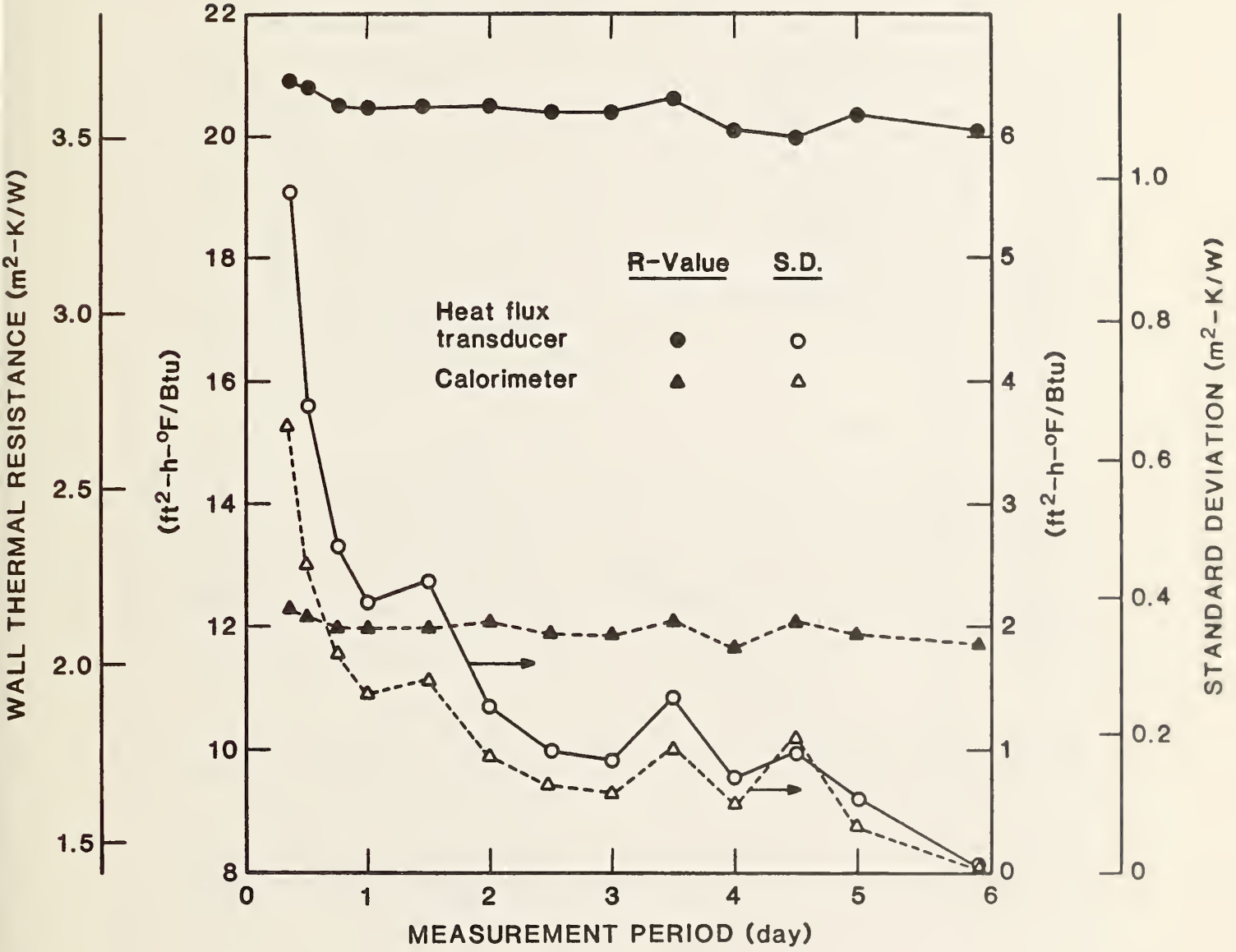

Figure 8.6 Effects of Measurement Period on Average Wall R-Values Determined by Heat Flux Transducer and Calorimeter

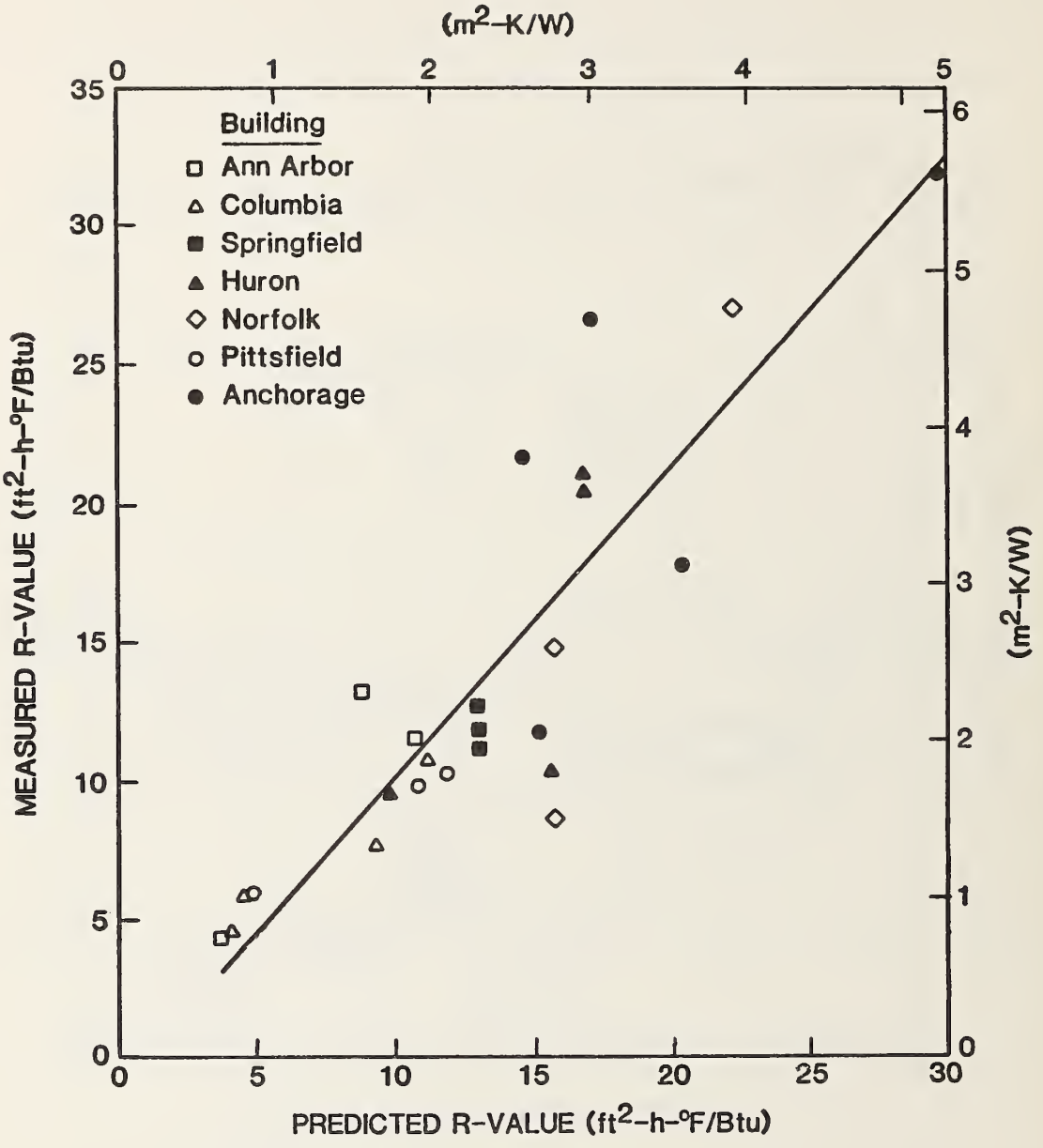

Figure 8.7 Comparison between the Measured Thermal Resistance and the Predicted Steady-State Resistance Values

9.0 Heat Losses Due to Thermal Bridges

9.1 Introduction

The thermographic inspection of the federal buildings revealed that four of the buildings have a number of highly conductive heat flow paths, referred to as thermal bridges, which conduct excessive heat around the insulation and cause abnormal escape of heat from the building. In better insulated buildings the heat losses associated with thermal bridges are more pronounced [28].

In general, a thermal bridge has a smaller cross-sectional area and contains material with less thermal resistance than the adjacent areas of the building envelope. During the heating season, the thermal bridge results in a rise in the external and a decrease in the internal surface temperature in the region of the building envelope where the thermal bridge occurs. The thermal bridge also causes a higher rate of outward heat flow relative to adjacent areas. During the cooling season, the process is reversed, resulting in increased heat gains. At external wall-floor interfaces, where concrete walls with layers of interior insulation are penetrated by concrete deck floors or internal walls, the thermal bridges may increase the envelope heat loss by 50% [30]. Condensation of moisture at interior surfaces can occur at the location of thermal bridges and cause rapid deterioration of building materials.

9.2 Description of the Thermal Bridges Found in the Building Envelopes

An example of structural thermal bridges found in the north wall of the office building located in Huron, SD is illustrated in the thermogram shown in figure 9.1. This thermogram was obtained from ground based thermographic inspections of the building envelope. The bright horizontal lines shown in the figure are thermal bridges at the exterior wall/intermediate floor intersection. The bright region in the right of figure 9.1 does not constitute a thermal bridge but rather is caused by the glass windows located near an entrance to the building.

Figure 9.2 shows a thermogram of the stone faced wall of the building located in Ann Arbor, MI. The horizontal and vertical bright lines in the picture indicate thermal bridges caused by the penetration of intermediate concrete slab floors and structural columns in the exterior wall. A thermogram showing the upper portions of the external walls of the building in Anchorage, AK is given in Fig 9.3. The horizontal and vertical bright stripes in this thermogram depict thermal bridges resulting from the penetration of concrete floors and structural columns through an insulated exterior wall.

Figure 9.4 shows thermal anomalies observed in a precast concrete panel of an exterior wall of the building in Columbia, SC. The long horizontal and vertical luminous lines show the thermal bridges caused by high heat conduction through the window overhangs and decorative columns that penetrated the insulated wall.

Construction details of the portions of the building envelope where the thermal bridges occurred in the buildings studied are shown in figures 9.6 through 9.8. The specification of the materials used in each wall section

is given in the table 9.1. As can be seen from figures 9.5 through 9.8, the insulation layers in these composite walls are penetrated by the concrete floor assemblies. The thermal conductivity and diffusivity of concrete are about 20 and 3 times greater, respectively, than those of glass fiber insulation. Significant heat flow through these paths during the heating and cooling seasons can be anticipated.

9.3 Instrumentation and Procedures

The equipment used to measure the rate of heat transfer through the building envelopes included heat flux tranducers and temperature sensors that were interfaced to a microcomputer. Each heat flux transducer consisted of a 4-inch (102 mm) diameter thin, flat circular disk with an embedded thermopile. The hot and cold junctions of the thermopile were located on opposite faces of the disk to measure the temperature gradiants and therefore the heat flow through it. The measurement system could simultaneously measure up to 13 temperatures and 15 heat fluxes. The computer continuously scanned all sensors, computed time-averaged values every 2 seconds. From these values average hourly values were computed and stored on a floppy disk for subsequent processing. Upon completion of the field tests, the heat flux transducers were calibrated using a guarded hot plate apparatus described in references 26 and 27. During the calibration the transducers were subjected to a range of uniform heat fluxes at the mean temperatures corresponding to those experienced during the field tests. The accuracy of the heat transducers calibration was estimated to be within $\pm$ 1%.

To perform field measurements, four to eight heat flux transducers were attached by masking tape to selected locations on the interior wall surfaces, one each on the structural beam and column, and four transducers on the roof assembly of the test building. The measurement stations were chosen based on the locations of thermal bridges found in the exterior thermograms of the buildings involved. During installation a stud finder was used to make certain that the transducers were not installed over metallic wall framing members.

Thermistors were used to measure the temperature of the air outside the building and the indoor air in close proximity of heat flux transducers. The sensing element of the thermistor was placed 6 in. (152 mm) from the exposed surface where surface heat flux was determined.

9.4 Test Results

The results of field measurements taken over a period of 2 to 16 days between February and May of 1983 are summarized in table 9.2. The air temperature and heat flow rate values shown in table 9.2 represent the mean values of daily average air temperatures and surface heat fluxes. Test periods consisting of multiples of 24-hours were chosen to minimize the transient effects on heat flow measurements and thermal resistance calculations associated with thermal storage within building components.

The thermal resistance values shown in table 9.2 represent average R-values, defined as the ratio of the average air-to-air temperature difference across the building envelope component to the average heat flow rate over the test period. Also presented are the corresponding predicted

steady-state thermal resistance values. Predicted resistance values were calculated from published data on the thermal properties of the building materials used, employing the series resistance method [8]. In performing these calculations the thermal resistances of air films was assumed to be 0.68 ft^2-h-^oF (0.12 m^2-K/W) on the inside surface and 0.17 ft^2-h-^oF (0.03 m^2-K/W) on the outside surface. These values are considered to be typical of interior and exterior vertical surfaces where the room is at normal temperature and when the exterior surface is exposed to a 15 mph (6.7 m/s) wind.

Table 9.2 shows that the measured and predicted R-values are in general agreement except for the structural column in the Anchorage building. The discrepancy observed in the Anchorage building is attributed to the fact that the simple parallel heat flow method used in performing the thermal resistance calculations is probably not applicable to the cases of the complex structural column and roof deck assembly.

Estimates of the contributions of thermal bridges to the heat losses in the office buildings measured are summarized in table 9.3. These data were derived from heat flux data obtained at the thermal bridges and computations (from an examination of the thermograms and architectural drawings) of the surface areas occupied by the thermal bridges. As can be seen in table 9.3 the thermal bridges resulted in a 62 to 118% increase in the rate of heat flow relative to the wall locations free from thermal bridges. The total cross-sectional area of the thermal bridges was estimated to occupy from 9 to 18% of the wall area depending upon the building. The overall effect of thermal bridges was to increase wall heat transmission from 10 to 21%.

The data presented in table 9.2 are for steady state conditions. However, the response of a thermal bridge is dynamic. Diurnal variations in the outdoor and indoor air temperatures and heat fluxes measured at each site are presented in figures 9.9 through 9.12. Also plotted in the figures are the temperature differences across the walls, and between the outdoor air and the air in the proximity of the structural beam and the roof deck inside the ceiling plenum.

Inspection of figures 9.9 to 9.12 shows that the temperature of the outdoor air varied periodically over 24 hours, with the minimum temperature occurring in the early morning and the peaks in the early afternoon. However, the indoor air temperatures were found to be stable throughout the 24-hour period. The rates of heat flow through the interior surfaces of various components were also found to fluctuate with time. Moreover, the temperature and heat flow data were about 90 degrees out of phase. Specifically, the maximum or minimum heat fluxes shown at the bottom of figures 9.9 to 9.12, were consistently lagging behind the temperature driving force by approximately 5.5, 7.5, 5.4 and 7.2 hours for the Huron, Ann Arbor, Anchorage, and Columbia buildings, respectively. These time differences were attributed to thermal storage.

9.5 Mathematical Modeling

In order to predict the amount of heat loss due to thermal bridges, a computer program called HEATING6 developed by Oak Ridge National Laboratory [31] was used to analyze the thermal fields around the exterior

wall/intermediate floor systems. This computer model uses a finite-difference method to solve multi-dimensional, steady-state and transient heat conduction problems associated with various types of complex structures.

A two dimensional heat flow model containing 1,059 nodes was developed. It simulates transient heat conduction within the multi-layered wall/floor system corresponding to the construction details at the Huron building (see figure 9.5). In executing the code it was assumed that the structure was exposed on one side to a time varying sinusoidal temperature, while on the other side the temperature remained constant throughout.

Figure 9.14 shows the predicted heat fluxes for the interior wall surface, the top of the slab floor, and the exposed surface of the lower inner wall containing the structural beam. These data were obtained by summing the contributions from the steady state condition with a temperature difference across the wall of 30.5°F (16.9°C), and a 24-hour periodic component having an amplitude of $\pm$ 12°F (6.7°C). These values were used because they corresponded to the changes observed in the outdoor air temperature on two consecutive days (see figure 9.9). A convective heat transfer coefficient of 1.47 Btu/h-ft^2-°F (8.35 W/m^2-K) was assumed for both the interior and exterior surfaces. The zero on the abscissa of figure 9.14 represents the intersection of the vertical interior wall surface and the top surface of the horizontal slab floor. Values below zero correspond to points along the top surface of the floor, or the lower wall containing the beam. Heat fluxes corresponding to heat flowing from inside to outside the building were assigned positive values. Added to figure 9.14 are the ranges of surface heat fluxes measured on April 7 on the interior wall surface at the mid-height of the structural beam at the Huron building. The agreement between the measured values and the predicted values is good as can be seen in figure 9.14.

It should be noted that the model predicts significantly higher heat fluxes at points such as the wall/floor corner and the concrete floor where measurements could not be made. An integration of the predicted heat fluxes over the area of the thermal bridge increases the contribution of the thermal bridge to the total wall heat loss by approximately a factor of two. However, additional experimental work is required to ascertain the heat fluxes along points on the thermal bridge where measurements could not be performed.

Figure 9.15 depicts the predicted heat flux on the exterior wall surface for several times throughout the day, plotted as a function of position. These values were calculated for an average air-to-air temperature across the wall of 40°F (22°C) and for an amplitude of $\pm$ 15°F (8.3°C). As the temperature level of the air adjacent to the exterior wall surface changed sinusoidally, the transient effect caused varying amount of heat to flow periodically in or out from the exterior wall. Moreover, as shown in figure 9.5, in the regions around the thermal bridges more heat was dissipated than in the adjoining areas.

9.6 Conclusions

The inspection of the exterior envelope of four federal office buildings using infrared thermography revealed the existence of thermal bridges. The

measurement of the heat flow through these thermal bridges using heat flow meters showed that the heat flux at the thermal bridges were from 62 to 118% greater than the heat flux on the insulated sections of the walls. Examination of thermograms obtained at each building and architectural drawings showed that the thermal bridges represented from 9 to 18% of the buildings insulated wall areas. Therefore, the thermal bridges increased the wall heat loss by approximately 10 to 21% relative to the same wall structures without thermal bridges. A two-dimensional finite difference heat flow model was used to simulate the transient response of the thermal bridge representing an exterior wall/intermediate floor system. At points at which heat flow measurements could be made, the model predicted the measured heat flux well. Moreover, the model predicted even higher heat fluxes at other points on the thermal bridge where measurements could not be made. Therefore, the total contribution of thermal bridges to heat loss is probably even greater, perhaps by a factor of two, than that cited above. Additional experimental work is needed to confirm this possibility.

Table 9.1

Details of Building Components in Thermal Bridge Measurements

A. The Huron building

1. Wall located below acoustical tile ceiling:
4 in. (102 mm) face brick, 6 in. (152 mm) light-weight concrete masonry unit, 3 in. (76 mm) semirigid glass fiber insulation board, and 0.63 in. (16 mm) gypsum wallboard.

2. Wall inside the ceiling plenum:
Same as above.

3. Structural beam in the ceiling plenum:
4 in. (102 mm) face brick, 4 in. (102 mm) light-weight concrete masonry unit, 3 in. (76 mm) semirigid glass fiber insulation, and W24x84 steel beam with a 2 in. (51 mm) minimum fire proofing.

4. Structural column:
4 in. (102 mm) face brick, 4 in. (102 mm) concrete masonry unit, structural column with 2 in. (51 mm) spray-on fire proofing, and 0.63 in. (16 mm) gypsum wallboard on metal studs as column enclosure.

B. The Ann Arbor building

1. Wall below the suspended ceiling:
0.5 in. (13 mm) Quarry tile, 1 in. (25 mm) metal lath and motor bed, 10 in. (254 mm) concrete masonry unit, 1.5 in. (38 mm) semirigid glass fiber insulation board, and 0.63 in. (16 mm) acoustic wall panel.

2. Beam section inside the ceiling plenum:
0.5 in. (13 mm) Quarry tile, 1 in. (25 mm) metal lath and motor bed, 4 in. (102 mm) concrete masonry unit, and W21x44 steel beam with spray-on fire proofing.

3. Structural column:
0.5 in. (13 mm) Quarry tile, 1 in. (25 mm) metal lath and motor bed, 10 in. (254 mm) concrete masonry unit, 1.5 in. (38 mm) glass fiber blanket insulation, structural column with spray-on fire proofing, and 0.63 in. (16 mm) plaster on 0.63 in. (16 mm) gypsum lath on 3.3 in. (84 mm) metal studs.

C. The Anchorage building

1. Wall below the suspended ceiling:
5 in. (127 mm) precast concrete panel, 3 in. (76 mm) semirigid glass fiber insulation board, 4 in. (102 mm) glass fiber batt insulation, and 0.63 in. (16 mm) foil backed gypsum wallboard on metal studs.

2. Wall inside the ceiling plenum:
5 in. (127 mm) precast concrete panel, 3 in. (76 mm) semirigid glass fiber insulation board with spray-on fire proofing.

3. Roof deck in the ceiling plenum:
1 in. (25 mm) concrete paver, 3 in. (76 mm) semirigid glass fiber insulation board, and 6 in. (152 mm) light weight aggregate concrete roof slab on corrugated steel deck connecting to wall structure.

4. Structural column:
5 in. (127 mm) precast concrete panel, 3 in. (76 mm) semirigid glass fiber insulation board, 20 x 20 in, (508 x 508 mm) steel column with spray-on fire proofing, and 0.63 in. (16 mm) gypsum board as column enclosure.

D. The Columbia building

1. Wall below acoustic tile ceiling:
12 in. (305 mm) precast concrete panel, 2 in. (51 mm) glass fiber blanket insulation, and 0.63 in. (16 mm) gypsum wallboard on 2 in. (51 mm) metal studs.

2. Wall above acoustic tile ceiling:
8 in. (203 mm) precast concrete panel, 24 in. (610 mm) air space inside concrete overhang, 3 in. (76 mm) precast concrete panel, 2 in. (51 mm) glass fiber blanket insulation, and 0.63 in. (16 mm) gypsum wallboard on 2 in. (51 mm) metal studs.

3. Concrete wall inside the ceiling plenum:
15 in. (381 mm) precast concrete panel.

4. Concrete beam inside the ceiling plenum:
10 in. (254 mm) precast concrete panel, and 18 in. (457 mm) reinforced concrete beam.

Table 9.2

Measured Heat Flow Rates and Thermal Resistance Values of Building Components in Thermal Bridge Analysis

Building	Component	Daily Average Air Temp °F (°F) Hot Side	Cold Side	Daily Average Heat Flow Rate Btu/h-ft² (W/m²)	Thermal Resistance ft²-h-°F/Btu (m²-K/W) Measured Value	Predicted Value
Huron, SD	1. Wall	66.9 (19.4)	37.9 (3.3)	1.42 (4.48)	20.4 (3.59)	16.9 (2.97)
	2. Upper Wall	63.8 (17.7)	37.9 (3.3)	1.23 (3.88)	21.0 (3.70)	16.9 (2.97)
	3. Structural	63.8 (17.7)	37.9 (3.3)	2.49 (7.85)	10.4 (1.83)	15.6 (2.75)
	4. Structural Column	66.6 (19.2)	37.9 (3.3)	3.02 (9.52)	9.5 (1.67)	9.7 (1.71)
Ann Arbor, MI	1. Wall	68.1 (20.1)	39.4 (4.1)	2.49 (7.85)	11.5 (2.03)	10.6 (1.87)
	2. Structural	65.1 (18.4)	39.4 (4.1)	5.85 (18.44)	4.4 (0.77)	3.7 (0.66)
	3. Structural	68.9 (20.5)	39.4 (4.1)	2.22 (7.00)	13.3 (2.34)	8.8 (1.55)
Anchorage, AK	1. Wall	73.2 (22.9)	50.6 (10.3)	0.70 (2.21)	32.0 (5.64)	29.9 (5.27)
	2. Upper Wall	69.2 (20.7)	50.6 (10.3)	0.86 (2.71)	21.7 (3.81)	14.6 (2.56)
	3. Roof Deck-Webs Lower	69.6 (20.9)	50.6 (10.3)	1.07 (3.37)	17.8 (3.13)	20.4 (3.59)
	Upper	69.6 (20.9)	50.6 (10.3)	0.64 (2.02)	29.6 (5.21)	17.1 (3.01)
	4. Structural Column	69.2 (20.7)	50.6 (10.3)	1.59 (5.01)	11.7 (2.06)	15.1 (2.66)

Building	Component	Daily Average Air Temp °F (°F) Hot Side	Cold Side	Daily Average Heat Flow Rate Btu/h-ft² (W/m²)	Thermal Resistance ft²-h-°F/Btu (m²-K/W) Measured Value	Predicted Value
Columbia, SC	1. Wall	70.3 (21.3)	47.9 (8.8)	2.08 (6.56)	10.8 (1.89)	11.2 (1.97)
	2. Upper Wall	69.1 (20.6)	47.9 (8.8)	2.76 (8.70)	7.7 (1.35)	9.4 (1.66)
	3. Concrete Wall	69.1 (20.6)	47.9 (8.8)	4.75 (15.0)	4.5 (0.79)	3.9 (0.68)
	4. Concrete Beam	69.1 (20.6)	47.9 (8.8)	3.64 (11.5)	5.8 (1.03)	4.5 (0.78)

Table 9.3

Estimates of the Heat Losses Resulting from Thermal Bridges

Office Building	Increased Wall Heat Flow Rate* (%)	Percent of Wall Occupied by Thermal Bridge	Percent Increase in Total Wall Heat Flow Caused by Thermal Bridge
Huron, South Dakota	108	9	10
Ann Arbor, Michigan	62	17	11
Anchorage, Alaska	118	18	21
Columbia, South Carolina	74	16	12

*Note: The ratio of the heat flux difference between the walls with and without thermal bridges to the surface heat flux at the wall with no thermal bridges.

Figure 9.1 Thermal Bridges Found in the Exterior Wall of the Huron Office Building

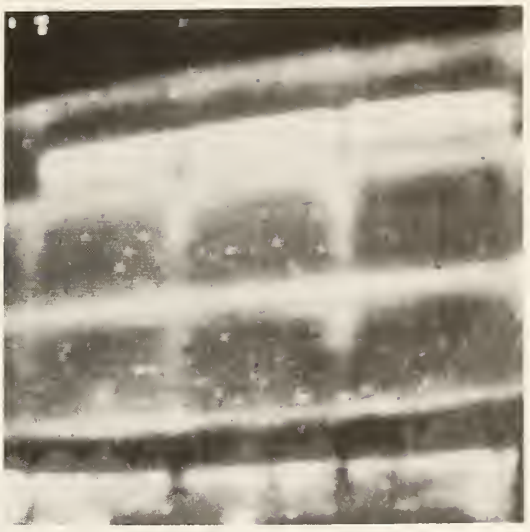

Figure 9.2 Thermal Bridge Occurring in the Ann Arbor Building

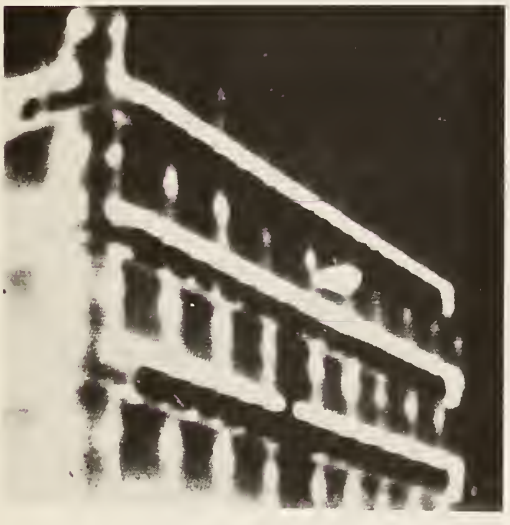

Figures 9.3 Thermal Bridges Observed in Upper Floors of the Anchorage Building

Figure 9.4 Thermal Bridges Occurring in the Columbia Building

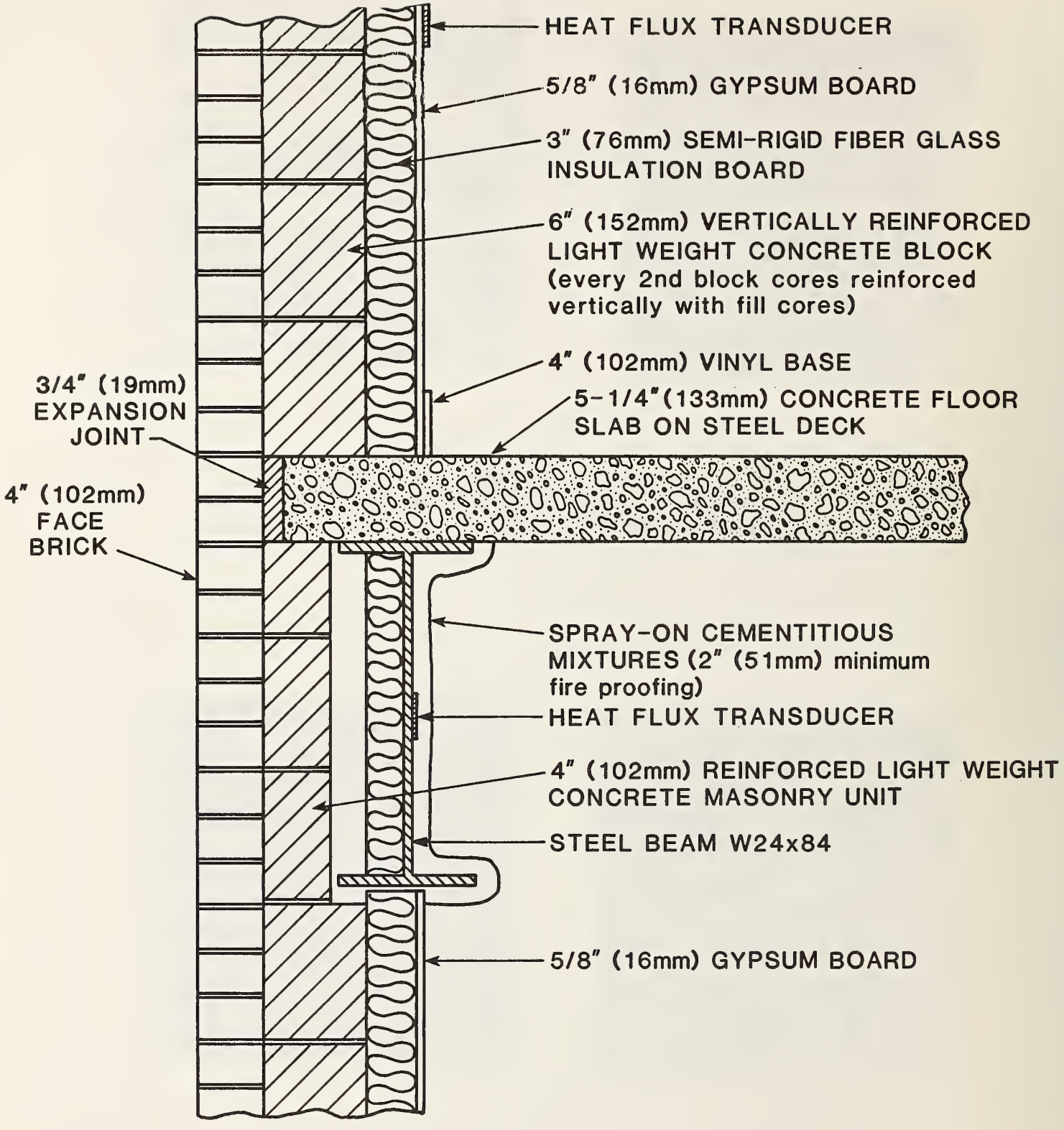

Figure 9.5 Construction Details and Sensor Locations on the Exterior Wall in the Huron Office Building

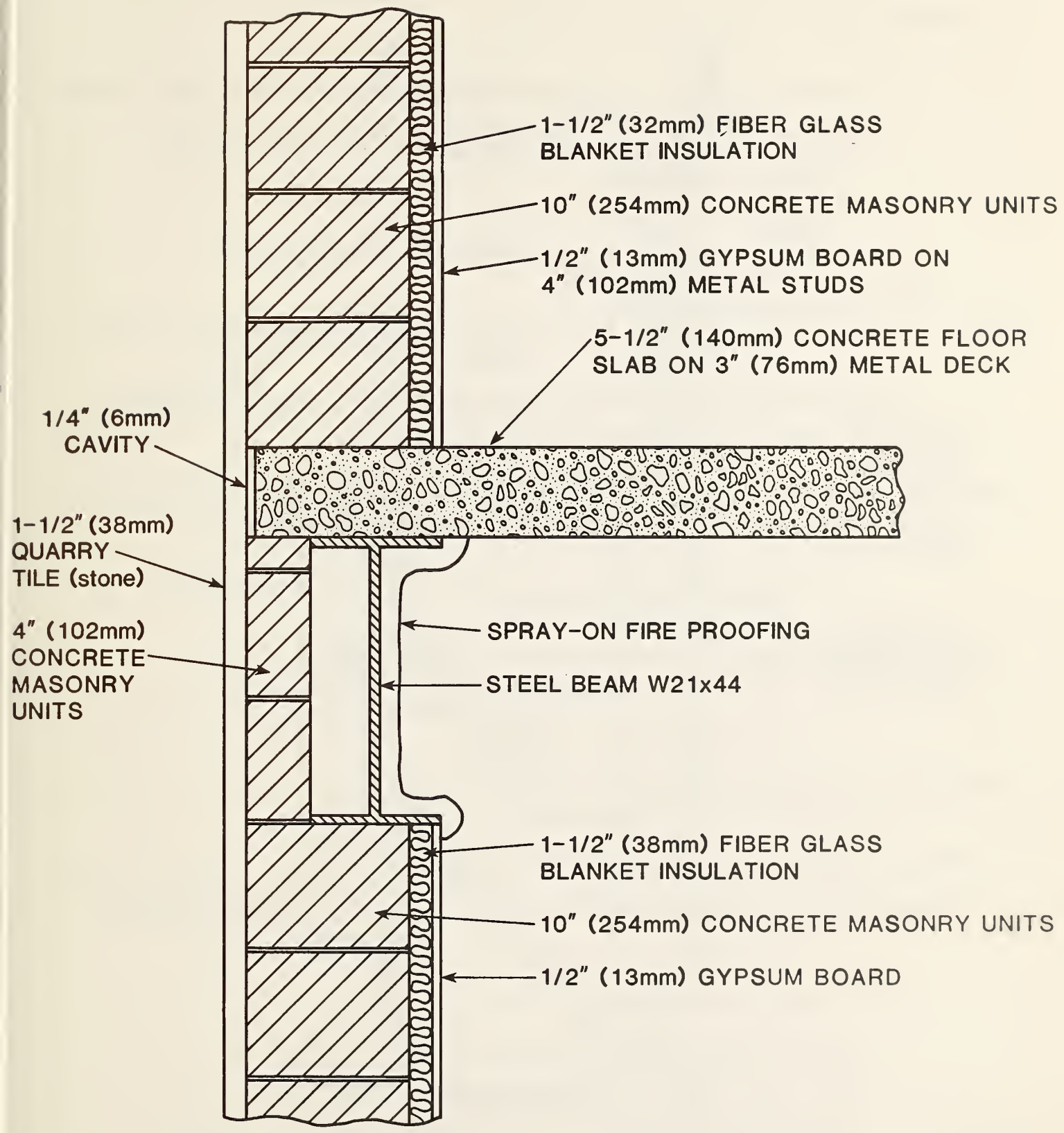

Figure 9.6 Construction Details of the Exterior Wall in the Ann Arbor Office Building

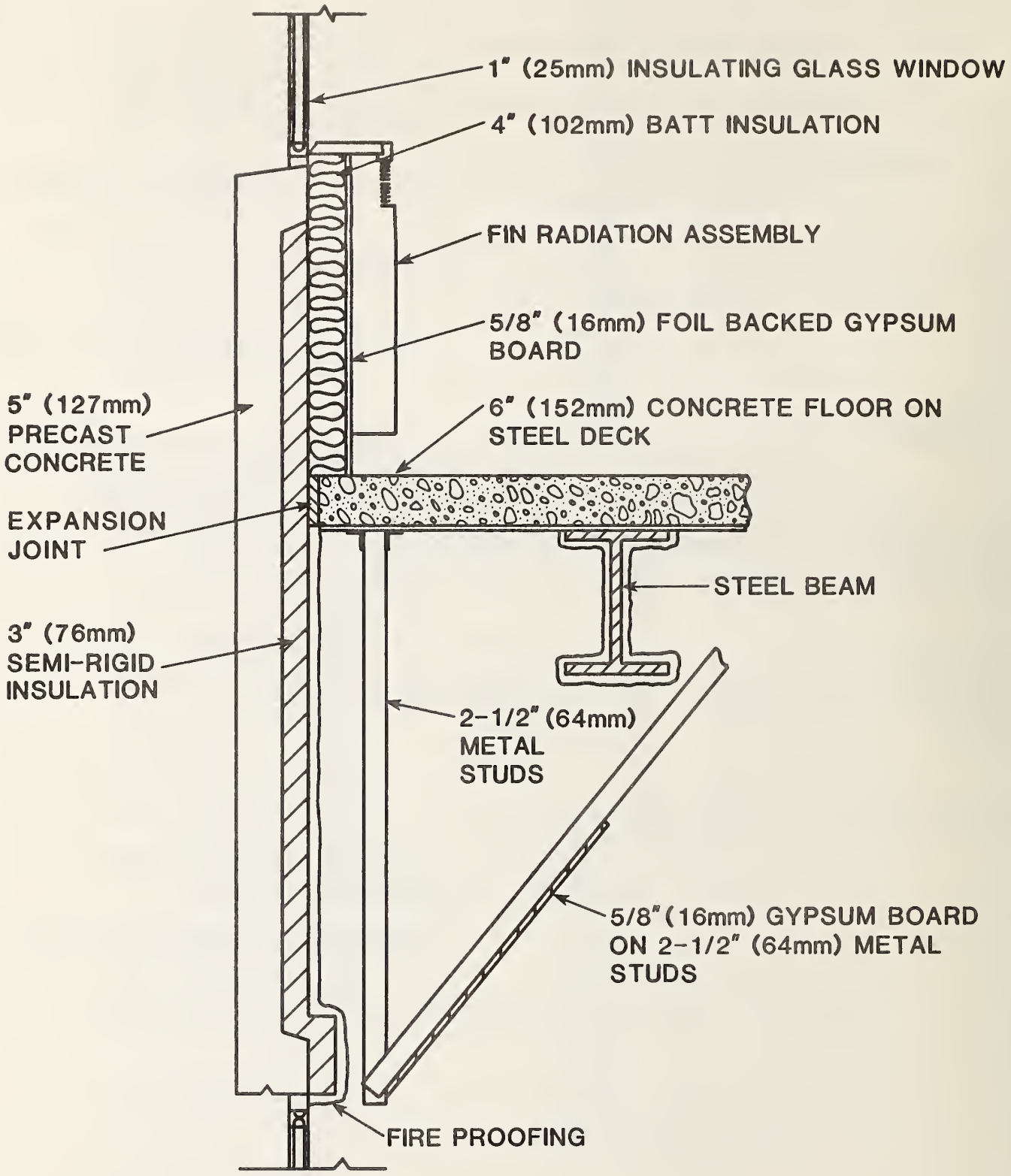

Figure 9.7 Construction Details of the Exterior Wall in the Anchorage Office Building

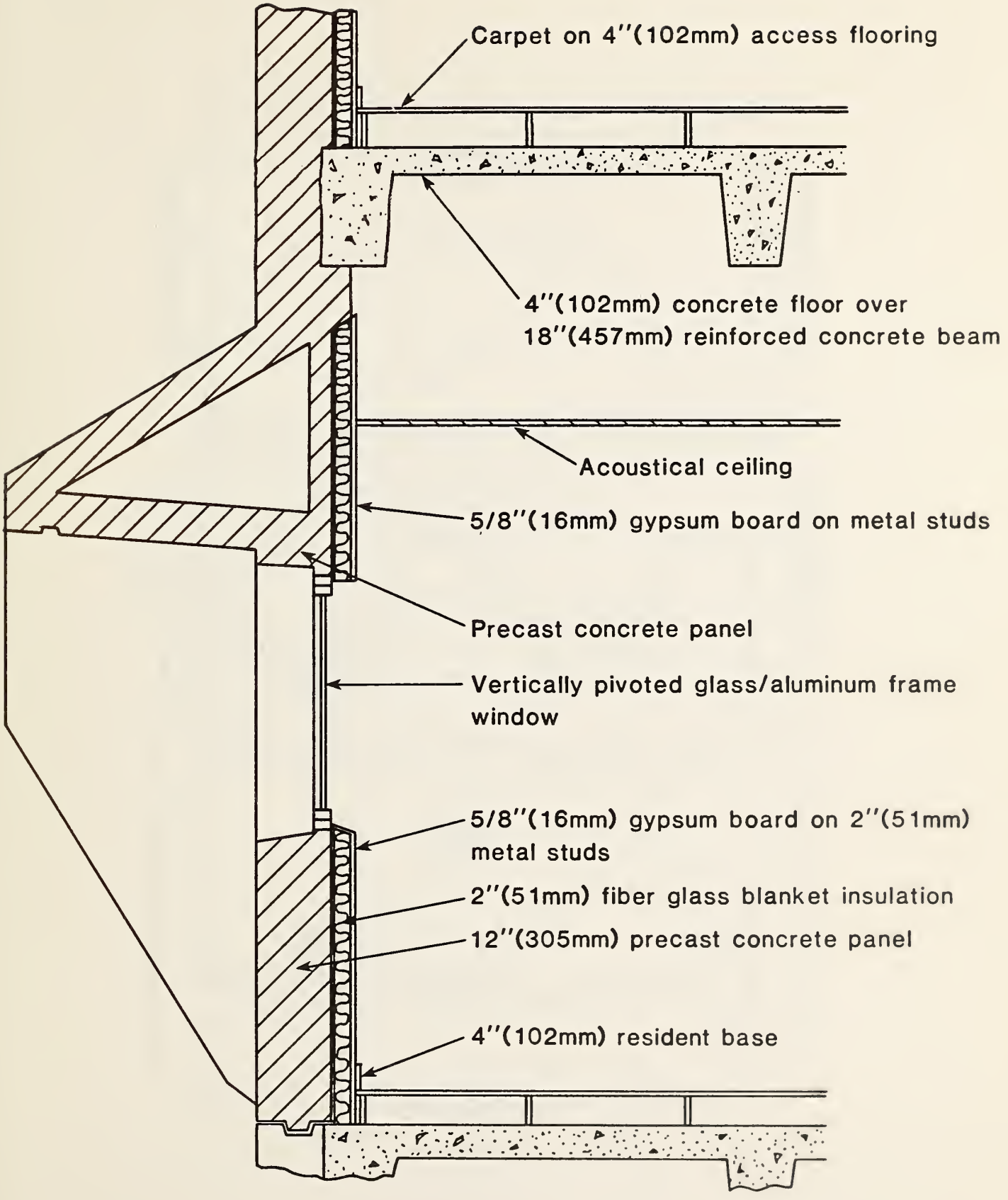

Figure 9.8 Construction Details of the Exterior Wall in the Columbia Office Building

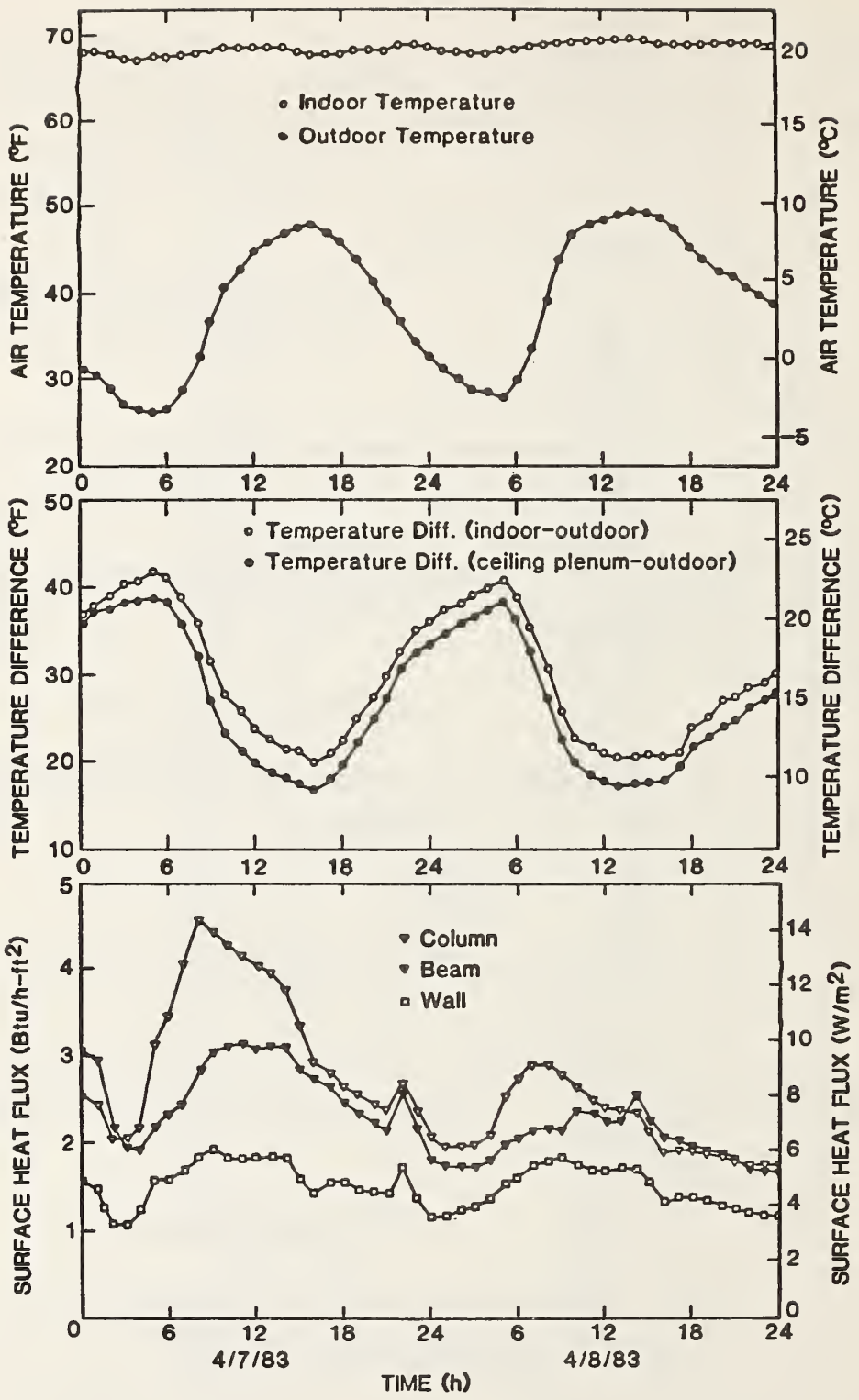

Figure 9.9 Temperature and Heat Flux in the Huron Building as a Function of Time

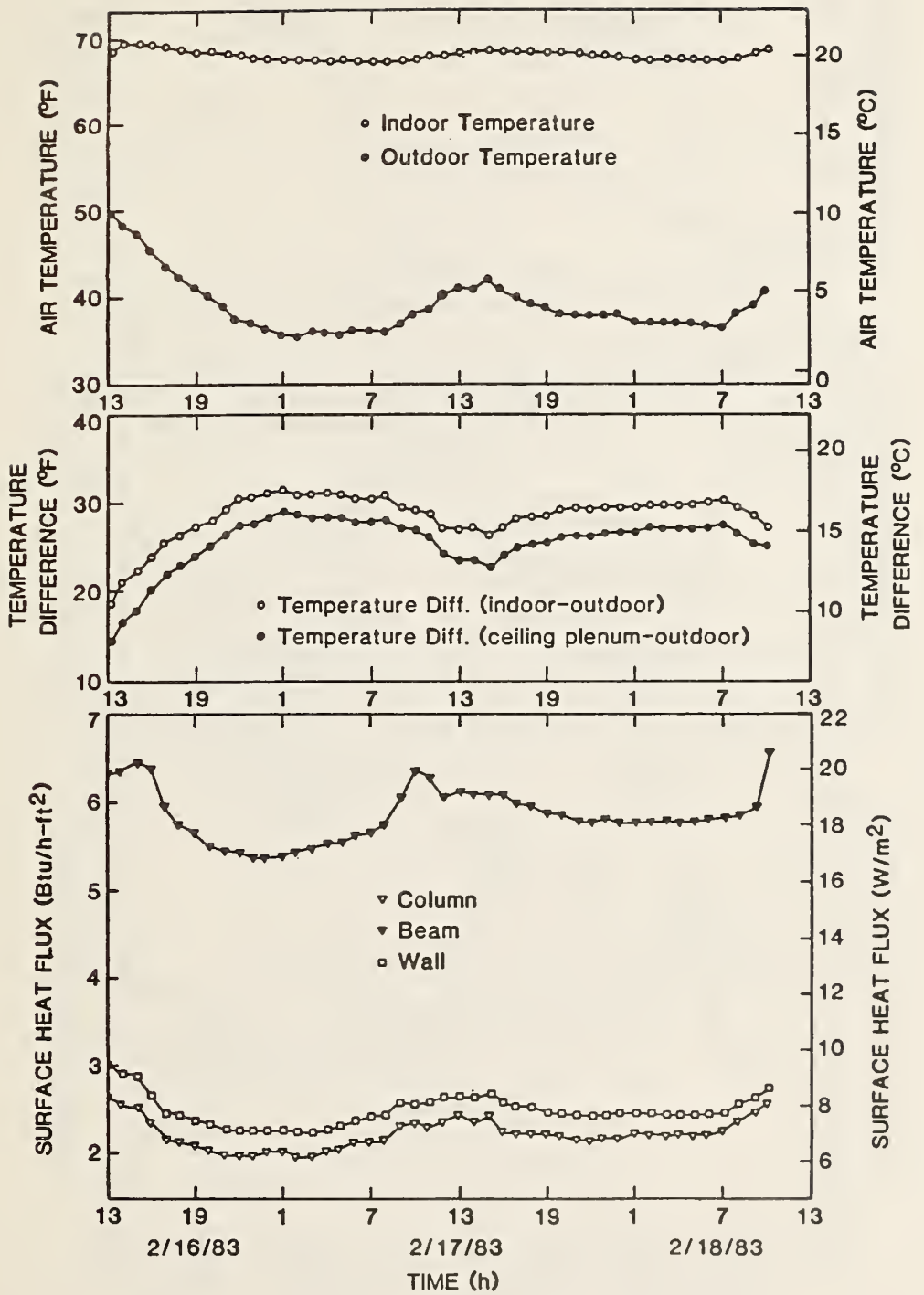

Figure 9.10 Temperature and Heat Flux in the Ann Arbor Building as a Function of Time

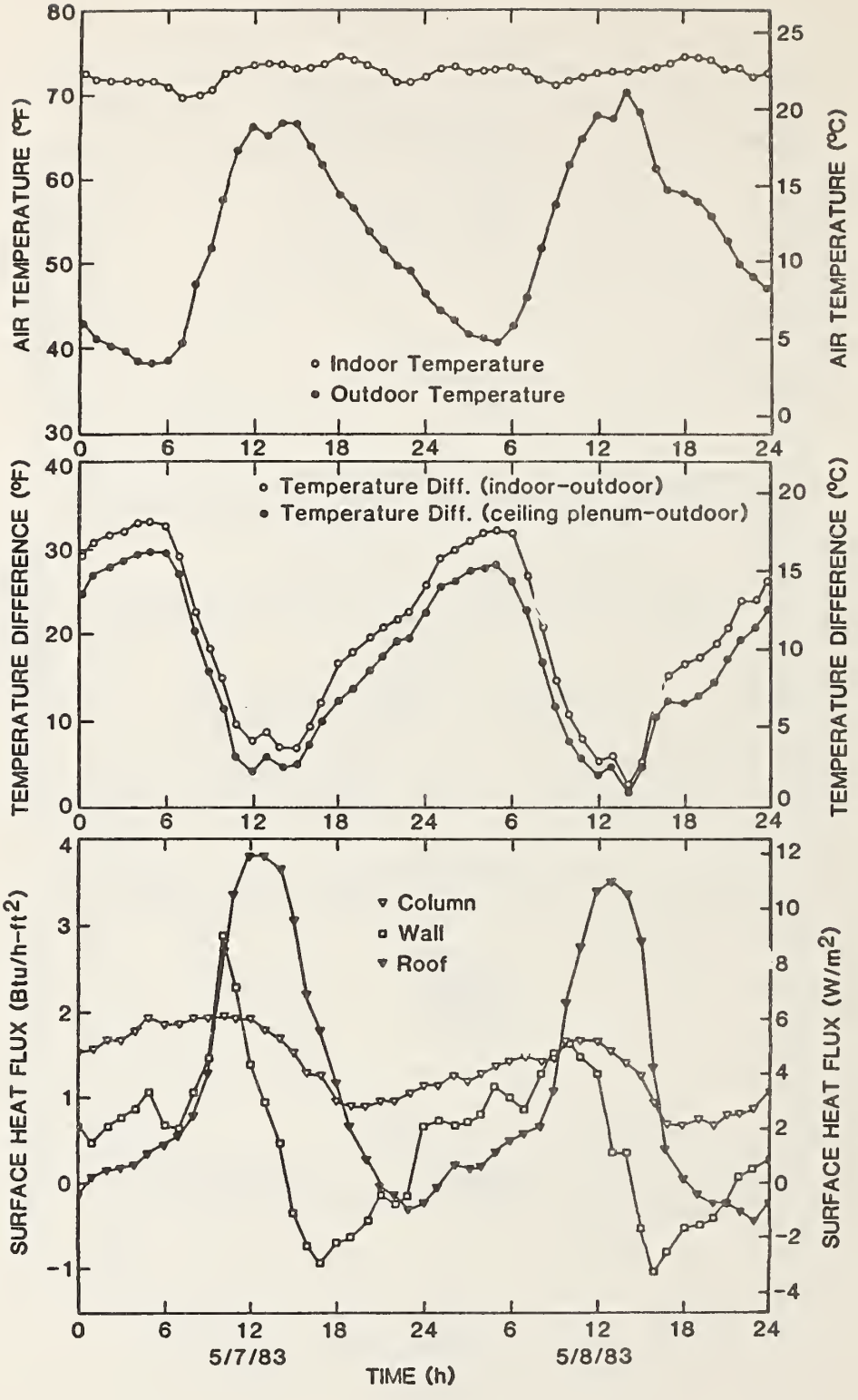

Figure 9.11 Temperature and Heat Flux in the Anchorage Building as a Function of Time

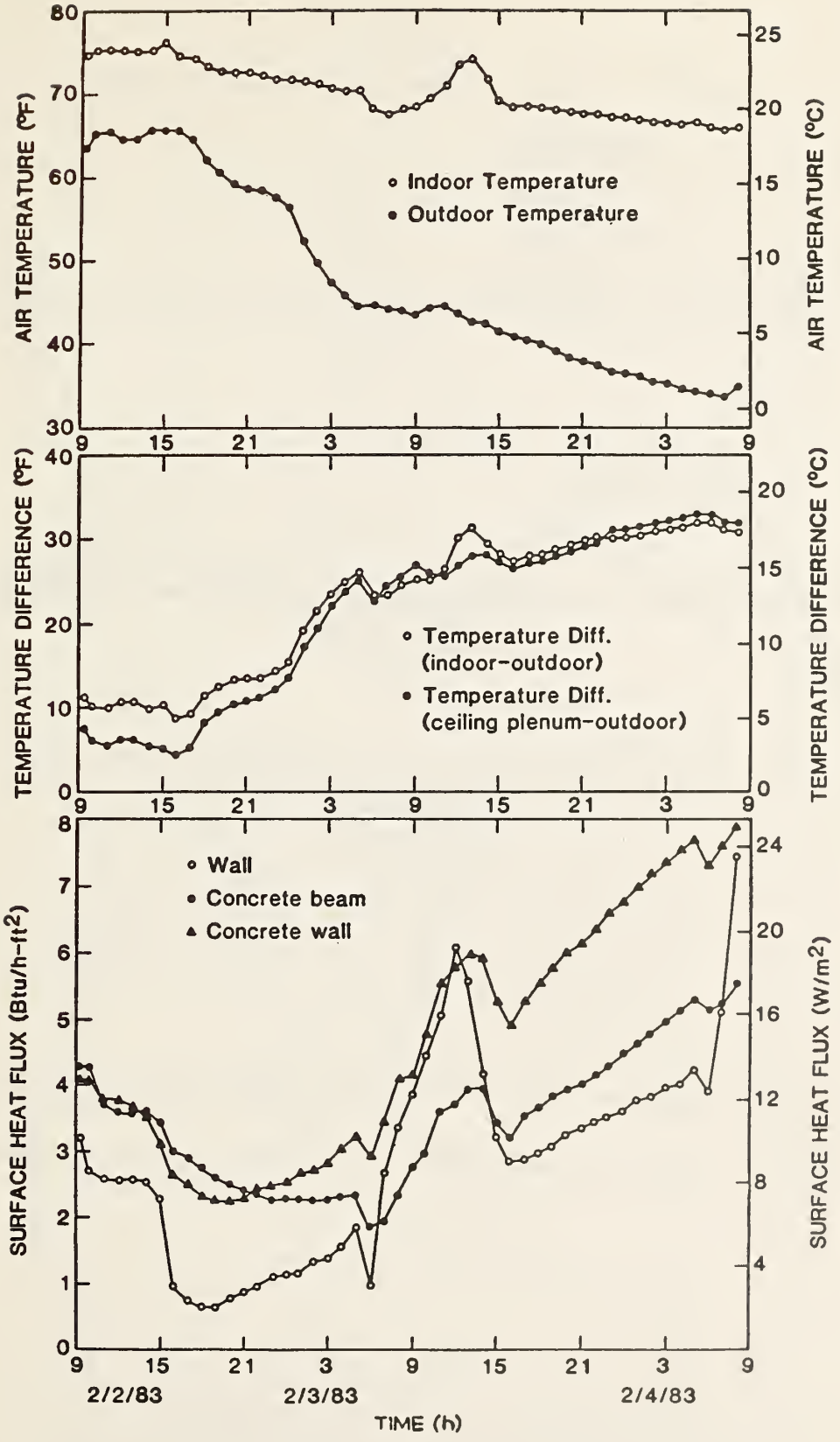

Figure 9.12 Temperature and Heat Flux in the Columbia Building as a Function of Time

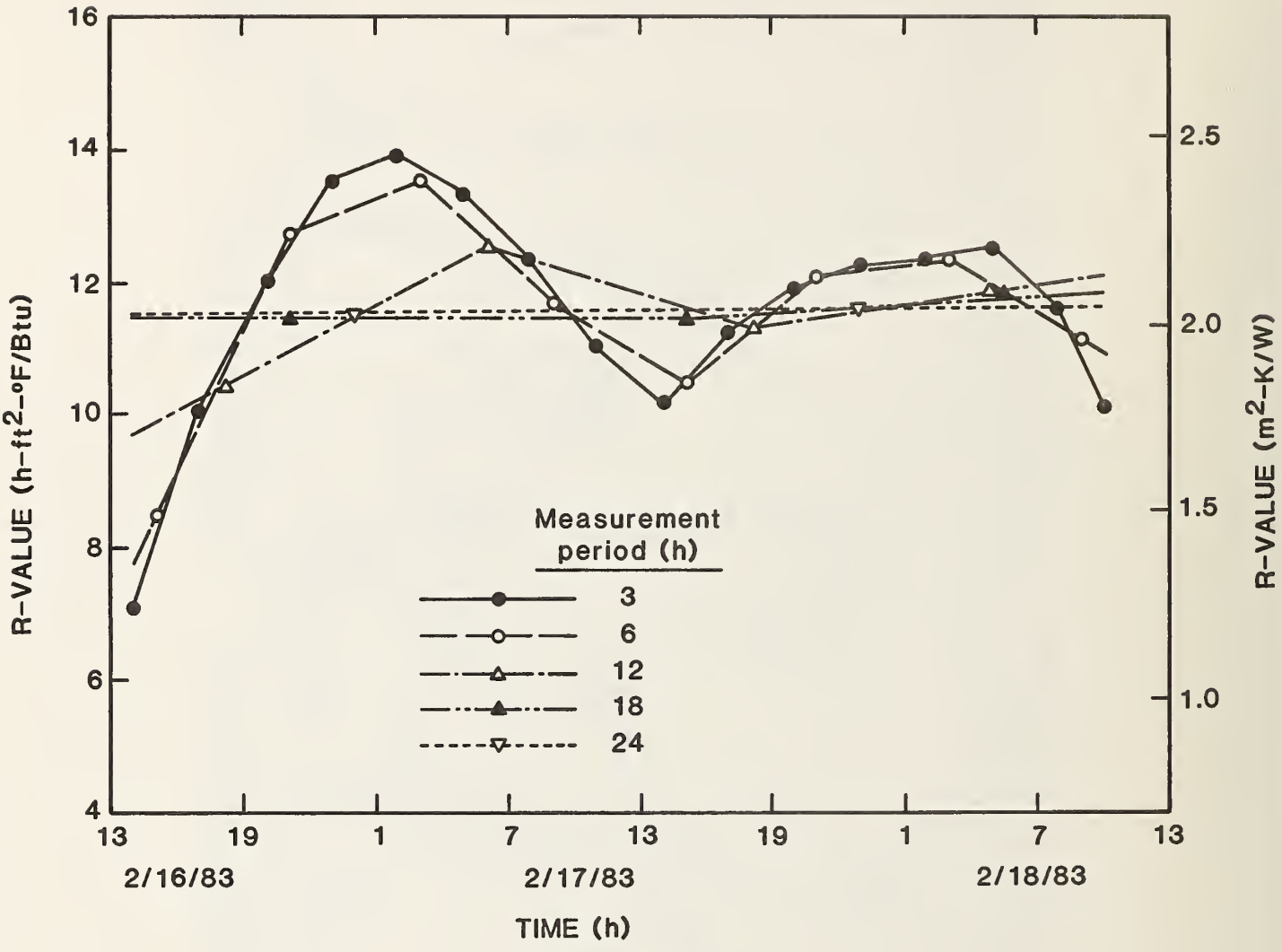

Figure 9.13 Wall Thermal Resistance Values Plotted as a Function of the Length of the Measurement Period for the Ann Arbor Building

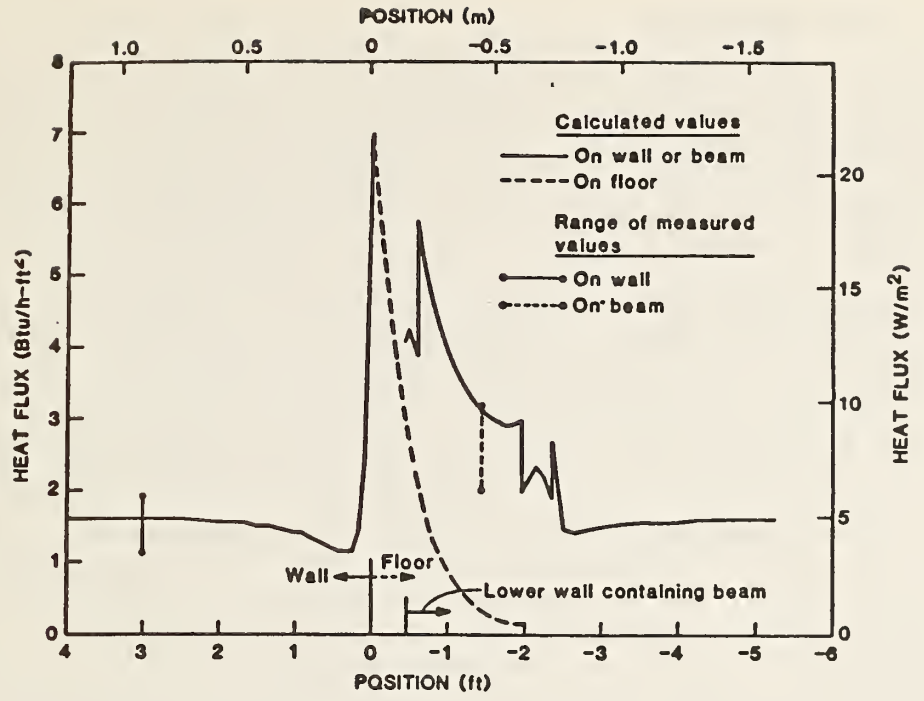

Figure 9.14 Comparison of Calculated Heat Flux on the Inside Surface with Measured Values

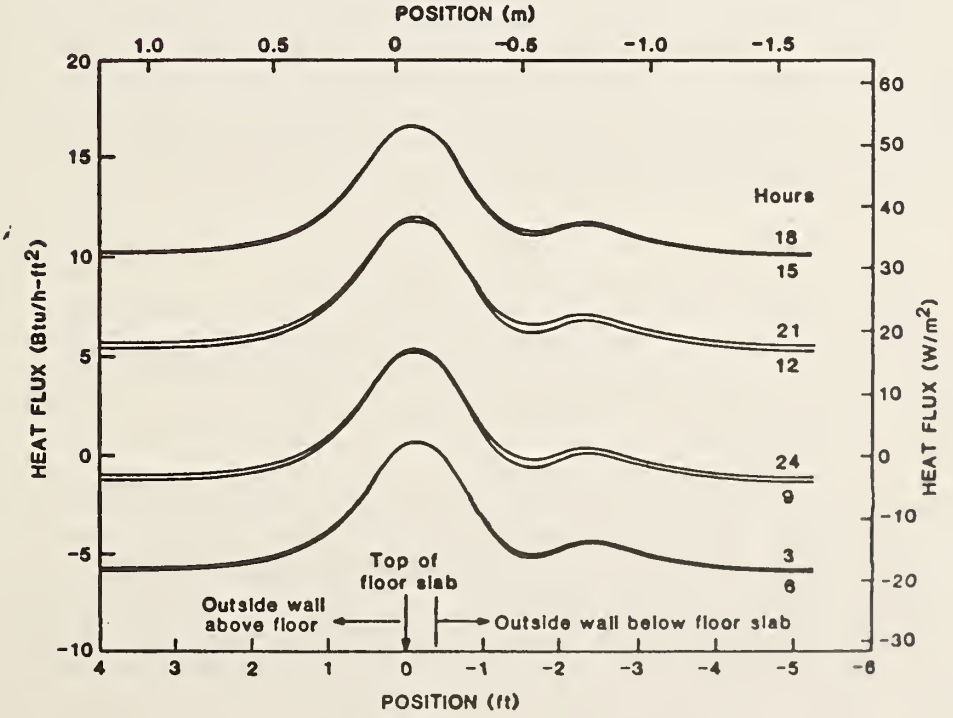

Figure 9.15 Calculated Outside Surface Heat Flux Distribution

10. SUMMARY AND CONCLUSIONS

The application of diagnostic measurements to eight federal office buildings revealed that, though most of these buildings were built to energy conservation guidelines, all contained serious defects which compromised their energy performance. Ground based thermographic surveys showed that from 6 to 18 percent of the insulated wall areas of the building contained thermal defects, including missing insulation, thermal bridges, defective ceiling and floor insulation and convection within insulation. Buildings with overhangs and indentations appear to have severe problems in those areas. Aerial thermographic surveys performed by private contractors on three large federal office buildings were technically capable of detecting thermal deficiencies in the built-up roof system of the buildings if used with a walk-on inspection of the roof. However, the inspection of the roofs revealed a defect in only the Columbia building. The private contractors who performed the aerial thermographic inspections also required walk-on thermographic inspections to identify deficiencies observed by the aerial inspections. This fact calls into question the economy of aerial thermographic inspections unless large roof areas or many buildings are inspected. It was not possible to collect useful thermographic data for the inverted membrane roof of the Anchorage federal building. Audits of office buildings with spot radiometers in order to determine in-situ thermal resistances did not produce consistent results. These audits did produce qualitatively correct results; however, thermographic inspections are probably a more efficient way to obtain the same results. Tracer gas tests of the eight federal buildings determined that the buildings experienced average air infiltration rates of 0.2 to 0.7 air changes per hour and that air infiltration accounted for 23% to 61% of the design heat loads, being over 50% for four of the federal office buildings. Table 10.1 gives an estimate of the components of the building envelope to the building design load, using the measured average air infiltration rates. Table 10.2 and figure 10.1 compare these estimated building design loads to the FY1981 energy used for space heating normalized to the building floor area and the degree day of the site. Figure 10.2 shows a plot of the conductive component of the design load and the FY1981 energy used for space heating.

Given the simple assumptions of this analysis, the correlation between the estimated design losses and the energy consumed for space heating is remarkable. From figure 10.2 it is clear that there is a component missing from the design conductive losses needed to explain the energy used for space heating. The analysis presented in tables 10.1, 10.2 and figure 10.1 seems to indicate that air infiltration almost completely explains this missing energy component.

The whole building tightness tests of the federal office buildings showed that per unit surface area these buildings were no tighter than typical U.S. homes. There seemed to be a relationship between the results of the building tightness tests and the measured air infiltration rates; however, the model developed by Shaw and Tamura to predict air infiltration rates using the results of the building tightness tests underpredicted the air infiltration. The testing of the windows using a fan pressurization technique showed that all the windows were leakier than the ASHRAE standard for windows. However the windows leakage accounted for only about 20% of the total building leakage. The measurement of the thermal resistance of

sections of the exterior envelope using heat flow meters and portable calorimeters showed that the measured thermal resistance deviated from the design thermal resistances by an average of 14%, with the worst case being 45%. An analysis of the heat losses due to the thermal bridges detected by thermography in four of the federal office buildings indicated that the thermal bridging increased the total opaque wall heat losses from 9 to 20 percent. The thermal bridging due to steel framing members increased the heat loss by up to 30 percent.

The measured minimum ventilation rate in two of the tighter federal buildings were only 20 and 50 percent of the ASHRAE Standard 62-1981 recommendation for office buildings with smokers. Three of the federal office buildings had minimum ventilation rates in excess of this recommendation by more than 20%, thus increasing the heating or cooling requirements under extreme weather conditions.

A brief summary of the findings of the diagnostic testing of each federal office building follows:

Anchorage

The Anchorage federal building uses about 28,500 Btu/yr·ft^2 (89.8 kWh/yr-m^2) for space heating. This is a well constructed building which is tight and well insulated - though air infiltration accounts for over 55% of the building load. The major defect is the thermal bridging resulting from the manner in which the precast panels were suspended (increasing the wall heat loss by about 20%). The wall area in the section above the suspended ceiling was not insulated to the same level as the wall area below the suspended ceilings. This was done by design; however, it is not justifiable from a heat transfer point of view. Visual inspection of the roof showed many areas with separations and fissures in the rigid insulation; however limited heat flow measurement did not detect a serious reduction in thermal resistance in the roof insulation system. During the extreme winter conditions, this building is often operated with closed dampers during occupied periods and has ventilation rates which are only 39% of those recommended by the ASHRAE ventilation standard for a building with smokers.

Ann Arbor

This building is a very poor energy performer. It is consuming about 132,000 Btu/yr·ft^2 (416 kWh/yr-m^2) for space heating. It has a high air infiltration rate of about 0.7 air changes per hour, which accounts for about 48% of the building heating load. The building has over 14,000 ft^2 (1,300 m^2) of glass area which contributes to about 26% of the heat load. The opaque walls constitute 18% of the heat load and the roof about 8%. About 18% of the wall area showed thermal defects when inspected by thermography. The thermal resistances of the wall section were close to the predicted values when the insulation was properly installed. The design of the building resulted in thermal bridging which increased the wall heat loss by about 8%.

Columbia

The Columbia federal building uses about 20,035 Btu/yr·ft^2 (63.1 kWh/m^2-yr) of energy for space heating. Air infiltration accounts for about 52% of the space heating load (0.4 air changes per hour). Air conditioning accounts for about 23% of the electrical energy use of the building. The building has operable windows which are quite leaky and which account for about 31% of the building leakage. About 17% of the wall area of the building has thermal defects, the most serious of which was air penetration around the insulation. This was caused by the manner in which the steel framing was installed in the building; an approximately one inch gap was left between the exterior concrete panels and the framing, and the insulation was hung in the framing cavities. The building also had thermal bridging which increased the heat flow through the wall by about 10%. The manner in which the insulation was installed in the wall area about the suspended ceiling was incorrect, allowing air movement through the insulation and leaving exposed exterior wall uninsulated. The minimum ventilation rate of this building was 51% above that required for an office building with smokers, thus adding to the space conditioning loads in extreme weather conditions.

Fayetteville

The Fayetteville federal building uses about 30,000 Btu/ft^2·yr (94.5 kWh/m^2-yr) for space heating. It is basically an uninsulated building built before the federal energy conservation guidelines were developed. In terms of energy use per unit floor area per degree day it is the second worst performer. The space heating load consists of 48% transmission through the opaque walls, 25% through the glass, 23% by air infiltration (0.33 air changes per hour) and 3% through the roof. The major deficiency of the building is the existence of large, uninsulated wall areas including large sections of spandrel glass. The building has serious leakage problems at the interface of the glass and spandrel walls and the structural columns. The first and fourth floors have serious leakage in the overhangs in the return air plenum. The building has adequate minimum ventilation; however, the ventilation rate is strongly wind dependent, indicating that much of the ventilation is being supplied by air leakage and not through the outside air supply ducts.

Huron

The Huron federal building used 21,514 Btu/ft^2·yr (67.8 kWh/m^2-yr) for space heating. This building is the tightest building of the eight tested, having an air infiltration rate of 0.2 air changes per hour. The space heating load consists of 19% transmission through the glass areas, 31% through the opaque wall areas, 17% through the roof and 33% by air infiltration. The framing members of the opaque wall increased the heat flow by about 30% above the design value of the insulation. Thermal bridging at the floor/wall interface caused another 10% increase in heat flow through the opaque wall areas. The minimum ventilation rate of this building was only 26% of the minimum requirements for a building with smokers.

Norfolk

The Norfolk federal building uses about 10,588 Btu/ft^2·yr (33.4 kWh/m^2-yr) of electricity (on-site) for space heating. The building heat loss consists of 27% transmission through the glass areas, 15% through the opaque wall areas, 6% through the roof and 15% by air infiltration (0.52 air changes per hour). The building had serious defects in the insulation in the overhangs over the garage and front entrance. The thermal resistance of the insulated walls was only 54% of the predicted values. The minimum ventilation rate was 90% of that recommended for an office building with smokers.

Pittsfield

The federal building in Pittsfield, MA uses about 51,200 Btu/ft^2·yr (161 kWh/m^2·yr) for space heating. The largest component of the heat load is air infiltration, accounting for 36% of the load (0.3 air changes per hour). The opaque walls contribute about 22% of the heat transmission, the roof 21% and the glass area 19%. The minimum ventilation rate of the building is 90% of the requirement for a building with smokers. Thermography showed that about 18% of the exterior wall area had defects, the most serious being air penetration around the insulation. The measured thermal resistance of the walls was about 13% less than the predicted thermal resistance.

Springfield

The Springfield federal building was a newly constructed office building and therefore there were no previous fuel records for the building. Twenty-three percent of the heat loss of the building is due to transmission through the glass areas, 11% through the opaque wall areas, 5% through the roof and 61% by air infiltration (0.52 air changes per hour). The insulation of the exterior walls consisted of rigid foam insulation applied to the concrete panels in such a way that air could leak around the insulation and into the air cavity between the steel framing. The effective thermal resistance of this wall construction was only 52% of the predicted value. The ventilation and air infiltration rates of the building had a strong temperature dependence which could be due to the leakiness of the building or a ventilation system control problem.

Table 10.1

Estimate of Above Grade Design Heat Losses (UA)

	Anchorage	Ann Arbor	Columbia	Fayette-ville	Huron	Norfolk	Pitts-field	Spring-field
Glass	19%	26%	27%	25%	19%	27%	19%	23%
Wall	15%	18%	16%	48%	31%	15%*	22%	11%
Roof	10%	8%	3%	3%	17%	6%	22%	5%
Air Infil-tration	55%	48%	42%	25%	33%	52%	37%	61%
UA Btu/ hr·F	55,813	30,697	78,201	18,877	10,470	37,985	4,732	39,196
(W/°C)	(29,423)	(16,183)	(41,226)	(9,951)	(5,520)	(20,025)	(2,495)	(20,663)
UA/Area Btu/hr·ft^2·F)	0.123	0.626	0.362	0.516	0.163	0.220	0.270	0.290
(W/°C-m^2)	(0.698)	(3.552)	(2.054)	(2.928)	(0.925)	(1.248)	(1.532)	(1.646)

*Contains underside of overhangs.

Table 10.2

Comparison of Energy Consumed for Space Heating versus Transmission Losses (UA)

	Energy Consumed* per Floor Area per Degree Day		UA per Day per Floor Area	
	Btu/day·ft^2·°F	(W/m^2-°C)	Btu/day·ft^2·°F	(W/m^2-°C)
Anchorage	2.9	0.38	3.0	0.39
Ann Arbor	11.9	1.56	14.9	1.96
Columbia	7.8	1.02	8.7	1.14
Fayetteville	10.1	1.33	12.4	1.63
Huron	2.6	0.34	3.9	0.51
Pittsfield	6.7	0.88	7.0	0.92
Norfolk +	4.2	0.55	5.3	0.70

* Assumes 1 gal oil = 140,000 Btu (148 MJ)
1 cu ft gas = 1,000 Btu (1.05 MJ)

+ Assumes - 3,412 Btu/Kwh and 70% efficiency for other buildings.

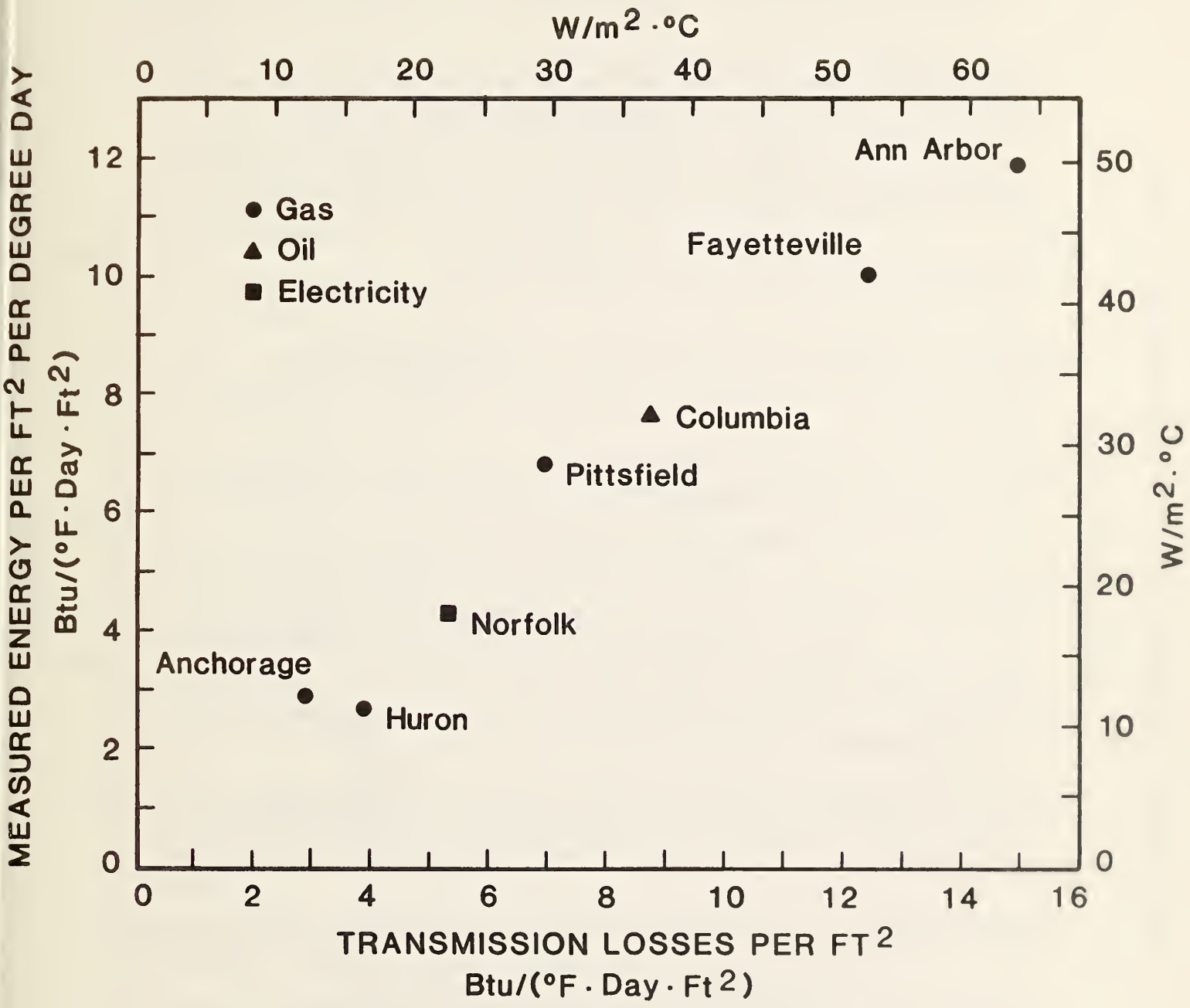

Figure 10.1 Comparison of Transmission Losses and Energy Consumed for Each Building

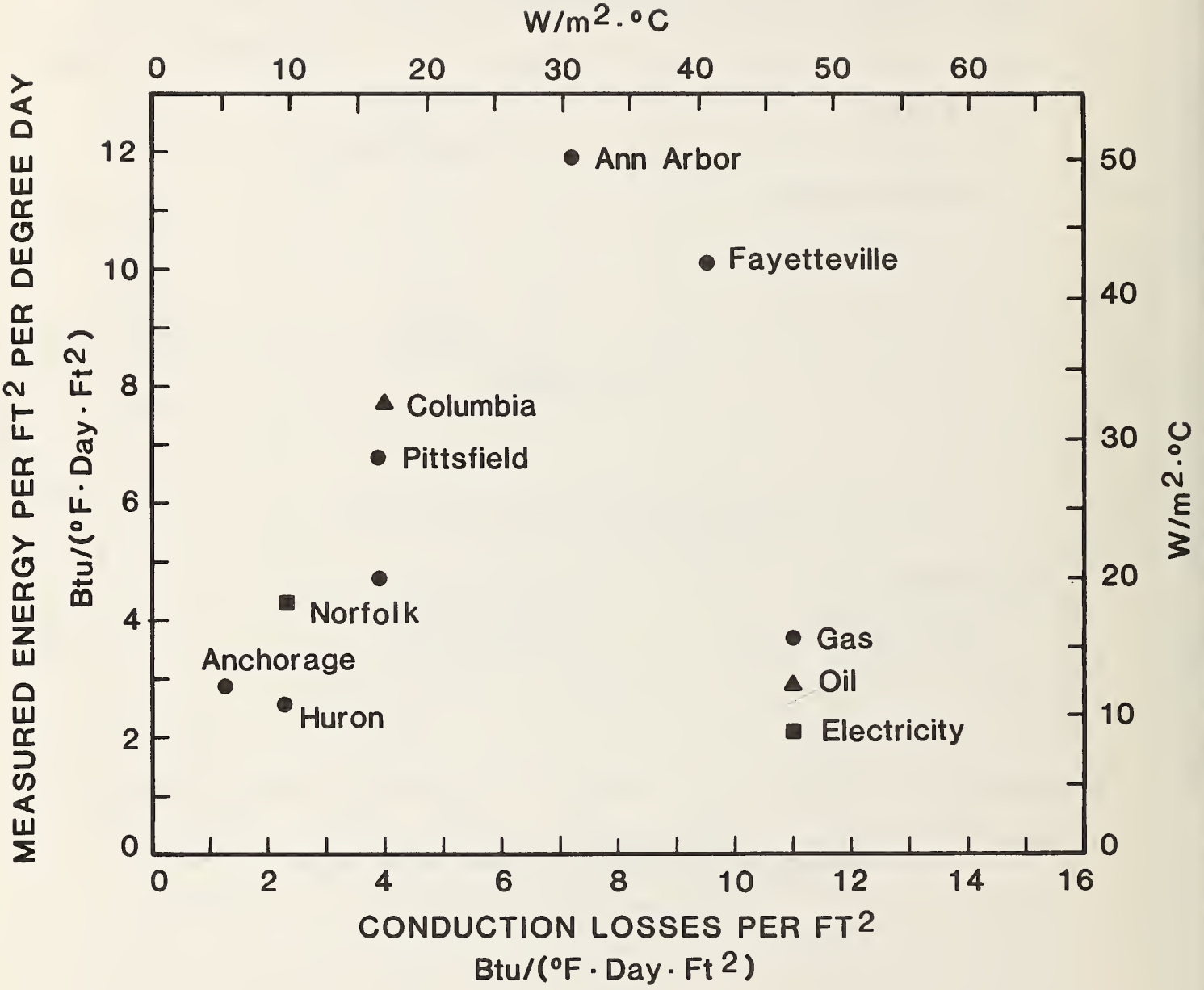

Figure 10.2 Comparison of Conduction Transmission Losses and Energy Consumed for Each Building

REFERENCES

1. Grot, R.A., Burch, D.M., Silberstein, S., Galowin, L., "Measurement Methods for Evaluation of Thermal Integrity of Building Envelopes," NBSIR 82-2506, National Bureau of Standards, Washington, DC, 1982.

2. Ouzts, K.B., Vanier, J.G., and Brotherson, D.E., "A Comparison of Infrared Flyover, Infrared Walkover, and Visual Inspection Techniques for Detecting Roof Moisture Anomalies," an Internal Conference on Thermal Infrared Sensing for Diagnostics and Control (Thermosense VI) Proceedings SPIE 446, pp. 122-129, Bellingham, WA, 1983.

3. Aerial Infrared Thermography of the Federal Building, Springfield, MA, Aeromarine Surveys, Inc., New London, CT, May 7, 1983.

4. Wallace, J.R., Thermographic Inspection Report, Wallace Thermographics Co., Richmond, VA, June, 1983.

5. Town, R.H., "Infrared Survey for Federal Building," C Street, Anchorage, AK. Infrared Technology of Alaska, Inc., Anchorage, AK, No. AP6546, April, 1983.

6. Spot Radiometer Energy Audit, Federal Building in Huron, SD, Donahue and Associates, Inc., Madison, WI, 1983.

7. Spot Radiometer Energy Audit, Federal Building in Ann Arbor, MI, Donahue and Associates, Inc., Madison, WI, 1983.

8. ASHRAE Handbook of Fundamentals, The American Society of Heating, Refrigerating and Air Conditioning Engineers, Inc., 1981.

9. Treado, S.J., and Burch, D.M., "Evaluation of Hand-Held Infrared Thermometers for Wall Thermal Resistance Determination," NBSIR 79-1736, July, 1979.

10. Burch, D.M., and Krintz, D.F., "Using High-Resolution Hand-Held Radiometers to Measure In-Situ Thermal Resistance," in International Conference of Thermal Infrared Sensing for Diagnostics and Control (Thermosense VI) Proceedings SPIE 446, pp. 24-32, Bellingham, WA, 1983.

11. "Application of Infrared Sensing Devices to the Assessment of Building Heat Loss Characteristics," ANSI/ASHRAE Standard 101-1981.

12. ASHRAE Standard 62-81, Ventilation for Acceptable Indoor Air Quality, American Society of Heating, Refrigerating, and Air-Conditioning Engineers, Inc., 1981.

13. ASTM E 779-81, "Standard Practice for Measuring Air Leakage by the Fan-Pressurization Method," American Society for Testing and Materials, 1981.

14. Kronvall, J., "Testing of Homes for Air Leakage Using a Pressure Method," ASHRAE Transactions, Vol. 84(I), 1978.

15. Shaw, C.Y., Sander, D.M., Tamura, G.T., "Air Leakage Measurements of the Exterior Walls of Tall Buildings," ASHRAE Transactions, Vol. 79(II), 1973.

16. Shaw, C.Y., "Air Tightness: Supermarkets and Shopping Malls," ASHRAE Journal," March 1981.

17. ASTM E 283-73, "Standard Test Method for Rate of Air Leakage Through Exterior Windows, Curtains, Walls and Doors," the American Society for Testing and Materials, 1973.

18. Svensson, A., "Methods for Measurement of Airflow Rates in Ventilation Systems," Bulletin M83:11, The National Swedish Institute for Building Research, 1983.

19. Persily, A.K., Grot, R.A., "Air Infiltration and Building Tightness Measurements in Passive Solar Residences," Journal of Solar Energy Engineering, Vol. 106, No. 2, 1984.

20. Tamura, G.T., Shaw, C.Y., "Studies of Exterior Wall Air Tightness and Air Infiltration of Tall Buildings," ASHRAE Transactions, Vol. 82(I), 1976.

21. Weidt, J.L., Weidt, J., Selkowitz, S., "Field Air Leakage of Newly Installed Residential Windows," DoE/ASHRAE Conference on the Thermal Performance of Exterior Envelopes of Buildings, Orlando, Florida, December 1979.

22. Ward, I.C., Sharples, S., "An Investigation of the Infiltration Characteristics of Windows and Doors in a Tall Building Using Pressurization Techniques," Report BS 68, Department of Building Science, University of Sheffield, 1982.

23. Tamura, G.T., "Measurement of Air Leakage Characteristics of House Enclosures," ASHRAE Transactions, Vol. 81(I), 1975.

24. Shaw, C.Y., Tamura, G.T., "The Calculation of Air Infiltration Rates Caused by Wind and Stack Action for Tall Buildings," ASHRAE Transactions, Vol. 83(II), 1977.

25. Hunt, C.M., Treado, S.J., "Air Exchange Measurements in a High-Rise Office Building," DoE/ASHRAE Conference on the Thermal Performance of Exterior Envelopes of Buildings, Orlando, FL, December, 1979.

26. ASTM C 177-76, "Standard Test Method for Steady-State Thermal Transmission Properties by Means of the Guarded Hot Plate," the American Society for Testing and Materials, 1976.

27. Powell, F.J., Rennex, B.J., "NBS Line-Heat-Source Guarded Hot Plate for Thick Materials," Proceedings of the ASHRAE/DoE Conference on Thermal Performance of the Exterior Envelopes of Buildings II, Las Vegas, NV, ASHRAE SP 38, December, 1982.

28. Brown, W.C. and Schuyler, G.D., "In-Situ Measurements of Frame Wall Thermal Resistance," ASHRAE Transactions, Vo. 88(I), 1982.

29. Brown, W.C. and Schuyler, G.D., "A Calorimeter for Measuring Heat Flow Through Walls," Proceedings of the ASHRAE/DoE Conference on Thermal Performance of the Exterior Envelopes of Buildings, Kissimmee, FL, ASHRAE SP 28, December, 1979.

30. Granum, H., "The Role of the Building Envelope," in `Building Research World Wide,´ edited by the Norwegian Research Institute, 1980.

31. Elrod, D.C., Giles, G.E. and Turner, W.D., "HEATING6: A Multidimensional Heat Conduction Analysis with the Finite-Difference Formulation," Union Carbide Corporation, Nuclear Division, ORNL/NUREG/CSD-2/V2, Oak Ridge, TN, October, 1981.

Appendix A

Economic Methodology for Selecting Optimal Energy Diagnostic Techniques for Federal Office Buildings

Because application of the various energy diagnostic techniques discussed in the previous chapters of this report causes the user to incur costs, a method is needed to decide whether such expenditures are economically justified. The purpose of this chapter is to describe and illustrate an economic methodology that addresses two types of decisions: (1) determining whether a particular diagnostic technique is cost effective for a given federal office building; and (2) selecting the most cost-effective technique from among a set of techniques, any one of which could be applied to a particular building or building component. The first type of decision arises when there is only one diagnostic technique worth considering for a particular application. This situation may prevail because economic or technical considerations limit the availability of alternative techniques. The second type of decision arises when more than one technique can be considered for an application, and they differ either in their associated costs or benefits.

A.1. Data Requirements

Implementation of the economic methodology presented in this section depends on the availability of two types of data: (1) cost data and (2) benefits data.

A.1.2 Cost Data

The cost data required for the methodology include all expenditures associated with carrying out each diagnostic technique being studied. The major cost items that need to be taken into account are specified in the Cost Data Collection Form for Diagnostic Tests presented in exhibit A.1. The significant distinction to be observed on this form is the one that exists between fixed and variable costs. Item 2 covers fixed costs, which are defined as those costs that are invariant with respect to the size of the building component being diagnosed. The primary examples of fixed costs are those arising from the transport of equipment, materials, and personnel to and from the building site. In addition, equipment costs (item 4) frequently tend to be fixed costs whenever the size and number of pieces of equipment do not have to be tailored to the size of the component being diagnosed.

Variable costs of the diagnostic technique are listed under item 3. These costs, such as for labor and materials, tend to vary in proportion to the size of the building component being diagnosed.

The background data covered in item 1 on the form include the component size, which quantifies how many physical units the particular diagnostic test is to cover for the building in question. The physical unit of measure chosen to represent size in this sense should be the unit that most directly affects the costs of the diagnostic test. This

Exhibit A.1

COST DATA COLLECTION FORM FOR DIAGNOSTIC TESTS

1. GENERAL BACKGROUND DATA

1.1 Date of Test: _____

1.2 Building Name and City: _____

1.3 Diagnostic Technique: _____

1.4 Component Diagnosed: _____

[Give name or description of component whose energy-related performance is being diagnosed.]

1.5 Component Size: _____

[Express size of component in whatever physical units (i.e., f, f^2, or f^3 most directly affect the costs of the diagnostic test.]

2. FIXED COSTS OF DIAGNOSTIC TEST

[Fixed costs are invariant with respect to size of component diagnosed.]

2.1 Transport of Equipment and Materials to and From Site

a. Packing, Shipping, Insurance: _____

b. Time in Transit: _____

2.2 Personnel Transport to and From Site

a. Air, Train Fare: _____

b. Local mileage or vehicle rental fee: _____

c. Time in transit: _____

2.3 Special Factors Affecting Fixed Costs

a. Crew size: _____

b. Number and weight of pieces of equipment: _____

c. Other?: _____

3. VARIABLE COSTS OF DIAGNOSTIC TEST

[Variable costs tend to vary <u>in proportion</u> to the size of component diagnosed.]

3.1 Labor at Site

[Itemize crew members by skill category and give hours worked and hourly wage for each category.]

a. Skill type:	_____	_____	_____
b. Hours:	_____	_____	_____
c. Wage ($/hr):	_____	_____	_____
d. Total cost:	_____	_____	_____

3.2 Materials

[Itemize each material or energy type used and give the quantity and unit cost of each; also indicate whether the item is reusable by entering the number of times the item is customarily used (i.e., if not reusable, enter 1).]

a. Material:	_____	_____	_____
b. Quantity:	_____	_____	_____
c. Unit cost:	_____	_____	_____
d. Total cost:	_____	_____	_____
e. Times Usable:	_____	_____	_____

3.3 Special Factors Affecting Variable Costs

a. Type of heating/cooling equipment: _____

_____

[Give features of equipment which affect variable costs, such as the size, number of units, location of units, and distance apart.]

b. Other: _____

_____

4. EQUIPMENT

[Describe each piece of diagnostic equipment used (4.1). Give current cost of purchasing equivalent equipment (4.2), the number of years of expected useful service life (4.3), the average number of site visits in a typical year (4.4), and the maintenance and repair costs per year (4.5). As an alternative to (4.2) through (4.5), given the equivalent rental rate per visit (4.5).]

		Equipment #1	Equipment #2	Equipment #3
4.1	Description	_____	_____	_____
		_____	_____	_____
4.2	Current Cost ($)	_____	_____	_____
4.3	Life (Yrs)	_____	_____	_____
4.4	Visits (#/Yr)	_____	_____	_____
4.5	M&R Cost ($/Yr)	_____	_____	_____
[4.6	Rent ($/Visit)]	_____	_____	_____

component size variable is the physical dimension to which the variable cost items are expected to be approximately proportional. Under this assumption of variable cost proportionality, total diagnostic costs can be modelled as a linear function of the component size variable. The algebraic expression for this function is:

$$C = F + V * S, \qquad (A.1)$$

where C = a variable representing total costs of the diagnostic test for the component ($);

F = a parameter representing fixed diagnostic test costs, i.e. costs which are invariant with respect to component size ($);

V = a parameter representing variable diagnostic test costs, i.e. costs which vary in proportion to component size ($/unit); and

S = a variable representing component size, measured in physical units (units).

Given a statistically valid sample of data on the variables, C and S, for each diagnostic technique, it is possible to derive reasonably precise, unbiased estimates of the parameters, F and V, using standard least squares regression methods. Alternatively, if only a small sample of cost data is available with information on each cost item as specified in exhibit A.1, then approximate values for the parameters F and V can each be directly derived from the separate data on Fixed and Variable Costs, respectively. This alternative procedure for deriving F values involves first summing all the costs under item 2 (Fixed Costs) and adding to that sum all those cost entries listed under item 4 (Equipment) which are not expected to vary as a function of S (1). This first step must be carried out for each building sampled for the diagnostic technique in question. These Fixed Cost values must then be averaged across all the buildings in the sample to obtain the F value. Similarly, an approximate value for the parameter V can be found by first totaling the Variable Costs under item 3 of exhibit 1 and adding to this total all those cost entries from item 4 (i.e., Equipment) which are expected to vary in proportion to S. This Variable Cost value is to be computed for each building and then averaged across all buildings sampled to arrive at the approximate value of V.

Whichever method is used to estimate the values of the parameters, F and V, it must be assumed that both parameters will be fairly constant for a given diagnostic technique. This is, a single value can be assigned to F and a single value can be assigned to V for a given technique. Moreover, because economic resources must be used to carry out the diagnostic tests,

---

(1) Because most capital equipment is "lumpy" (i.e., it comes in limited, discrete sizes) rather than continuously variable, the cost entries under item 4 will usually be included in the cost function as part of fixed costs, F. If the range of interest in the analysis extends beyond the capacity of one discrete size of equipment, then the cost function becomes a step function and discontinuous at endpoints of the equipment capacity ranges.

the value of C in expression (A.1) is positive. This means that either F or V must be positive (since Component Size, S, is positive. Indeed, it is reasonable to expect that the true values of both F and V for most diagnostic techniques are positive. Based on this information regarding the probable ranges of values for F and V, the linear relationship between C and S given in expression (A.1) can be illustrated graphically as shown in exhibit A.2.

A.1.3 Benefits Data

The benefits data needed to implement the methodology are basically derived from an economic comparison of two situations: (1) retrofitting the building for energy conservation according to the recommendations that result from the application of the diagnostic technique; and (2) retrofitting the building without the benefit of the specific information or recommendations derived from the diagnostic technique. This economic comparison is conducted in terms of the discounted present values of the net dollar savings (i.e., energy cost reductions minus the cost of retrofitting) from the two sets of energy conservation retrofits. In other words, the benefits of a diagnostic technique are based on the discounted present value of the net dollar savings over the remaining life of the building that are directly attributable to applying the technique.

The first step involved in estimating the present value of the net savings attributable to each diagnostic technique is to identify the two sets of all mutually compatible energy conservation retrofit options that would be considered for economic evaluation both in the absence and in the presence of the technique. Which retrofit options are identified in this process would be influenced generally by the type of building, the fuel used for heating and cooling, and the climatic conditions of the geographic location. For each of the candidate retrofit options identified, economic data must be collected as specified in exhibit A.3. Once the necessary economic data have been gathered, a life-cycle cost (LCC) evaluation of each retrofit option must be conducted along the lines described in Life-Cycle Costing Manual for the Federal Energy Management Program (2). The result of the LCC evaluation should then be compared with a benchmark LCC evaluation of installing no retrofits at all. If the LCC of the retrofit option is greater than that of the benchmark, the retrofit should not be installed. If the LCC of the retrofit is less than that of the benchmark, then the difference between the two LCC values represents the net savings attributable to that retrofit option. The sum of these positive net savings estimates across all retrofit options that would be installed (i.e., those options considered that were found to have LCC values less than that of the benchmark) in the presence of the diagnostic technique must be compared with the sum of the corresponding positive net savings across all the retrofit options that would be installed in the absence of the diagnostic technique. The difference between these two sums represents an estimate of the net savings directly attributable to the application of the diagnostic technique. This net savings estimate will be referred to as the Benefits (B) of the technique.

---

(2) Rosalie T. Ruegg, Life-Cycle Costing Manual for the Federal Energy Management Programs, National Bureau of Standards Handbook 135 (Revised May, 1982), Washington, DC: U.S. Department of Commerce,1982.

Exhibit A.2

Cost (C) of Applying a Diagnostic Technique as a Linear Function of Building Component Size (S)

Exhibit A.3

ECONOMIC DATA SHEET FOR GSA RETROFIT OPTIONS

1. Building Name _____ 2. City _____

3. Component _____ 4. Date _____

	Option #1	Option #2
5. Specifications	_____	_____
	_____	_____
	_____	_____
	_____	_____
	_____	_____
6. Scaffolding Needs (Check One)		
a. None (Inside access)	_____	_____
b. Swing (Suspended)	_____	_____
c. Stage (Built-Up)	_____	_____
7. Max. Working Dist. (f) (Omit if 6.a is checked)	_____	_____
8. Job Dimensions		
Length (f)	_____	_____
Area (f^2)	_____	_____
Sizes (f x f)	_____	_____
Number	_____	_____
9. Expected Cost ($)	_____	_____
10. Expected Life (yrs.)	_____	_____
11. Expected Reduction in Annual Purchased Energy		
Oil (Gal./yr.)	_____	_____
Gas (Therms/yr.)	_____	_____
Electric (kWh/yr.)	_____	_____
12. Additional Comments	_____	_____
	_____	_____
	_____	_____
	_____	_____
	_____	_____

Exhibit A.3 (continued)

General Instructions:
Use a separate data sheet for each building component to be retrofitted. If there are more than two retrofit options to be considered for a particular building component, use additional data sheets.

Items 1 and 2: Fill in the name of the building and the city in which it is located.

Item 3: Indicate which building component is to be retrofitted, e.g., roof, exterior walls, doors, windows. Be sure to use a separate sheet for each component.

Item 4: Today's date.

Item 5: Give a detailed description of the retrofit work to be done under each option. Specify the type, thickness, and quality of all materials to be used, give the tolerances and performance specifications to be met, and also indicate any special circumstances of the job that might affect materials or labor costs (e.g., whether the retrofit work area will be occupied by office workers). Attach separate, if necessary.

Item 6: Indicate whether and what type of scaffolding will be required. If all the work can be done from the inside, check 6.a. If swing scaffolding that is suspended from the top of the building wall can be used, check 6.b. If stage scaffolding that is built-up from the ground is needed, check 6.c.

Item 7: Indicate the maximum required working distance (f) from the top of the building to the work area for swing scaffolding (6.b), or from the ground to the work area for stage scaffolding (6.c.).

Item 8: Indicate in detail the complete dimensions of the retrofit job. For caulking and weatherstripping, give the crack length, in feet (f); for walls and roofs, give the area in square feet (f^2); and for windows and doors, give both the height and width of each different size, in feet (f), as well as the number of windows and doors of each size. Attach separate sheet if necessary.

Item 9: Give a rough estimate of the total cost of the retrofit option for that component, if the work were done today under a union contract.

Item 10: Give the expected life of the retrofit, of the building component, or of the entire building, whichever is shortest.

Item 11: Estimate the reduction in annual purchased energy expected to result from this retrofit option being applied to this building component. Be sure to state estimated savings in terms of units of purchased energy, rather than in terms of changes in heating or cooling loads. These purchased energy savings should be given in gallons of fuel oil, therms of natural gas, kilowatt-hours of electricity, or some combination of these three. If demand charges are expected to be affected, indicate the reduction in kilowatts expected for each billing period (month) affected.

Item 12: Provide any additional information that might affect the costs or benefits of the retrofit option. If any local building contractor has been identified as capable of accomplishing the retrofit, please given name and phone number. Also information on which local utility companies serve the building would be helpful, as would the name and phone number of the building engineer or superintendent.

Once sufficient Benefits data have been collected for a particular technique over a range of building component sizes, an explicit relationship can be derived between Benefits and component size. It is expected that this relationship could be represented reasonably well by the following algebraic expression:

$$B = P * S, \qquad (A.2)$$

where B = a variable representing the estimated Benefits of the diagnostic technique for the building component ($);

P = a parameter representing the combined effects on B resulting from local climatic factors, the cost of energy, the discount rate, and the conversion efficiencies of the mechanical equipment ($/unit); and

S = a variable representing building component size, measured in physical units (units).

The value of P for a given building will depend on the local climatic factors affecting the building energy use, the current and projected future cost per unit of purchased energy, and the heating and cooling conversion efficiencies of the mechanical equipment used in the building. For a specific building in a particular location, these factors are held fixed, so that the value of P would not change because of them. Another important factor affecting the value of P is the discount rate used to compute the LCC values of the retrofit options on which the estimate of B is based. The discount rate can be considered as a constant even in the analysis of several different Federal buildings since a common rate of seven percent is prescribed for evaluating energy conservation investments under the Federal Energy Management Programs. Consequently, P can be considered as a positive constant for any particular building and diagnostic technique. This means that the general relationship given in expression (A.2) can be illustrated graphically as shown in exhibit A.4.

A.2. Evaluation of a Single Diagnostic Technique

The first type of decision addressed by this methodology concerns the case in which there is only one diagnostic technique available that can be reasonably applied to the particular building component being analyzed. This situation would arise when there simply is only one technique or when one technique clearly dominates all the others with respect to ease of application, effectiveness, and cost. The basic objective of the methodology in such a case would be to determine whether the single technique is expected to yield sufficient economic benefits to cover the costs of applying the diagnostic technique. As has been shown, both the benefits and costs of the technique can be expressed as functions of a common variable, the size of the building component being analyzed. The methodology takes advantage of this fact by determining the breakeven value of this common variable. That is, the methodology finds that critical value of the building component size below which the diagnostic technique is not cost effective, and above which it is cost effective. As an illustration, this type of analysis is graphically depicted in exhibit A.5 for air infiltration measurements using the diagnostic technique of tracer gas decay.

As can be seen in exhibit A.5, both the benefits and costs of using the tracer gas dilution method to measure air infiltration are functions of the volume of the enclosed space in the building. Because of the presence of positive fixed costs and the proportional nature of the benefits function, the building component sizes (i.e., in this case, the volume of the building) to the left of (or less than) the Breakeven (BE) volume at which the two curves intersect, the costs of this diagnostic technique exceed its expected benefits. For this range of smaller building volumes, therefore, the technique was found not to be cost effective. In contrast, for building volumes greater than BE, the benefits exceed the costs, making the technique cost effective in this larger building volume range. This BE value will always occur in the positive range of building component sizes, as long as two conditions are fulfilled: (1) the slope of the benefits function must exceed that of the cost function (i.e., $P > V$), and (2) there mut be positive fixed costs (i.e., $F > 0$). If the first of these conditions is not met, then there is no positive BE value, and the diagnostic technique being evaluated can be said not to be cost effective over the entire range of building component sizes. In other words, without a positive BE value, the technique would not be cost effective for any building size. If the first condition is met while the second condition is not, then the BE value would occur at the origin, which would mean that the diagnostic technique is cost effective for all building component sizes.

A.3. Evaluation of Alternative Diagnostic Techniques

The second type of decision addressed by this methodology concerns the case in which there is more than one diagnostic technique available to be applied to the analysis of a particular building component. The objective of the methodology in this case is to find the technique which would yield the greatest benefits net of costs for the size of building component being analyzed. To accomplish this, expression (1) should be subtracted from expression (2) for each of the diagnostic techniques to be compared in order to form a combined expression for the Net Benefits (NB):

$$NB = B - C = P * S - F - V * S = -F + (P - V) * S, \qquad (A.3)$$

where all of the variable and parameters are as previously defined. This expression is to be evaluated for the building component size being studied and then the technique with the highest value of NB is the one that should be chosen. Because F is a positive constant, the intercept of NB will be negative, which means that for the lowest range of building component size there will be no diagnostic technique that is cost effective. Because the values of F and of the slopes of expression (A.3) are likely to be different for each diagnostic technique, there will be breakpoints separating the ranges of component size for which a particular technique has the highest NB. This is graphically illustrated with hypothetical data for the case of two diagnostic techniques in exhibit A.6. As can be seen from the graph, neither of the techniques is cost effective for the lowest range (i.e., below 19 thousand sf) of building envelope size. In the middle range of building envelope size (i.e., between 19 and 50 thousand sf), the spot radiometry method yields the highest value of NB, and in the highest range (i.e., above the breakpoint at 50 thousand sf), the heat flow meter method becomes more cost effective. The economic evaluation of more than two alternative diagnostic techniques is conducted in a similar manner.

Exhibit A.4

Benefits (B) of Applying a Diagnostic Technique as a Proportional Function of Building Component Size (S)

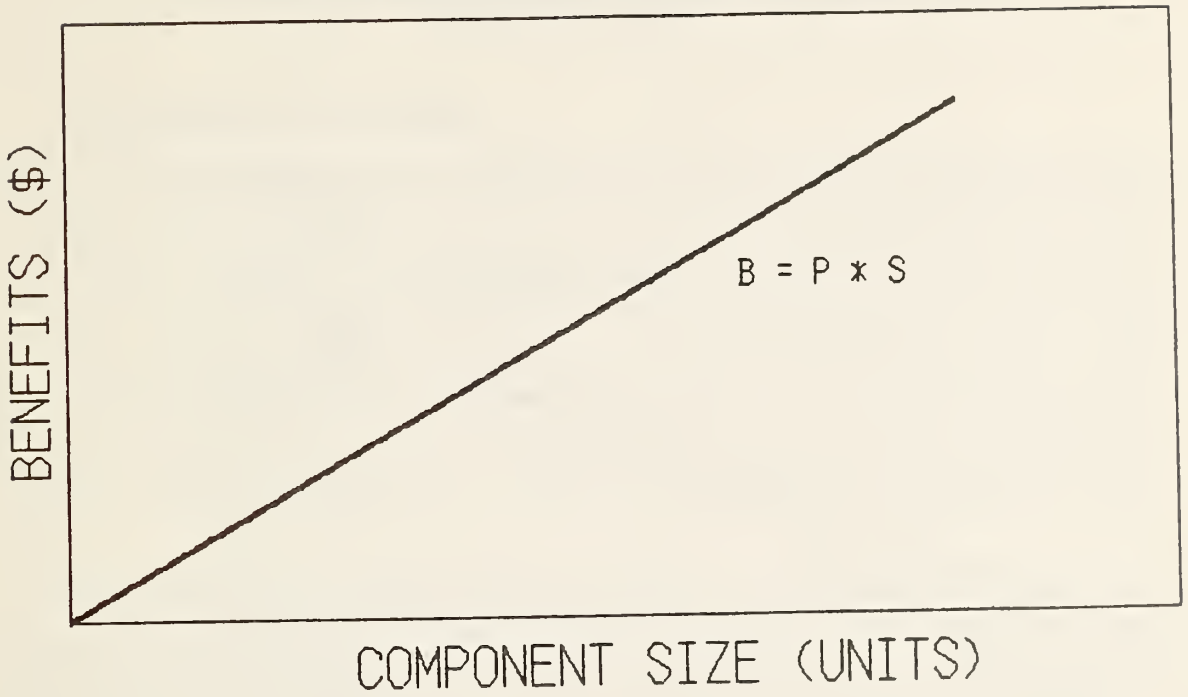

Exhibit A.5

Economic Analysis of a Single Diagnostic Technique: Air Infiltration Measured by Tracer Gas

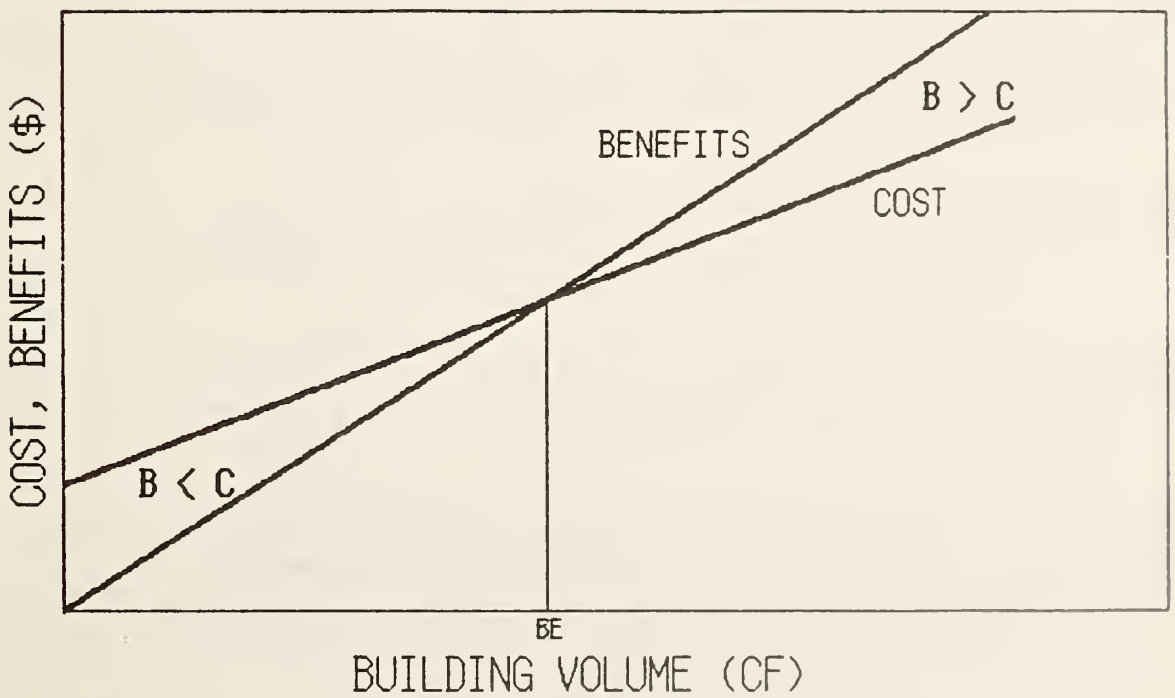

Exhibit A.6

Economic Analysis of Two Alternative Diagnostic Techniques:
Conduction Measured by Heat Flow Meters or Spot Radiometry

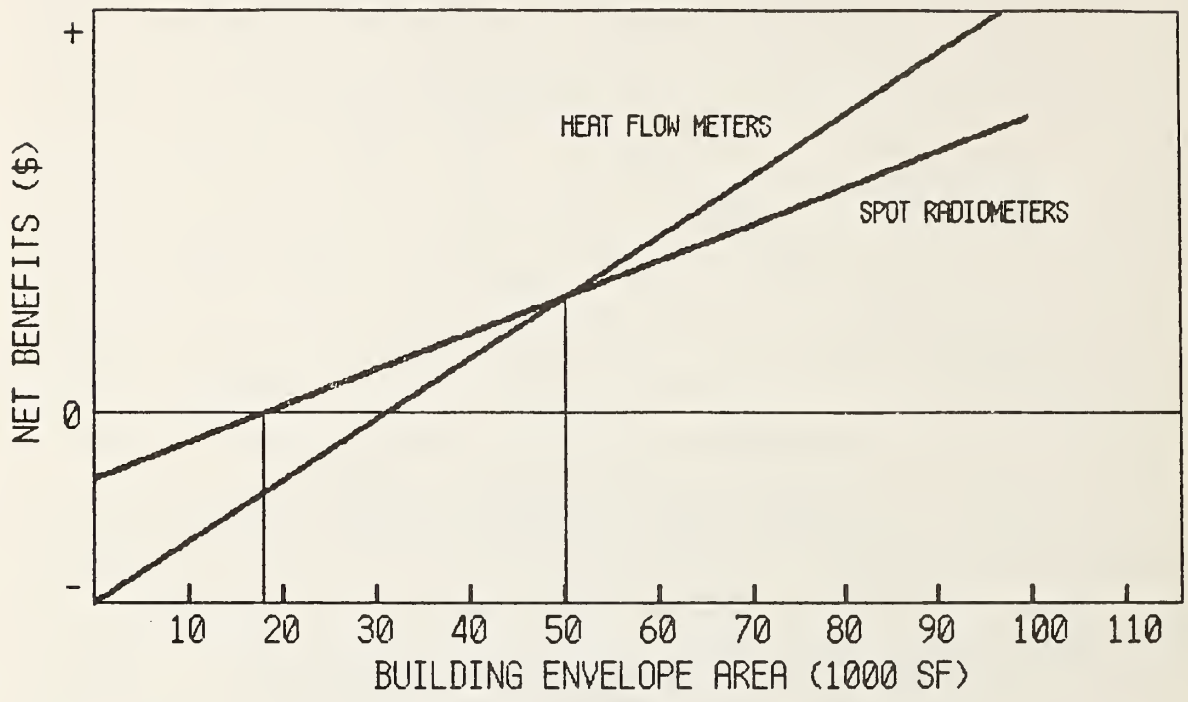

Appendix B

Specifications for Aerial Infrared Thermography
Roof Inspections

1. Guidelines and Requirements

Scope - Aerial Thermographic surveys will be performed by fixed wing or helicopter with suitable equipment for airborne measurement procedures. The contractor(s) will be required to visit and inspect the building(s) selected for the aerial thermographic survey. The aerial thermographic survey will be conducted in a manner consistent with the requirements indicated, part 3. The aerial surveys will be performed in such a manner as to result in production of photographic, TV film and/or other documentation of the infrared data from such inspections with sufficient detail to permit the identification and location of defects and thermal anomalies for each building. A conventional aerial photograph(s) should bee taken during daylight hours of the same scene displayed in the thermal image.

The contractor(s) will prepare and transmit a reproducible report which will contain a comprehensive detailed description of the inspection survey, methods and procedures for data collection, the photographic and other data or information derived, analysis and interpretation of the survey, and recommendations for remedial actions.

The contractor(s) will conduct the survey within a reasonable time period when the building(s) are heated and the roof is clear of water, dew, snow or ice. The survey, when conducted under clear sky conditions, may have ambient air temperature differences of 30°F (17°C) below the building interior air temperature; for other than clear sky conditions the temperature difference should be at least 40°F (22°C). For all cases, the outside ambient air temperature should not exceed 45°F (7°C). The survey should be at least four hours after sunset, sky conditions homogeneous, and wind speed less than 15 mph (7 m/s).

The spatial resolution of the scanner shall be one foot square (object plane resolution at the flight path nadir). The actual usable field of view shall not exceed $\pm$ 45° with respect to the flight path nadir.

A method of displaying the scanner video signal or thermal map to the operator to facilitate proper settings of controls. Data may be recorded directly on hard copy film or other medium in analog or digital form suitable for processing by the contractor(s) into hard copy thermograms.

Two internal black body reference sources are desired for the line scanner to display radiance temperature range in the thermal image. Instrument sensitivity requirements for anticipated minimum resolvable temperature difference (MRTD) shall be indicated in the proposal for exterior (air) temperatures and wind speeds in the vicinity of the building(s).

Operation and Data Record - Scanners should be operated within aircraft speed and altitude envelopes to provide the required resolution, continguous line scanning (or overscanning) or building roof surfaces. Undesirable motions should not seriously degrade the thermal image.

The following data should be recorded:

1. Date of survey
2. Time of survey
3. Outdoor ground-level temperature
4. Wind speed at ground level
5. Sky conditions (i.e., clear, solid overcast, etc.)
6. Flight line location and orientation
7. Approximate ground speed and altitude of aircraft
8. Site conditions (i.e., foliage, roofs having low emittance,etc.)

Staff Qualifications - Aerial infrared thermography should be undertaken by trained personnel. The training requirements are similar to those of level II in the Canadian training program*. The interpretation of aerial thermograms must take into account overflight conditions, environmental conditions at the time of data collection, and knowledge of the particular structure and surface conditions (dry, wet, etc.).

Experience and/or Capabilities - The organization and staff that will participate in the project shall be described in sufficient detail to enable evaluation of capabilities to perform the proposed effort. For the purpose of the evaluation of the proposals on a competitive basis the information provided to accomplish the inspection, survey, report, staffing, organization qualifications, and costs will be weighed as factors in determining the contract award(s).

2. Exceptions

Exceptions to any lists, guidelines or requirements may be permitted provided that explanation describing consistency with good commercial practices or experiences are provided as a basis for technical evaluation by NBS.

---

*Public Works Canada Training, Level I (thermographic), Level II (Thermographic), Level III (Building Science).

3. Use of Other Equipment

Where the normal commercial roof survey and inspection processes require other devices, instruments or integral for inspections with roof analysis services beyond infrared aerial measurement methods such equipment and their intended purposes shall be stated in the proposal and reported on in the final document, when used in this investigation.

Appendix C

Specifications for Energy Audits with Spot Radiometers for Temperature or Radiosity Measurements

1. Guidelines and Requirements

Scope - Conduct public building energy audits with measurements utilizing temperature or radiosity spot radiometers, perform data analysis and interpretation of measurements and audits to determine deficiencies in smaller federal buildings, prepare remedial actions recommendations, and submit a report documenting the results for:

- o Estimated heat loss from major building components
- o Thermal anomalies and deficiencies
- o Identified measures for energy saving retrofits

The contractor(s) will prepare a reproducible report which will contain a comprehensive detailed description of the inspection survey, use of spot radiometers, the methods and procedures for data collection, data, photographic and other appropriate information derived for analysis, calculations and interpretation of the survey and recommendations for remedial actions.

The contractor(s) will be required to visit and inspection the building(s) selected for the audits and measurements. The inspections, audits and measurements will be conducted in a manner consistent with the requirements indicated, part 3. The audits and measurements will be performed in such a manner as to result in reproducible format data sheets, or other records, with sufficient detail and summary findings developed onsite to permit independent review and analysis of the results, location of defects and anomalies and heat loss estimation.

The contractor(s) will conduct the audits and measurements within a reasonable time period when the building(s) are heated. The indoor-to-outdoor temperature difference shall exceed 18°F (10°C). The building heating plant shall be turned off 30 minutes prior to the measurements. The measurements should not be carried out sooner than three hours after sunset. Interior shading devices should be closed. A suitable calibration method shall be provided; accurate outdoor temperature measurement by thermometer is required.

Requirements - The contractor(s) shall provide the proposed (blank) spot radiometer data record and audit format sheets to be applied for the audit measurement inspections. Conduct the building(s) survey in accordance with the following provisions:

Equipment Specifications

Temperature spot radiometer resolution to within $\pm$ 0.5°F (0.3°C).
Tabulation of uncertainties as a percent error in measuring the thermal resistance of walls and measurements of temperature differences are to be provided in the proposal.
Reference surface provisions for calibrating the radiometer shall be provided and described.
The technique for determination of equivalent black body (reflected radiation) reference temperature measurement of the surroundings shall be provided and described.
Auxiliary temperature measurement for thermal resistance determination with radiosity equipment is required.

Operation and Data Record - The radiometers should be calibrated with reference surfaces provided by manufacturers or comparable methods. Data on prepared formats should be recorded to show:

1. Date, time and location of inspection.
2. Measured values from instruments.
3. Outdoor temperature and wind conditions.
4. Site weather conditions.
5. Audit inspection findings.
6. Photographs of observable defects.

Staff Qualifications - Audits with spot radiometers inspection survey and measurements should be undertaken by personnel trained as energy auditors and have training to level I for a paraprofessional as indicated by the Canadian Training Program.*

Experience and/or Capabilities - The organization and staff that will participate in the project shall be described in sufficient detail to enable evaluation of capabilities to perform the proposed effort with spot radiometers. For the purpose of the evaluation of the proposals on a competitive basis the information provided to accomplish the inspection, survey, report, staffing, organization qualifications, and costs will be weighed as factors in determining the contract award(s).

2. Exceptions

Departure from any listed guidelines or requirements may be permitted provided that spot radiometers will not be made subordinate to other equipment, devices or imaging techniques categorized as essential equipment to conduct an instrumented audit inspection. The supporting rationale must be technically valid and reflect a high quality level for good commercial practices or from experience, and provided as a basis for evaluation to NBS.

---

*Public Works Canada Training Program, Level I (Thermographic), Level II (Thermographic), Level III (Building Science).

3. Use of Other Equipment

Where normal commercial audit practice requires other supplementary devices, instruments regarded as integral for inspections such equipment and their intended purposes are to be described, stated in the proposal and reported on in the final document, when used in this investigation.

☆U.S. GOVERNMENT PRINTING OFFICE: 1985 491 097 36664

FORM NBS-114A (REV.11-84)

U.S. DEPT. OF COMM. BIBLIOGRAPHIC DATA SHEET (See instructions)	1. PUBLICATION OR REPORT NO. NBSIR 85-3147	2. Performing Organ. Report No.	3. Publication Date SEPTEMBER 1985

4. TITLE AND SUBTITLE

Evaluation of the Thermal Integrity of the Building Envelopes of Eight Federal Office Buildings

5. AUTHOR(S) Richard A. Grot, Andrew K. Persily, Y. May Chang, Jin B. Fang, Stephen Weber and Lawrence S. Galowin

6. PERFORMING ORGANIZATION (If joint or other than NBS, see instructions)

NATIONAL BUREAU OF STANDARDS
U.S. DEPARTMENT OF COMMERCE
GAITHERSBURG, MD 20899

7. Contract/Grant No.

8. Type of Report & Period Covered

9. SPONSORING ORGANIZATION NAME AND COMPLETE ADDRESS (Street, City, State, ZIP)

General Services Administration
18th and F Streets
Washington, DC 20405

10. SUPPLEMENTARY NOTES

☐ Document describes a computer program; SF-185, FIPS Software Summary, is attached.

11. ABSTRACT (A 200-word or less factual summary of most significant information. If document includes a significant bibliography or literature survey, mention it here)

Diagnostic test methods were applied to eight federal office buildings in order to assess the applicability to these measurement methods for determining the thermal integrity of the building envelope. The eight federal office buildings were located in Anchorage, AK; Ann Arbor, MI; Columbia, SC; Fayetteville, AR; Huron, SD; Norfolk, VA; Pittsfield, MA and Springfield, MA. These buildings ranged in size from 20,000 ft^2 (1,900 m^2) for the building in Pittsfield to 520,000 ft^2 (48,000 m^2) for the Anchorage federal building. They were all constructed within the last ten years. The diagnostic tests which were applied to these buildings were ground infrared thermographic inspection, aerial infrared thermographic inspection, spot radiometry, air infiltration and ventilation rate measurement using tracer gas decay, building tightness testing using fan pressurization, component tightness testing, and measurement of the thermal conductance of major wall sections using portable calorimeters and heat flow meters. This report presents and discusses the results of these tests.

12. KEY WORDS (Six to twelve entries; alphabetical order; capitalize only proper names; and separate key words by semicolons)
Air infiltration; building diagnostics; building thermal integrity, fan pressurization; field measurements; spot radiometers; thermal bridges; thermographic inspection; tracer gas techniques; U-value measurements.

13. AVAILABILITY

☒ Unlimited

☐ For Official Distribution. Do Not Release to NTIS

☐ Order From Superintendent of Documents, U.S. Government Printing Office, Washington, DC 20402.

☒ Order From National Technical Information Service (NTIS), Springfield, VA 22161

14. NO. OF PRINTED PAGES 200

15. Price